A STUDY OF TWO-DIMENSIONAL PANEL FLUTTER

Thesis by

Malcolm Harvey Lock

In Partial Fulfillment of the Requirements

For the Degree of

Doctor of Philosophy

California Institute of Technology

Pasadena, California

1961

ACKNOWLEDGMENT

The author is very happy to take this opportunity to express his deep appreciation to Dr. Y. C. Fung for his help and encouragement in carrying out this research. He has found great pleasure in undertaking this study and the help of those who made it possible is gratefully acknowledged.

He also wishes to express his thanks to Mr. M. E. Jessey for the design of the electronic equipment employed in the experimental phases of this study. His thanks are also due to Mrs. Dorothy Eaton for carrying out the numerous calculations and to Miss Helen Burrus and Mrs. Betty Wood for their help in preparing the manuscript.

This study has been greatly aided by the Air Force Office of Scientific Research which is currently sponsoring a research program in panel flutter at the Institute. This aid is gratefully acknowledged.

SUMMARY

An investigation of the problem of the flutter of two-dimensional flat panels is undertaken. The research is largely devoted to investigating the adequacy of the ideal flutter theory that has been employed to predict flutter boundaries for such panels. A series of panel flutter experiments carried out in the GALCIT 4" x 10" transonic wind tunnel at Mach numbers up to 1.5 are described in detail. Before the results of these experiments are compared with the predictions of the theory some further analytical studies of the flutter problem are presented that enable a more critical comparison of theory and experiment to be made. These analyses treat some aspects of the problems of transonic and supersonic panel flutter. The nature of the energy exchange at flutter is also considered. This latter study throws considerable light upon the flutter process as described by the ideal theory and also clarifies the breakdown of certain approximate unsteady aerodynamic theories in the low supersonic flow region ($1 < M < 1.5$). Comparison of theory and experiment reveals considerable differences between the theoretical and experimental flutter boundaries at the lower supersonic Mach numbers. The agreement between theory and experiment improves at Mach numbers above about 1.4. The possible sources of the apparent inadequacy of the theory at the lower supersonic Mach numbers are discussed.

TABLE OF CONTENTS

LIST OF FIGURES

LIST OF FIGURES (Cont'd)

LIST OF SYMBOLS

a	Velocity of sound in the undisturbed flow
A_m	Generalized co-ordinates describing the plate motion (see equations 1.12, 1.16 and 2.5)
b	Plate semi-chord
B_1	Amplitude of the initial deflection of the plate (see Section 2.2.)
C_{mn}	Coefficients appearing in the generalized aerodynamic force in a supersonic flow (see Section 2.2.)
D	$= \frac{Eh^3}{12(1-\nu^2)}$, bending rigidity of the plate
E	Young's modulus of the plate material
g	Structural damping coefficient
h	Plate thickness
k	$= \frac{\omega b}{U}$, reduced frequency of flutter
k_o	$= \frac{2\omega_o b}{U}$, stiffness parameter
M	Mach number of the flow
N_x	Mid-plane tension per unit span; tension positive
$p_a(x, o^+, t)$	Aerodynamic pressure induced by the deflection Z_a acting upon the upper surface of the plate
$p(\omega)$	Power spectrum of the response of the plate
Q_n	The nth generalized force (see equation 1.8, 1.11 and 2.6)
R_I	Energy contribution per cycle at flutter arising from the integral term in equation (3.1)
R_x	Energy contribution per cycle at flutter arising from the $\frac{\partial Z_a}{\partial x}$ term in equation (3.1)

R_T	Energy contribution per cycle at flutter arising from the $\frac{\partial Z_a}{\partial t}$ term in equation (3.1)
S	$= \frac{4N_x b^2}{\pi^2 D}$, mid-plane stress parameter
t	Time variable
T_{mn}	Coefficients appearing in the generalized aerodynamic force in a transonic flow (see equations 1.9 and 1.11)
U	Velocity of the undisturbed flow
U_δ	Fluid velocity at the edge of the boundary layer, defined as 99 per cent of the freestream velocity
$W_a(x)$	Downwash (see equation 1.4)
$\bar{x}$	Streamwise co-ordinate
x	$= \frac{\bar{x}}{b}$, dimensionless streamwise co-ordinate
$Y(x)$	Plate mode shape
z	Spatial co-ordinate
$Z_a(x, t)$	Vertical deflection of the plate, positive upwards
$\phi(x, z, t)$	Aerodynamic perturbation velocity potential
μ	$= \frac{\rho_s h}{2b\rho}$, mass ratio of the panel to air
ν	Poisson's ratio
ρ	Density of the undisturbed air
ρ_s	Density of the plate material
ω	Flutter frequency
ω_o	Fundamental frequency of free vibration, rad. per sec.

β $= \dfrac{2kM^2}{(M^2-1)}$, the supersonic reduced frequency

$\bar{\delta}$ Ratio of the amplitude of vibration of the plate to the plate chord

δ_B Boundary layer thickness, defined as the height above a solid boundary where the fluid velocity reaches 99 per cent of the freestream value

INTRODUCTION

Elastic plates, when suitably perturbed, will exhibit various natural modes of lateral vibration, wherein all points of the plate will vibrate at the same frequency. The frequency, damping and spatial shape of these modes are dependent upon the plate characteristics and the medium in which the plate is immersed. These modes of vibration are positively damped in still air, due to the action of aerodynamic and internal damping. The nature of these modes will change when the plate is exposed to an airstream and it is possible that the damping in a particular mode may vanish at some airspeed. The plate may then exhibit undamped harmonic oscillations. These oscillations are referred to as "panel flutter". Further change of airspeed may lead to a divergent oscillation and the eventual fatigue failure of the plate. This phenomenon appears to be of practical concern in supersonic flight (Ref. 1).

The possibly disastrous consequences of panel flutter stimulated a number of analytical studies of the problem (Refs. 2, 3, 4, 5, 6, 7 and 8). These studies were largely devoted to the prediction of flutter boundaries for two-dimensional panels exposed to supersonic airstreams (i.e. the conditions were sought whereby the panels could exhibit undamped harmonic oscillations). The analyses were performed under several simplifying assumptions concerning the flow and plate properties and the amplitude and velocity of the plate motion was required to be such that the problem could be linearized. Even so, the complications introduced in this ideal theory by the aerodynamic

pressure term appearing in the plate equation of motion necessitated the use of approximate methods of solution. Two general approaches were employed. The first was the use of methods of solution whereby the integro-differential equation of motion was reduced to a system of linear algebraic equations (e.g. the Galerkin method or the assumption of generalized co-ordinates). The second approach consisted of the use of approximate aerodynamic theories, such as the quasi-steady and linear piston theories, that simplified the equation of motion to such an extent that exact solutions could then be readily obtained. The analysis, however, proved to be extremely sensitive to the approximations employed and difficulties arose with both methods. The Galerkin method applied to the membrane flutter problem, at Mach numbers that were high enough to permit the use of the linearized aerodynamic piston theory, failed to yield a convergent result, whereas the exact solution to the same simplified problem showed that all membranes would be stable (Ref. 6). On the other hand, the quasi-steady aerodynamic theory, although apparently successful at high Mach numbers ($M > 1.6$), proved to be inadequate at the low supersonic Mach numbers ($1 < M < 1.5$). A flutter analysis performed with this theory (Ref. 4) predicted that all panels would flutter if the supersonic Mach number was less than $\sqrt{2}$, whereas the results of analyses using the complete linearized aerodynamic pressure yielded finite flutter boundaries (i.e. plates with sufficiently large thickness ratios $(\frac{h}{2b})$ would not flutter).

By recourse to further analysis (Refs. 1 and 9) the difficulty with the Galerkin method was shown to be associated with the membrane problem. Flutter boundaries for plates (finite bending stiffness) could

be satisfactorily obtained using this method. It was also noted (Ref. 10) that the quasi-steady aerodynamic pressure expression, which consists of the zero and first order terms of a frequency expansion of the complete linearized result, could be expected to be unsatisfactory in the neighborhood of $M = \sqrt{2}$, where the first order frequency contribution vanished; however, this reasoning did not explain the failure of the theory at Mach numbers well below $\sqrt{2}$. The general trends predicted by the ideal theory are shown in Figure 2 where stability boundaries are presented for simply supported panels at sea level flight conditions. The results for clamped edge panels are similar and exhibit the same general features. The boundaries at Mach numbers less than 1.56 were calculated using the complete linearized aerodynamic pressure and the analysis indicates that this region is critical in the sense that large thickness ratios are required to prevent flutter. The possibility of panel flutter in a transonic flow ($M \approx 1$) has not been investigated. The analysis in this flow region would require the use of a transonic aerodynamic theory.

From this brief summary of the previous work it is seen that the prediction of flutter boundaries is rather difficult and that great care has to be exercised when employing approximate methods to obtain a solution. However, the problem itself that has been analyzed is already highly idealized with regard to the assumed fluid and plate properties. In particular, a drastic assumption is that the fluid is inviscid. By this means the no-slip boundary condition along the surface of the plate, which leads to a partially subsonic boundary layer and appreciable viscous stresses in the immediate neighborhood of the surface, has been circumvented and replaced by the simpler tangential flow condition.

The predictions of this ideal theory, which have already been shown to be extremely sensitive to assumptions within the limited framework of the theory, are therefore open to some doubt and the question arises as to how realistic a description of the panel flutter phenomenon is presented by such a theory. This question can only be answered by experiment and it is here that the panel flutter investigation is at its weakest. Apart from some work at Mach number 1.3 (Ref. 11), which established the existence of the phenomenon and investigated the effect of mid-plane stresses upon flutter, no systematic experimental investigation of the panel flutter phenomenon, especially in the low supersonic flows, is yet available and the predictions of the ideal theory remain unchecked.

The present investigation comprises a further study of the flutter of two-dimensional flat panels and is largely directed to investigating the adequacy of the ideal flutter theory. A series of panel flutter experiments were undertaken in the GALCIT 4" x 10" transonic wind tunnel at Mach numbers up to 1.5. Two-dimensional conditions were represented as closely as was possible. The flutter phenomenon was carefully investigated in the low supersonic region and flutter boundaries were obtained between Mach numbers 1.15 and 1.5. These experiments are described in the first part of this paper. Before comparison of the experimental results with the theory is undertaken, some further theoretical studies of the panel flutter phenomenon are presented. These studies were stimulated by certain features of the experiments and their results enable a more critical comparison of theory and experiment to be made. The first of these studies consists of an

investigation of the possibility of transonic panel flutter. This analysis is undertaken under certain parametric restrictions associated with the use of a linearized transonic aerodynamic theory. The flutter of a simply supported plate exposed to a sonic airstream (M = 1) is investigated assuming that the plate motion is describable by a small number of generalized co-ordinates. A study of the flutter of simply supported panels at the low supersonic Mach numbers is next presented. In particular the effects of internal damping and small initial curvature upon the flutter boundaries at these Mach numbers are investigated. Finally an analysis of the energy transfer between the airstream and the plate during the flutter motion is presented. The analysis is undertaken by examining the solutions of some previous panel flutter investigations. The results of this study throw considerable light upon the flutter processes as described by the ideal theory and clarify the breakdown of the quasi-steady aerodynamic theory for flutter analysis at the low supersonic Mach numbers.

The comparison of theory and experiment in the low supersonic region is presented in the final part of this paper. Considerable disagreement is found between the theoretically predicted flutter boundaries and the experimental results at Mach numbers less than about 1.4. The agreement between theory and experiment improve at the higher Mach numbers. The possible sources of the apparent inadequacy of the theory at the lower supersonic Mach number are discussed.

PART I

AN EXPERIMENTAL STUDY OF PANEL FLUTTER

1.1. General Remarks

In the experimental program to study the flutter of two-dimensional flat panels, the subsonic and low supersonic flow regions were chosen for the investigation. The experiments were carried out in the GALCIT 4" x 10" transonic wind tunnel at Mach numbers up to 1.5. A detailed description of the transonic wind tunnel may be found in Reference 12. The model and the wind tunnel installation were designed to represent two-dimensional conditions as closely as was possible. Furthermore it was attempted to produce a good representation of the condition of zero mid-plane stress in the test panels. The panels were installed in the ceiling block of the wind tunnel such that the panel surface would lay flush with the ceiling surface (Figure 3). In order to make some allowance for the sidewall boundary layers the span of the test panels were made slightly less than the width of the wind tunnel test section. The test panels were attached to a mounting frame at their leading and trailing edges. The streamwise edges of the panels were free. Ideally the space behind the test panel, the venting chamber, would be vented to the free stream static pressure, however, early experiments revealed that small pressure differentials (of the order of 0.4 ~ 0.5 cm Hg) would exist between the chamber pressure and the free stream static pressure. These pressure differentials could produce mid-plane stresses in the test plates, which in turn could change the flutter boundaries (see for example Reference 6). To reduce the possible

development of such stresses the trailing edges of the panels were mounted upon a light flexure support (see detail in Figure 3). The effective mass of this flexure was small compared to the mass of a typical test panel and for small amplitude lateral motion (amplitude < plate thickness) this support is considered to represent a partially restrained (against rotation) edge boundary condition.

A boundary layer would be present upon the wind tunnel ceiling during the tunnel operation. Measurements were made of the velocity profile of this layer over the test panel installation. The measurements were taken on the tunnel centerline. The thickness of the boundary layer, defined as the height above the solid surface where the flow velocity reached 99 per cent of the free stream velocity, was found to be of the order of 0.34" - 0.40". The velocity profiles were typical of a turbulent boundary layer (see Figure 4). Boundary layer pressure fluctuations acting upon the surface of the test panels were used as a source of excitation of the panels in the non-flutter region. The lateral motions of the plates that were induced by the airstream were measured and analyzed at different flow Mach numbers. The flutter boundaries were estimated from these measurements. Harmonic analysis of the plate motion yielded certain of the natural frequencies of the test panels at the different Mach numbers. By this means the origin of the flutter mode was identified and the importance of the other plate modes assessed. Flutter boundaries were determined in the low supersonic flow region and certain general features of the phenomenon obtained.

1.2. Test Panels and Equipment

The test panels were manufactured from thin brass sheet (0.010" to 0.0155" thickness) and were attached to a brass mounting frame at their leading and trailing edges. The chord length of the panels varied between 3.14" and 3.79". The leading edges of the panels were soldered directly to the mounting frame. This method of attachment was considered to be a close approximation to the clamped edge boundary condition. The trailing edges of the panels were mounted upon a flexure support (see detail in Figure 3) that would allow a small amount of horizontal movement in the plane of the plate. A Z section flexure, manufactured from 0.006" thick phosphor bronze sheet, was employed. The horizontal deflection-load characteristics of the flexure were linear up to at least 2 lbs. load. The flexure stiffness being found to be approximately 77 lbs. per inch. Permanent deformation of the flexure would occur at less than 4 lbs. load.

This type of support was found necessary to reduce the development of mid-plane stresses in the test panels. Such stresses, which have an appreciable effect upon the flutter boundaries, could be easily developed by static pressure differentials across the plates, by thermal effects and by mechanical distortion of the mounting frame when it is inserted in the wind tunnel. The flexure support conveniently circumvented these difficulties and had the added advantage of reducing the effect of any small initial curvature of the test panels (the effect of small initial curvature would appear as a mid-plane stress term in the plate equation of motion). It should be added that insofar as the pressure differential problem is concerned this means of support leads

to the development of bending stresses, rather than mid-plane stresses, that resist the pressure acting upon the plate. However, such initial bending stresses, as opposed to initial mid-plane stresses, are expected to have little influence upon the plate bending frequencies and this is taken as an indication that the flutter boundaries are relatively insensitive to this effect.

The flexure is extremely light, the effective mass with respect to flexural vibration of the plate being of the order of 10 per cent of the mass of a typical test panel. For small amplitude lateral motion of the test panels (amplitude < plate thickness) the associated horizontal motion of the trailing edge will be proportional to the square of the lateral amplitude (assuming that the flexure is fully effective in preventing any mid-plane stresses) and, for the panels under consideration, will therefore be much smaller than the lateral motion. This fact, coupled with the small effective mass of the flexure, suggests that the horizontal motion will have little influence upon the linear vibration characteristics of the test panels*. The flexure supporting trailing edge is therefore expected to behave as a partially restrained (against rotation) edge. Experimental determination of the frequencies of flexural vibration of the various test panels supports this view. These flexural vibration frequencies are found to be intermediate to the corresponding values calculated for plates with clamped-clamped and clamped-simply supported boundary conditions (see Table I).

*The preceding argument applies to the case of perfectly flat panels. The linear vibration characteristics of slightly curved panels would be affected. In fact, if the flexure is fully effective then the curved plate should vibrate at the natural frequencies of the corresponding flat panel. However, the boundary conditions of this corresponding flat panel are not expected to be affected by the horizontal motion.

The mounting frame, to which the test panels were attached, fitted into the ceiling block of the wind tunnel such that the surface of the test panel would lay flush with the ceiling surface. To reduce the effect of the sidewall boundary layers the streamwise edges of the plates were set approximately 0.22" from the tunnel walls. A gap of about 0.038" was left between these edges of the panel and the mounting frame. These gaps served to vent the chamber behind the panels to the free stream static pressure.

The wind tunnel was of the closed circuit type and had a test section that was 4" wide and approximately 10" deep. The Mach number of the flow was varied continously by two screw jacks which controlled a flexible nozzle on the tunnel floor block. A second smaller nozzle was mounted downstream of the working section. The supply pressure was kept at atmospheric pressure throughout the tests. The supply temperature was kept between 30 - 32^{o}C. The test section Mach number was estimated from static pressure measurements taken upon the mounting frame and the ceiling liner. Ten static pressure taps were provided for these measurements. Three taps were located upstream of the model, three more taps were downstream of the model and four taps were located on the mounting frame itself. The pressure in the venting chamber behind the test panels was also measured. Pressure measurements taken from these taps during the experiments indicated that good flow conditions were obtained over the test panel installation. The estimated variation of Mach number over the panel chord was of the order of 0.5 - 1 per cent of the average estimated Mach number. The spanwise variation of the free stream Mach number was of the same

order of magnitude. For the determination of the free stream Mach number from these static pressure measurements it is assumed that the airstream has expanded isentropically from the stagnation conditions and that the wall static pressure is equal to the free stream static pressure (i.e. negligible pressure gradient through the boundary layer). Because the boundary layer on the panel installation was relatively thick this latter assumption was checked and was verified to be reasonable. The error in Mach number estimation arising from this source being of the order of 1 per cent of the free stream Mach number.

When the wind tunnel was in operation a turbulent boundary layer was present over the surface of the test panel. Lateral motion of the panel was induced by the pressure fluctuations present in this layer and the plate response was measured by an inductance pickup. This pickup was located in the chamber behind the panel, being positioned on the tunnel centerline at 2.2" downstream of the test panel leading edge position. The pickup, which employed a 100 kilocycle carrier system, had the advantage of permitting simultaneous static and dynamic measurements of the plate motion. The signal from the pickup was relayed to a harmonic analyser (Technical Products TP 627 and TP 626), a Ballantine true root mean square meter and a Moseley automatic plotter. Precise determination of the plate frequencies was accomplished with the use of a Hewlett Packard oscillator and a Berkeley type 5501 counter. A Dumont type 411 oscilloscope was also employed in the analysis of the plate response.

A number of panels with thickness ratios($\frac{h}{2b}$) varying from 0.00297 to 0.0046 were tested. The various thickness ratios were obtained by varying both the thickness and chord length of the panels. The chord lengths were varied between 3.14" and 3.79". The majority of the tests were made with 0.0125" thick panels. The panel widths were kept at 3.56". Details of the different test panels are given in Table I. The theoretical natural frequencies of lateral vibration that are also presented in Table I were estimated for flat plates with clamped-simply supported and clamped-clamped boundary conditions using the results of Reference 13.

1.3. Test Procedure

(a) Still-air Vibration Tests.

After manufacture of each test panel the first few natural frequencies of flexural vibration of the panels would be obtained. These modes of vibration may be divided into two classes, namely (1) the "two-dimensional" modes, where the nodal lines are all essentially parallel to the fixed edges of the plate and, (2) the "three-dimensional" modes where nodal lines appear that are not parallel to the fixed edges. These latter modes are obtained as a consequence of the finite span of the panels. A series of nodal line positions at successive natural frequencies that were obtained for a typical test panel are shown in Figure 5. These nodal line positions were obtained using single frequency acoustic excitation of the test panel. The two-dimensional modes that are shown are the modes labeled (2, 0), (3, 0) and (4, 0) in the figure. Examples of the three-dimensional modes are those labeled (2, 1) and

(2, 2). The classification (a, b) indicates the number of nodal lines. The first number "a" denotes the number of nodal lines parallel to the fixed edges, the second number "b" denotes the number of nodal lines that are essentially parallel to the free edges of the panel.

The determination of these modes of vibration in still air is of some importance in connection with the wind tunnel tests. By tracing the natural frequencies of the plates at different Mach numbers to their still air values it is possible to identify the source of the flutter mode and to assess the importance of the three-dimensional plate modes in what is intended to be a two-dimensional experiment. The modes that were three-dimensional in still air are expected to remain three-dimensional when the plates are exposed to an airstream. It is also expected that the modes of plate vibration that were two-dimensional in still air will remain essentially two-dimensional. (i.e. the changes in mode shape produced in these modes by the airstream will be essentially uniform across the plate span). It is therefore required, for a two-dimensional experiment, that the flutter mode originates from a two-dimensional mode of plate vibration in still air.

To obtain the plate natural frequencies at the different Mach numbers advantage was taken of the fact that random pressure fluctuations would be acting upon the test panels and that these fluctuations would excite motion of the panels. The feasibility of using random excitation as a means of determining the natural frequencies was first investigated by conducting a series of experiments in which the test panels were subject to the noise field of an air jet (a convenient source

of random excitation). The plate response to such a loading was analyzed and the resulting power spectra yielded distinct peaks at frequencies which were found to be identifiable with the plate natural frequencies. A power spectra of the response of one of the test panels to jet noise is shown in Figure 6. The spectral peaks have been identified with the corresponding natural frequencies. The plate modes at these frequencies were obtained separately with the use of single frequency excitation of the test panel. The frequencies at which these spectral peaks occur were obtained by passing the pickup signal through a 2 cycle/sec bandwidth filter, locating the peak from the mean square signal meter incorporated in the analyser, and then beating the filtered signal against an oscillator signal. The frequency of the oscillator was determined using the Berkeley counter.

(b) Wind Tunnel Tests.

The wind tunnel test procedure consisted of measuring and analyzing the lateral motion of a given test panel at successive Mach numbers until the flutter speed for this panel was determined. This procedure would be repeated for different panels until a flutter boundary was established in the flow region of interest. The flutter points for the various test panels were estimated from the measurements of the panel response. Analysis of the panel response yielded the natural frequencies of the plates at the various Mach numbers.

Throughout the non-flutter region the plate response was of a highly irregular nature. The flutter motion on the other hand was very regular and was of appreciably greater amplitude. The different nature

of the two types of plate motion is clearly seen from the oscilloscope traces shown in Figure 7. The first trace shows a typical plate response in the non-flutter region. The second trace shows a typical plate response at flutter. The plate motion in the non-flutter region was found to be so irregular that the mean square plate response at a given Mach number, although averaged over several seconds, would fluctuate considerably. It was therefore found necessary to take a time average of these mean square measurements. Harmonic analysis of the plate response, as in the case of the jet noise excitation, revealed a series of spectral peaks at the natural frequencies of the panels (see Figure 8). The major contribution to the measured response was found to arise from the frequency band around the lowest natural frequency. An example of this is shown in Figure 9. The upper trace shows the variation of the measured mean square response of a test panel in the non-flutter region. The mean square response was obtained by averaging the measured plate deflection over about 5 seconds. The response was then filtered about the fundamental natural frequency of the plate, a 50 cycles/sec bandwidth filter was employed, and the mean square of this filtered response was obtained. This mean square response is shown in the lower trace in Figure 9. When taking average values of the two traces over several minutes and comparing the results it is found that the response in the frequency band around the fundamental frequency contributes about 75 per cent of the root mean square response of the plate. The mode of vibration of the plate corresponding to this frequency derives originally from the mode (2, 0). The contribution to the plate response from this frequency band is

therefore expected to be essentially two-dimensional. The non-flutter response was found to be larger in the subsonic flows than at the supersonic Mach numbers. This effect is believed to be due to disturbances from the wind tunnel diffuser being propagated upstream into the working section and exciting the panels. For supersonic flow the root mean square amplitude of the measured plate motion in the non-flutter region would be of the order of 0.0005" - 0.0015". During the flutter motion, root mean square amplitudes of the order of 0.016" were recorded. Root mean square amplitudes of this magnitude would correspond to actual amplitudes of the order of twice the plate thickness.

The approach to the flutter boundary would be characterized by a rapid increase in the amplitude of the plate response. The variation of the mean square plate response with Mach number at the flutter boundary of a typical test panel is shown in Figure 10. The exact determination of the flutter Mach number from such measurements is not possible. However, the rapid increase of the mean square response with Mach number allows a close estimate of the flutter Mach number to be made. The method employed was to choose as the flutter Mach number, some value at which the mean square response had increased appreciably (by a factor of 20 ~ 30) from an average value for the non-flutter region. At such a Mach number the major contribution to the response was the regular harmonic motion characteristic of the flutter region. Such a method is rather vague, however, the increase in the plate response as the flutter region is approached is so rapid that the method is practical. For example, for the case shown in Figure 10, computing the boundary using an increase factor of 30 instead of 20 would change the flutter Mach number by less than 1 per cent.

A certain amount of irregularity was present in the plate response at flutter, however, this irregularity was very small compared to the steady component of the mean square response (see Figure 11). This irregularity in the response was due to the continuing action of the random pressure fluctuations acting upon the test panel. Harmonic analysis of the plate response revealed in all cases that the flutter frequency was the lowest natural frequency of the panel. A power spectrum of the flutter motion of one of the test panels is shown in Figure 12. The other plate modes were still being excited by the pressure fluctuations but their contribution to the plate response was negligible compared to the flutter motion. The oscilloscope traces presented in Figure 13 show the flutter response of one of the test panels. The upper trace shows the total response. The second trace shows the response when it is filtered at the flutter frequency (a 2 cycle/sec bandwidth filter was employed) and the third trace shows the response in the frequency band around the second two-dimensional mode (i.e. the signal has been filtered at the plate natural frequency that originally derived from mode (3, 0) in still air). It should be noted that this frequency is not necessarily the frequency of mode (3, 0) in still air. In this connection it should also be remarked that the harmonic analysis of the plate motion at the different Mach numbers revealed very little change of the higher natural frequencies of the test panels from their still air values. The fundamental frequency of the test panels appeared to be more sensitive to the influence of the airstream. The typical behavior of the natural frequencies of the test panels are shown in Figure 14. The fundamental frequency (mode 2, 0) is found to decrease steadily in the subsonic range and to increase steadily with increasing supersonic Mach

number. The phenomenon in the subsonic range may however be due to the effect of wind tunnel interference. The fundamental frequency was also found to be rather difficult to locate at subsonic Mach numbers above about 0.6. The variation of the second natural frequency (mode 2, 1) of the panel is not plotted, the pickup location being unsuitable for the measurement of this mode.

1.4 Test Results

The results of the experimental program may be briefly stated as follows:

Panel flutter was observed only at the supersonic Mach numbers. Flutter boundaries were obtained in the low supersonic region between Mach numbers 1.15 and 1.5. The maximum thickness ratio $(\frac{h}{2b})$ required to prevent the flutter of "flat" panels at these Mach numbers was found to be slightly less than 0.0046. The panel thickness ratio requirements to prevent flutter were found to decrease slowly with increasing Mach number at Mach numbers above $M = 1.2$ (see Figure 15). The boundaries of the flutter region were quite distinct but proved to be rather sensitive to the test conditions. In particular, streamwise acceleration of the airstream over the length of the test panels, was found to change the flutter Mach number of the test panels from the values obtained when the airstream was essentially uniform. At the same time, the accelerating flow would produce static deflection of the test panels (due to the action of the pressure differential). It is believed that the observed changes of flutter Mach number are a consequence of these static deflections rather than being directly due to the non-uniformity of the flow which was small compared to the average Mach number.

The flutter boundary presented in Figure 15 that is denoted as the "flat" panel boundary was obtained for conditions wherein the measured static deflection of the test panels was less than a plate thickness. This boundary is expected to be representative of the flat panel case. Flutter points that were obtained when the test panels exhibited considerable static deflection (due to an accelerating airstream) are also shown in Figure 15. The flutter Mach number for these points was taken as the average Mach number over the panel chord. The corresponding values of the measured static deflection are shown, together with the measured frequency ratios $(\frac{\omega}{\omega_o})$, where ω_o denotes the frequency of the mode (2, 0) in still air and ω denotes the flutter frequency.

The flutter mode in all cases was found to derive from the fundamental two-dimensional mode of the test panels in still air (i.e. the flutter mode would be traced to the mode (2, 0) in still air. The maximum amplitude of the flutter mode appeared to be downstream of the mid-chord point of the panel. There was very little phase shift present in the flutter modes that were observed. The phase shift between the flutter motion at the 22 per cent and 65 per cent chord stations of the plate was estimated to be 2.5°, 1°, and 1° at Mach numbers of 1.18, 1.31, and 1.34 respectively. Visual observation of the flutter response revealed no detectable spanwise variation of the plate motion. The frequency ratios $(\frac{\omega}{\omega_o})$ of the "flat" panel flutter were found to vary from about 0.83 to slightly above unity. No "second mode" flutter was observed throughout the test series. (This second mode flutter would be a flutter mode originating from the

second two-dimensional mode of the test panels). No frequency coalescence was observed. The higher natural frequencies of the test panels were found to vary only slightly from their still air values.

It was not possible to extend the flutter boundaries in the supersonic region to Mach numbers less than about 1.15. This was due to the appearance of the wind tunnel normal shockwave in the working section. The presence of this shockwave upset the flow conditions of the experiments and prevented the determination of flutter boundaries.

Review of the experimental data indicates that good two-dimensional conditions were obtained in the experiments. As mentioned previously, no detectable spanwise variation of the flutter modes was observed. It was also found that the excitation of the measured three-dimensional plate modes was negligible compared to the plate response from the frequency band around the fundamental two-dimensional plate mode. A possible source of three-dimensional effects in the two-dimensional experiments could arise from the small differentials that were found to exist between the pressure in the venting chamber and the free stream static pressure, and which could produce an outflow from the venting chamber. Such an outflow, however, is expected to have little effect upon the main airstream and it is considered unlikely that any small, steady perturbation of the mainstream produced by this outflow would interact with the unsteady flutter phenomenon.

It is also considered that a good representation of the zero mid-plane stress condition was obtained. The low stiffness of the flexure support ensures that the mid-plane stresses developed by the effects of thermal expansion and by the action of static pressure

differentials will be negligible. For example, when considering a typical test panel that has deflected, under the action of a static pressure loading, into the form of a half sine wave with an amplitude of 0.060 inches, it is found that the mid-plane stress that is developed due to the flexure stiffness is only of the order of 4-6 psi. The development of mid-plane stresses by mechanical distortion of the mounting frame when it is installed in the wind tunnel would be revealed by measurable changes between the natural frequencies of the test panels measured in still air and measured when the panel was installed in the wind tunnel. The changes in the frequencies that were noted were small (of the order of 2-3 cycles/sec in the fundamental frequency). This finding indicates that any stresses that were developed by this means were also negligible. A conservative limit upon the magnitude of mid-plane stresses that were developed in the panels during the experiments is that they would be less than 20 psi. Previous flutter analysis has indicated that mid-plane stresses of this order of magnitude would produce such small changes of the flutter boundaries from the results for zero stress conditions that the experimental flutter boundaries may be considered representative of these zero stress conditions.

PART II

THEORETICAL STUDY OF PANEL FLUTTER

General Remarks

Before attempting to compare the results of the experiments with the theory, some further analytical studies of the two-dimensional panel flutter problem will be presented. These analyses were stimulated by the experiments and their results will enable a more critical comparison of theory and experiment to be made.

The problem of transonic panel flutter is first treated. The experimental results indicate that the flutter region is restricted to the supersonic Mach numbers and it is of some interest to determine whether the ideal theory will indicate such a feature of the phenomenon. To accomplish this it is necessary to extend the flutter analysis to the transonic flow region. Such an analysis is presented in the following section.

It is also necessary to undertake some flutter calculations at the low supersonic Mach numbers in order that the theoretical flutter predictions, used in the comparison of theory and experiment, are for conditions that are representative of the test panel conditions. Previous analysis (Ref. 6) has indicated that the flutter boundaries in the low supersonic region are sensitive to the effects of mid-plane stress and internal damping. The first of these effects may be safely neglected in the present calculations because the employment of a flexure support in the experiments ensures that the mid-plane stresses in the test panels will be negligibly small. However, the test panels certainly

possess some internal damping and this effect must be included in the calculations.

The effect of initial plate curvature upon the experimental flutter boundaries is considered to be drastically reduced by the use of the flexure support, however, the nature and actual magnitude of this effect upon the boundaries in the low supersonic region (assuming fixed edge plates) is not known. It is of some interest to obtain this information because it is conceivable that the changes of flutter speed (observed when the test panels exhibited appreciable static deflection) could be explained by this curvature effect. Accordingly, some flutter calculations are undertaken to obtain this information. These calculations also serve to estimate the error incurred when the curvature effect is neglected in the flutter calculations employed in comparison with the experimental "flat" panel flutter boundaries.

A third study that clarifies the flutter mechanism at the low supersonic Mach numbers is also presented. Examination of the energy transfer at flutter throws considerable light upon the flutter process as described by the ideal theory and the reason for the breakdown of the quasi-steady aerodynamic theory for flutter analysis in the low supersonic range becomes readily apparent.

All of these analyses are based upon the use of the ideal theory, which involves a combination of the simple linear plate theory with linearized irrotational flow theory. This theory is employed only to determine the infinitesimal amplitude flutter boundaries and cannot be used as such to compute the details of the large amplitude flutter occurring within the flutter region. The foundations of the ideal theory

rest upon the following set of assumptions concerning the fluid and plate properties and the flutter motion.

(a) The fluid is homogeneous and isotropic.

(b) The fluid is inviscid and non-heat conducting.

(c) The flow is irrotational and all perturbation velocities and pressures are small compared to the free stream velocity and pressure respectively.

(d) The plate material is homogeneous, isotropic and linearly elastic.

(e) The amplitude of the plate motion is small compared to the plate thickness.

(f) The normal stress σ_{zz} acting on surfaces parallel to the mid-plane of the plate is negligibly small compared to the bending stresses developed by the plate motion.

(g) All points that lie upon a linear element of the plate which is normal to the undeflected mid-surface of the plate remain on a straight line that is normal to the deflected mid-surface of the plate.

(h) The characteristic flutter time is large compared with the time that it takes an elastic wave to travel the length of the plate.

Of these assumptions perhaps the most suspect is that of an inviscid fluid. It is an experimental fact that at normal air densities the viscosity of air plays an extremely important role in determining the flow in the immediate neighborhood of a solid boundary, leading to the formation of the region of large velocity gradients and appreciable

viscous stresses associated with what is commonly known as the boundary layer. For steady, non-separating flow over a smooth surface of small curvature the boundary layer theory of fluid mechanics indicates that the pressure gradient through such a layer is negligible and that the inviscid theory with proper boundary conditions may be employed with reasonable success. The situation in the unsteady flow case is not so simple, especially when considering aeroelastic stability questions such as flutter, which tend to be rather sensitive problems, and it is by no means clear that arguments applied to the steady non-separating flow case have any bearing whatsoever on the unsteady problem.

The success of the ideal theory, which will justify such assumptions, will be measured later against the experimental data. But first the above mentioned analyses will be presented. For convenience this part of the investigation is divided into three sections, namely

Section 2.1. Two-dimensional Transonic Panel Flutter.

Section 2.2. Two-dimensional Supersonic Panel Flutter.

Section 2.3. Analysis of the Energy Transfer at Flutter.

Together with the assumptions (a) to (h) further restrictions are imposed upon the analysis in Sections 2.1 and 2.2. The restriction in the transonic case concerns the reduced frequency k ($k = \frac{\omega b}{U}$) and is associated with the use of a linearized transonic aerodynamic theory. The restriction in Section 2.2 concerns the supersonic reduced frequency $\bar{\omega} = \frac{2kM^2}{M^2 - 1}$ and is imposed to reduce the amount of computational labor involved in determining the flutter boundaries. No significant loss of accuracy is expected from the use of this simplification.

Section 2.1. - Two-Dimensional Transonic Panel Flutter.

2.1.1. General Remarks

The following sections consist of an analysis of the flutter of two-dimensional flat plates exposed to uniform transonic airstreams*. The analysis is performed under the assumptions (a) to (h), which form a basis for the use of the small disturbance inviscid flow theory and the linear plate theory. Furthermore, the following parametric restrictions, peculiar to the transonic flow region, are imposed

$$k \gg \tilde{\delta}^{2/3}, \qquad k = 0(1) \text{ and } k \gg |M^2 - 1|$$

(where $k = \frac{\omega b}{U}$ is the reduced frequency and $\tilde{\delta}$ is the ratio of the amplitude of lateral vibration to the plate chord). Lin, Reissner and Tsien (Ref. 14) have shown that the linearized flow theory may be employed in the transonic range if $k \gg \tilde{\delta}^{2/3}$. Furthermore, the equation governing the velocity potential may be reduced to a simple form if $k \gg |M^2 - 1|$. Nelson and Berman (Ref. 15) have employed this result to determine the forces acting upon a wing-aileron combination in a sonic airstream. A similar procedure is employed here to treat the panel flutter problem. With the above limitations clearly understood the following sections describe the panel flutter analysis for the transonic flow range. The aerodynamic terms required in the analysis are first developed and then expressions for the kinetic and strain energy of the plate are determined under the assumption that the plate deflection surface is describable by N generalized co-ordinates. Lagrange's

---

*The adjective transonic is employed here in a rather limited sense in that the analysis will be restricted to cases where the free stream Mach number is greater than or equal to unity.

equations of motion then yield a system of N linear algebraic equations from which the flutter conditions are obtained. Simply supported and clamped edge plates are treated and numerical results presented from a two mode analysis of a simply supported plate exposed to a sonic airstream. An alternative derivation of the transonic aerodynamic approximation, which emphasizes the physical significance of the theory, is presented in Appendix A.

2.1.2. Aerodynamic Pressure Expression

The aerodynamic pressure acting upon a harmonically oscillating plate exposed to a uniform transonic airstream is considered. The plate is initially flat and is of infinite span, being embedded in a flat rigid wall (see Figure 1). The wall is parallel to the uniform stream and extends to infinity in both the front and the rear of the plate. The flow is assumed to be isentropic and irrotational. The expression for the aerodynamic pressure on the plate is developed under the following restrictions.

$$k = 0(1), \qquad k \gg \tilde{\delta}^{2/3}, \qquad \tilde{\delta} \ll 1 \text{ and } k \gg \left| M^2 - 1 \right|.$$

Under these restrictions the equation governing the perturbation velocity potential $\phi(\bar{x}, z, t)$ is (Ref. 14)

$$2U \frac{\partial^2 \phi}{\partial \bar{x} \partial t} + \frac{\partial^2 \phi}{\partial t^2} - a^2 \frac{\partial^2 \phi}{\partial z^2} = 0. \tag{1.1}$$

For harmonic oscillations

$$\phi(\bar{x}, z, t) = \psi(\bar{x}, z)e^{i\omega t}. \tag{1.2}$$

The deflection surface of the plate may be written

$$Z_a(\bar{x}, t) = Y(\bar{x})e^{i\omega t} \qquad (o \leq \bar{x} \leq 2b).$$

The velocity potential $\phi(\bar{x}, z, t)$ satisfies the boundary conditions

$$\frac{\partial \phi}{\partial z}(\bar{x}, o^+, t) = \frac{\partial Z_a}{\partial t} + U\frac{\partial Z_a}{\partial \bar{x}} \qquad (o \leq \bar{x} \leq 2b;\ z = o^+),$$

$$\frac{d\phi}{dz} = 0 \qquad (\bar{x} < o,\ \bar{x} > 2b;\ z = o^+), \tag{1.3}$$

and

$$\phi(\bar{x}, \infty, t) = 0$$

In a supersonic flow ($M \geq 1$), the solution of (1.1), under the boundary conditions (1.3), evaluated upon the upper surface of the plate is

$$\phi(x, o^+, t) = -\frac{be^{i\omega t}}{\sqrt{2\pi k i M^2}} \int_o^x \frac{W_a(x - \xi)e^{-ik\xi/2}}{\sqrt{\xi}}\, d\xi \qquad (o \leq x \leq 2) \tag{1.4}$$

$$\phi(x, o^+, t) = 0 \qquad (x < o)$$

where

$$W_a(x) = i\omega Y(x) + \frac{U}{b}\frac{dY}{dx}$$

and

$$x = \frac{\bar{x}}{b}, \qquad \xi = \frac{\bar{\xi}}{b}.$$

The pressure is given by:

$$p_a(x, z, t) = - \rho \left\{ \frac{\partial \phi}{\partial t} + \frac{U}{b} \frac{\partial \phi}{\partial x} \right\}. \tag{1.5}$$

The pressure distribution on the surface is therefore:

$$p_a(x, o^+, t) = \frac{\rho U^2 e^{i\omega t}}{b\sqrt{2\pi k i M^2}} \left[\int_o^x \frac{e^{-ik\xi/2}}{\sqrt{\xi}} \left\{ \frac{d^2Y}{d\nu^2} + 2ik \frac{dY}{d\nu} - k^2 Y(\nu) \right\} d\xi + \frac{dY}{dx}(o) \frac{e^{-\frac{ikx}{2}}}{\sqrt{x}} \right] \tag{1.6}$$

where $\nu = x - \xi$.

It will be noted that there will be a singularity at the leading edge if $\frac{dY}{dx}(o) \neq 0$. This will be the case for simply supported panels. The singularity is integrable and the computation of the generalized forces will yield finite values.

The results for $\phi, \frac{\partial \phi}{\partial x}$, and $p_a(x, o^+, t)$ all become infinite for the steady state case ($k = 0$), which is a well known difficulty of the linearized theory.

2.1.3. Development of the Generalized Aerodynamic Forces

The results of the previous sections will now be employed to calculate the generalized aerodynamic forces required in the panel flutter analysis.

(a) Simply supported case.

Assume that the plate deflection surface may be represented by the following series

$$Y(x) = \sum_{m=1}^{N} A_m \sin \frac{m\pi x}{2}. \tag{1.7}$$

Each term of the series satisfies the simply supported boundary conditions at $x = 0$, $x = 2$.

The nth generalized force $Q_n^{(s)}$ is given by:

$$Q_n^{(s)} = -\int_0^2 p_a(x, o^+, t) \sin \frac{n\pi x}{2} \, b \, dx. \tag{1.8}$$

The expression for the pressure is of the form

$$p_a = \int_0^x f(x, \xi) d\xi$$

and the expression for $Q_n^{(s)}$ is of the form

$$Q_n^{(s)} = -\int_0^2 g(x) \left[\int_0^2 f(x, \xi) d\xi \right] dx.$$

An examination of the integrands shows that it would be advantageous to integrate with respect to x first. This may be done by interchanging the order of integration by applying Dirichlet's formula which states:

$$\int_0^2 dx \int_0^x g(x) \, f(x, \xi) d\xi = \int_0^2 d\xi \int_\xi^2 g(x) \, f(x, \xi) dx.$$

Carrying out this procedure and integrating with respect to x we find that

$$Q_n^{(s)} = \frac{-\rho U^2 e^{i\omega t}}{\sqrt{2\pi k i M^2}} \left(\sum_{m=1}^{N} T_{mn}^{(s)} A_m \right) \tag{1.9}$$

where

$$T_{nn}^{(s)} = \left[\frac{C_7^{(n)}}{2\sqrt{\theta}} \int_0^{2\theta} \tilde{J}(t)dt + \frac{C_8^{(n)}}{2\sqrt{\delta}} \int_0^{2\delta} J(t)dt + \frac{i\sqrt{2}\, C_9^{(n)}}{4} \right]$$

$$T_{mn}^{(s)} = \frac{1}{i\sqrt{2\pi}} \left[\frac{C_1^{mn}}{2\sqrt{\alpha}} \int_0^{2\alpha} \tilde{J}(t)dt + \frac{C_2^{mn}}{2\sqrt{\beta}} \int_0^{2\beta} J(t)dt \right.$$

$$\left. + \frac{C_3^{mn}}{2\sqrt{\delta}} \int_0^{2\delta} J(t)dt + \frac{C_4^{mn}}{2\sqrt{\theta}} \int_0^{2\theta} \tilde{J}(t)dt. \right]$$

and

$$\tilde{J}(t) = J_{-1/2}(t) - i\, J_{1/2}(t); \quad J_{-1/2}(t) = \left(\frac{2}{\pi t}\right)^{1/2} \cos t$$

$$J(t) = J_{-1/2}(t) + i\, J_{1/2}(t); \quad J_{1/2}(t) = \left(\frac{2}{\pi t}\right)^{1/2} \sin t$$

The $J_{\pm 1/2}(t)$ are Bessel functions of order $\pm 1/2$. The coefficients $T_{mn}^{(s)}$ satisfy the relationship

$$T_{mn}^{(s)} = (-1)^{m+n}\, T_{nm}^{(s)}.$$

The expression (1.9) for the generalized force is of a particularly convenient form. For given m, n the $T_{mn}^{(s)}$ depend only upon k. Tables of the Fresnel integrals appearing in equation (1.9) are available (see for example Ref. 16). The expressions for the coefficients C_i^{mn} appearing in the $T_{mn}^{(s)}$ are given in Appendix B. The limits of integration that appear above are $2\alpha = m\pi + k$; $2\theta = n\pi + k$; $2\beta = m\pi - k$, $2\delta = n\pi - k$.

(b) Clamped edge case.

The generalized force expression is developed for the case when the plate deflection surface is represented by a series of Iguchi functions:

$$Y(x) = \sum_{m=1}^{N} A_m F_m(x), \tag{1.10}$$

where

$$F_m(x) = \frac{x}{2}\left(\frac{x}{2} - 1\right)^2 + (-1)^m \frac{x^2}{4}\left(\frac{x}{2} - 1\right) - \frac{1}{m\pi} \sin\frac{m\pi x}{2}.$$

Each term of the series satisfies the clamped edge boundary conditions at $x = o$, $x = 2$.

The nth generalized force is

$$Q_n^{(c)} = -\int_o^2 p_a(x, o^+, t)\, F_n(x)\, b\,dx,$$

where $F_n(x)$ is the nth Iguchi function.

Proceeding as before we find that

$$Q_n^{(c)} = \frac{-\rho U^2 e^{i\omega t}}{\sqrt{2\pi k i M^2}} \left[\sum_{m=1}^{N} T_{mn}^{(c)} A_m \right], \tag{1.11}$$

where the $T_{mn}^{(c)}$ (are functions of m, n, and k satisfy the relation

$$T_{mn}^{(c)} = (-1)^{m+n} T_{nm}^{(c)}.$$

These coefficients are more lengthy than the coefficients appearing in the simply supported case. Their explicit forms are given in Appendix B.

2.1.4. Panel Flutter Analysis

The flutter of a thin elastic plate exposed to a uniform two-dimensional transonic stream over its upper surface is considered. The plate is of infinite span and is attached to a rigid wall at its leading and trailing edges. The plate is initially flat and lies flush with the surface of the wall (see Figure 1). The air below the plate is still and is assumed to be vented to the free stream static pressure. Acoustic pressures developed on the lower surface of the plate are neglected. The structural or internal damping of the plate material is also neglected. If flutter exists, then the plate will oscillate harmonically under the action of the aerodynamic pressures developed by its motion. It is assumed a priori that the reduced frequency $k(k = \frac{\omega b}{U})$ is such that the linearized aerodynamics developed in the previous sections may be used. The deflection surface of the mid-plane of the plate is represented by a series of functions satisfying the plate boundary conditions. The flutter analysis is undertaken using the Lagrange equation of motion.

(a) Simply supported panels.

Let $Z_a(x, t)$ denote the deflection surface of the mid-plane of the panel. It is assumed that $Z_a(x, t)$ may be expressed as

$$Z_a(x, t) = \sum_{m=1}^{N} A_m(t) \sin\frac{m\pi x}{2}, \qquad (1.12)$$

where the $A_m(t)$ are regarded as generalized co-ordinates. Each term in the above series satisfies the simply supported boundary conditions. Let N_x denote the mid-plane force/per unit width in the panel. (N_x is taken to be constant). Under the assumptions of the small deflection plate theory, the strain energy of the plate is expressed as

$$V = \frac{D}{2}\int_0^{2b} \left(\frac{\partial^2 Z_a}{\partial \bar{x}^2}\right)^2 d\bar{x} + \frac{N_x}{2}\int_0^{2b} \left(\frac{\partial Z_a}{\partial \bar{x}}\right)^2 d\bar{x},$$

where $D = \frac{Eh^3}{12(1-\nu^2)}$ and N_x denotes the mid-plane force/unit width in the panel. The kinetic energy T of the plate may be written as

$$T = \frac{\rho_s h}{2}\int_0^{2b} \left(\frac{\partial Z_a}{\partial t}\right)^2 d\bar{x},$$

where ρ_s denotes the density of the plate material. The Lagrange equation of motion for a system that is describable by N generalized co-ordinates (A_1, A_2, ... A_N) is

$$\frac{d}{dt}\left(\frac{\partial T}{\partial \dot{A}_n}\right) + \frac{\partial V}{\partial A_n} = Q_n^{(s)}, \qquad (n = 1, 2, \ldots . N) \qquad (1.13)$$

where $Q_n^{(s)}$ is the nth generalized force and $\dot{A}_n$ denotes the time derivative of A_n. We now substitute the series (1.12) into the expressions for the kinetic and strain energy of the plate. The results

of this substitution are then introduced into equation (1.13) and the indicated differentiations are performed. We now assume that the plate motion is harmonic and write

$$A_m(t) = A_m e^{i\omega t}, \qquad (m = 1, \ldots N)$$

where the A_m are constants. Finally, we substitute equation (1.9) into the Lagrange equation. The system of equations (1.13) is then written as

$$\left[-4k^2 + k_o^2 \left\{ n^4 + n^2 S \right\} \right] A_n = \frac{-2}{\mu \sqrt{2\pi k i M^2}} \left[\sum_{m=1}^{N} A_m T_{mn}^{(s)} \right] \qquad (1.14)$$

$$(n = 1, 2, .. N)$$

where

$$k_o^2 = \frac{\pi^4}{4b^2 U^2} \left(\frac{D}{\rho_s h} \right), \qquad \mu = \frac{\rho_s h}{2\rho b}, \qquad S = \frac{4N_x b^2}{n^2 D}.$$

In the matrix form the equations (1.14) may be expressed as

$$\left[\mathcal{D}(k, M, \mu, k_o, S) \right] \begin{bmatrix} A_1 \\ \vdots \\ A_n \end{bmatrix} = \begin{bmatrix} 0 \\ \vdots \\ \vdots \end{bmatrix} \qquad (1.15)$$

For a non-trivial solution the determinant $\left| \mathcal{D}(k, M, \mu, k_o, S) \right|$ must vanish. The determinant is generally complex valued. The vanishing

of the real and imaginary parts of this determinant yields two equations from which two of the parameters may be determined after the remaining parameters have been specified.

(b) Clamped edge panels.

The plate deflection surface is assumed describable by a series of Iguchi functions.

$$Z_a(x,t) = \sum_{m=1}^{N} A_m(t)\, F_m(x). \tag{1.16}$$

Each term of this series satisfies the clamped edge boundary conditions at $x = o$, $x = 2$.

Taking the first two terms of (1.16) and proceeding as before, we find that the equations of motion reduce to the form

$$\left[-4k^2 + k_o^2 \left\{ 1 - \pi^2 S \left(\frac{I_{11}^{(2)}}{I_{11}^{(4)}} \right) \right\} \right] A_1 = \frac{-\left\{ A_1 T_{11}^{(c)} + A_2 T_{21}^{(c)} \right\}}{I_{11}^{(o)} \mu \sqrt{2\pi k i M^2}},$$

$$\left[-4k^2 + k_o^2 \left(\frac{I_{11}^{(o)}}{I_{22}^{(o)}} \right) \left(\frac{I_{22}^{(4)}}{I_{11}^{(4)}} \right) \left\{ 1 - \left(\frac{I_{22}^{(2)}}{I_{22}^{(4)}} \right) \pi^2 S \right\} \right] A_2 \tag{1.17}$$

$$= \frac{-\left\{ A_1 T_{12}^{(c)} + A_2 T_{22}^{(c)} \right\}}{\mu I_{22}^{(o)} \sqrt{2\pi k i M^2}},$$

where

$$\mu = \frac{\rho_s h}{\rho(2b)}; \quad k_o^2 = \left(\frac{I_{11}^{(4)}}{I_{11}^{(o)}} \right) \left(\frac{D}{\rho_s h} \right) \frac{1}{4b^2 U^2}; \quad S = \frac{4N_x b^2}{\pi^2 D},$$

and

$$I_{mp}^{(r)} = \int_0^1 F_m(\eta) \frac{d}{d\eta} (F_p(\eta))\, d\eta = (-1)^r I_{pm}^{(r)} .$$

The integrals $I_{mp}^{(r)}$ have been evaluated in Reference 17. Expressed in matrix form the equation (1.17) becomes

$$\begin{bmatrix} & & \\ & (k, M, k_o, \mu, S) & \\ & & \end{bmatrix} \begin{bmatrix} A_1 \\ \\ A_2 \end{bmatrix} = \begin{bmatrix} 0 \\ \\ 0 \end{bmatrix} \qquad (1.18)$$

The flutter conditions are determined as before. It is found to be convenient to specify k, S and M and to solve for $\frac{1}{\mu}$ and k_o. Because $\frac{k_o}{\mu} = \text{constant} \sqrt{(\frac{\rho}{\rho_s})^3 \frac{E}{U^2(1-\nu^2)}}$ it is seen that each panel material and flight condition specifies a hyperbola which intersects the flutter boundaries on the $\frac{1}{\mu}$, k_o plane. The minimum panel thickness ratio may be determined from this intersection.

2.1.5. Numerical Calculations and Conclusions

Calculations were undertaken for a two mode analysis of a simply supported panel exposed to a sonic airstream ($M = 1$). The plate was assumed to have zero mid-plane stress and the deflection surface was represented by the first two terms of the series (1.12). The numerical procedure was as follows: a value of k was assumed, the coefficients $T_{mn}^{(s)}$ were computed and then the flutter determinant was solved for the corresponding values of $\frac{1}{\mu}$ and k_o. The reduced frequency k was varied from 0.001 to 1.5. No real-valued roots of of the mass parameter $\frac{1}{\mu}$ or the stiffness parameter k_o were

obtained for real k, leading to the conclusion that harmonic oscillations at these reduced frequencies were not possible (at least to this order of approximation). The variation of $\left| \mathrm{Im} \frac{1}{\mu} \right|$ and $\left| \mathrm{Im}\, k_o \right|$ with k is shown in Figure 16 where it is seen that $\left| \mathrm{Im} \frac{1}{\mu} \right|$ increases with increasing k and $\left| \mathrm{Im}\, k_o \right|$ decreases with increasing k. To further investigate the nature of the solution, the determinantal equation was expanded for large k. The Fresnel integrals appearing in the coefficients $T_{mn}^{(s)}$ were replaced by their asymptotic expansions. Terms of $0(\frac{1}{k^{3/2}})$ were neglected. The generalized forces $Q_1^{(s)}$, $Q_2^{(s)}$ then reduce to the form

$$Q_n^{(s)} = \frac{-\rho U^2 e^{i\omega t}}{\sqrt{\pi i M^2}} \left[(-1)^n \frac{4}{3} A_n + ik A_m + 0(\frac{1}{k^{1/2}}) \right] \quad (n = 1, 2).$$

The determinantal equation becomes

$$16(ik)^4 + \frac{16}{\mu}(ik)^3 + (ik)^2 \left\{ 68k_o^2 + \frac{4}{\mu^2} \right\} + ik \left\{ \frac{34 k_o^2}{\mu} \right\} + 16 k_o^4 = 0.$$

If $k_o \sim 0(k)$, $\frac{1}{\mu} \sim 0(k)$ then all the terms are of the same order of magnitude. Assuming real k and separating the equation into its real and imaginary parts the following solutions are found.

$$k_o = \frac{k}{2}, \frac{1}{\mu} = 0. \qquad k_o = \pm \left(\frac{16}{34}\right)^{1/2} k.$$

$$k_o = 2k, \frac{1}{\mu} = 0. \qquad \frac{1}{\mu} = \pm 2k \left[\left(\frac{16}{34}\right)^2 - 1 \right]^{1/2}.$$

The first solutions corresponds to vibration in vacuum and are of no interest here. It is seen that $\frac{1}{\mu}$ is imaginary in the second solution

and that the $\left| \text{Im} \frac{1}{\mu} \right|$ increases linearly with k indicating that flutter is not possible at these higher reduced frequencies.

To summarize, the analysis was performed under the restrictions $k \gg \tilde{\delta}^{2/3}$, $k = 0(1)$, $k \gg |M^2 - 1|$, $\tilde{\delta} \ll 1$, and $M \geq 1$. A two mode analysis of a simply supported panel exposed to a sonic airstream was carried through. Solutions of the flutter determinant indicated that harmonic oscillations were not possible at reduced frequencies between 0.001 and 1.5. Examination of the asymptotic form of the determinantal equation for large k revealed no such oscillations (for finite $\frac{1}{\mu}$). It is therefore concluded that, to this degree of approximation, harmonic oscillations of a simply supported plate exposed to a sonic stream are not possible.

Section 2.2. - Two-Dimensional Supersonic Panel Flutter.

2.2.1. General Remarks

The problem of two-dimensional flutter in a supersonic flow is now investigated. This problem has been treated previously by many authors, see for example References 1, 4, 5, 6, 7, 8, 9, 10, 18, and 19. The results of these earlier analyses led to the conclusion that the low supersonic region ($1 < M < 1.5$) was critical for panel flutter and that the simplified aerodynamic theories, such as the quasi-steady and linear piston theories, could not be employed for flutter analysis at these Mach numbers. The purpose of the following analysis is to study the effects of internal damping and initial plate curvature upon the flutter boundaries at the low supersonic Mach numbers. The analysis is undertaken for simply supported panels. The results of the internal

damping study are later employed in conjunction with results from References 1 and 6 (which treated the clamped edge panel in a supersonic stream) to provide flutter boundaries for comparison with the experimental data for "flat" panels. The boundary conditions of the test panels are considered to be intermediate between the simply supported and clamped edge cases and the comparison between theory and experiment will be based upon the assumption that the theoretical flutter boundaries corresponding to the test panels will be intermediate between the boundaries for these two plate conditions. The flutter calculations for the simply supported and clamped edge panels therefore provide the two limiting cases against which the experimental results may be compared.

The effect of plate curvature upon the flutter boundaries is greatly reduced by the flexure support employed in the experiments, however, it is of interest to determine the general nature and the order of magnitude of this effect in the low supersonic range. This information is used to estimate the error incurred by neglecting curvature effects in the theoretical flutter calculations that are compared with the experimental data for "flat" panels and is also employed in the discussion of the changes of flutter speed of given test panels that were observed when the test panels exhibited static deflection under the influence of a slightly accelerating flow.

The analysis proceeds as in Section 2.1. under the assumptions of linearized irrotational flow theory and linear plate theory. To simplify the calculations, the linearized aerodynamic pressure expression is approximated under the assumption that $\bar{\omega} = \frac{2kM^2}{(M^2-1)} < 3$.

The flutter boundaries calculated from this simplified result agree very well with the boundaries obtained from more extensive calculations.

2.2.2. Aerodynamic Pressure and Generalized Force

Consider a two-dimensional flat plate embedded in a plane rigid wall and exposed to a uniform supersonic airstream (see Figure 1). When the plate oscillates harmonically the deflection surface may be expressed as

$$Z_a(x, t) = Y(x)e^{i\omega t}.$$

According to the linearized irrotational flow theory, the aerodynamic pressure acting upon the upper surface of the plate is

$$p_a(x, o^+, t) = \frac{\rho U^2 e^{i\omega t}}{b\sqrt{M^2-1}}\left[\frac{dY}{dx} + ik\frac{(M^2-2)}{(M^2-1)}Y(x) + \frac{k^2}{(M^2-1)^2}\int_o^x Y(x)e^{-\frac{i\bar{\omega}(x-\xi)}{2}}F(x-\xi)d\xi\right], \tag{2.1}$$

where

$$F(x) = -\frac{(M^2+2)}{2}J_o\left(\frac{\bar{\omega}x}{2M}\right) + \frac{M^2}{2}J_2\left(\frac{\bar{\omega}x}{2M}\right) + 2iMJ_1\left(\frac{\bar{\omega}x}{2M}\right)$$

and

$$\bar{\omega} = \frac{2kM^2}{(M^2-1)}, \qquad k = \frac{\omega b}{U}, \qquad x = \frac{\bar{x}}{b}, \qquad \xi = \frac{\bar{\xi}}{b}.$$

The J_n are Bessel functions of the first kind.

The first two terms in equation (2.1) constitute the quasi-steady aerodynamic theory. The third term is essential for supersonic flutter analysis at Mach numbers less than 1.5. Luke (Ref. 18) has shown that the kernel $F(x)$ may be expressed as

$$F(x) = \sum_{r=1}^{q} \frac{1}{q} \left[2iM \cos\left(\frac{2r-1}{4q}\right)\pi \cdot \sin\left(x \cos\left(\frac{2r-1}{4q}\right)\pi\right) - \left\{ 1 + \cos^2\left(\frac{2r-1}{4q}\right)\pi \right\} \cos\left(x \cos\left(\frac{2r-1}{4q}\right)\pi\right) \right] + E_q, \tag{2.2}$$

where the remainder term E_q is

$$E_q = -2(M^2+1)J_{4q}(x) - \frac{M^2}{2}\left\{ J_{4q}(x) - 2J_{4q}(x) + J_{4q+2}(x) \right\} + 2iM \left\{ - J_{4q+2}(x) + J_{4q+1}(x) \right\}.$$

This result may be employed to approximate the kernel $F(x)$ by a sum of trigonometric functions. The $J_n(x)$ are Bessel functions of the first kind. For a limited range of the argument x, the $q = 1$ approximation from the above result may be improved upon by using

$$F_1(x) = \left[- \frac{(M^2+2)}{2} \cos\left(\frac{\pi x}{d_1}\right) + 2(\max J_1)\, iM \sin\left(\frac{\pi x}{d_2}\right) \right] \tag{2.3}$$

The coefficients d_1, d_2 are obtained by fitting $F_1(x)$ to $F(x)$ at the two lowest values of x where real $F(x)$ and $\frac{d}{dx}$ (Im $F(x)$) vanish respectively.

Thus

$$d_1 = 2u^* \quad \text{where } u^* \text{ is the first root of } -\frac{(M^2+2)}{2}J_o(u)+\frac{M^2}{2}J_2(u) = 0$$

and $d_2 = 2u^{**}$ where u^{**} is the smallest value of u for which $J_1(u)$ attains a relative maximum. The approximation (2.3) is employed hereafter in the flutter analysis and good results are expected for $\bar{\omega} < 3$. The flutter frequencies of interest for the plates under consideration are such that this condition is easily met when the flow Mach number is bounded away from unity.

Substituting equation (2.3) into equation (2.1) we find

$$p_a(x, o^+, t)= \frac{\rho U^2 e^{i\omega t}}{b\sqrt{M^2-1}}\left[\frac{dY}{dx}+\frac{(M^2-2)}{(M^2-1)}ikY(x)+\frac{k^2}{(M^2-1)^2}\int_o^x Y(\xi)F_2(x-\xi)d\xi\right], \tag{2.4}$$

where

$$F_2(x) = -\frac{(M^2+2)}{4}\left[e^{iW_1x}+e^{iW_2x}\right]+M(\max J_1)\left[e^{iW_3x}-e^{+iW_4x}\right]$$

and

$$W_{1,2} = \pm\frac{\bar{\omega}}{2M}\left[\frac{\pi}{d_1}\mp M\right], \qquad W_{3,4} = \pm\frac{\bar{\omega}}{2M}\left[\frac{\pi}{d_2}\mp M\right].$$

When the panel under consideration has simply supported boundary conditions the deflection surface may be represented by

$$Z_a(x, t) = \sum_{m=1}^{N} A_m(t)\sin\frac{m\pi x}{2}. \tag{2.5}$$

$$Q_n^{(s)} = -\int_0^2 p_a(x, o^+, t) \sin \frac{n\pi x}{2} \, b dx. \qquad (2.6)$$

Substituting equation (2.5) into equation (2.4) and then carrying out the integration in equation (2.6), we find

$$Q_n^{(s)} = -\frac{\rho U^2 e^{i\omega t}}{\sqrt{M^2 - 1}} \left(\sum_{m=1}^{N} C_{mn}^{(s)} A_m \right). \qquad (2.7)$$

The coefficients $C_{mn}^{(s)}$ are functions of k, M, m, and n. They satisfy the relationship

$$C_{mn} = (-1)^{n+m} C_{nm}.$$

The complete expressions for these coefficients are given in Appendix B.

2.2.3. Panel Flutter Analysis

The flutter analysis proceeds in exactly the same manner as in the transonic case. The plate deflection surface is assumed describable by a small number of generalized coordinates, the kinetic and strain energy of the plates are determined in terms of these co-ordinates and using the result (2.7) for the generalized force the Lagrange equations of motion are employed to calculate the flutter boundaries.

The only difference in the analyses, apart from the aerodynamic terms, arises from the inclusion of two effects that were previously ignored. The first of these concerns the influence of internal damping, imherent in the plate, upon the flutter boundaries. As mentioned in the Introduction the vibrations of plates in still air are found to be

positively damped and part of the energy dissipation arises from sources in the plate itself, in particular from internal friction due to motion and from heat conduction across the plate thickness arising from the straining of the plate elements. The complete damping process will be very complicated but a simple means of introducing damping into the analysis is provided by the use of the structural damping coefficient g. The stiffness parameter k_o^2 is simply replaced by $k_o^2(1 + ig)$, where the extra term represents a damping force proportional to the amplitude of motion and in phase with the velocity. This damping coefficient is independent of frequency and in practice the damping will be dependent upon frequency, however it will be remembered that the flutter frequencies in the experiments varied only slightly from their still air values so that the inclusion in the analysis of values of "g" determined from still air tests upon the models should be realistic.

The second effect treated in this analysis is of geometric origin. The question has arisen as to whether some small initial curvature of the panel will affect the flutter boundaries. This problem has been investigated by Yates and Zeijdel (Ref. 20) at Mach numbers 1.5 and 2.0, where it was found that a specified initial plate curvature was destabilizing up to some critical value of the curvature. This analysis simply extends the treatment to the low supersonic range. As mentioned previously, the effect of small initial curvature arises from the development of mid-plane stresses. Employing the boundary conditions of no horizontal motion of the plate boundaries it can be shown that a

mid-plane stress develops that is proportional to the integral of the perturbation displacement over the plate chord. The provision of a flexure support, specifically for the prevention of mid-plane stress development, therefore renders the test panels considerably less sensitive to any curvature effects. For the purpose of the analysis an initial plate deflection of the form

$$Y_1(x) = B_1 \sin \frac{\pi x}{2} \tag{2.8}$$

is assumed. The amplitude of the initial surface is restricted so that

$$(\frac{dY_1}{dx})^2 << 1.$$

Assuming that the deflection surfaces of the plates are describable by the two generalized co-ordinates so that

$$Y(x) = A_1 \sin \frac{\pi x}{2} + A_2 \sin \pi x, \tag{2.9}$$

the equation of motion, including the effects of structural damping and a specified initial curvature but assuming no applied mid-plane stresses, may be written as

$$\left[-4k^2 + k_o^2 (1 + ig)(1 + 6B_1^2 \frac{1}{h^2})\right] A_1 = \frac{-2}{\mu\sqrt{M^2-1}} \left[A_1 C_{11}^{(s)} + A_2 C_{21}^{(s)}\right]$$

$$\left[-4k^2 + 16 k_o^2 (1 + ig)\right] A_2 = \frac{-2}{\mu\sqrt{M^2-1}} \left[A_1 C_{12}^{(s)} + A_2 C_{22}^{(s)}\right] \tag{2.10}$$

The flutter boundaries are determined in the same manner as in the transonic panel flutter analysis.

2.2.4. Numerical Calculations

Flutter boundaries were first determined for initially flat panels at Mach numbers 1.2, 1.3, $\sqrt{2}$, and 1.56. The deflection surface of the panels were assumed describable by the first two terms of the series (2.5). The effects of acoustic radiation, structural damping and mid-plane stress were neglected. The boundaries obtained compare favorably with the results of more extensive computations (see for example Figure 17). The flutter boundaries presented in Figure 18 are for brass panels exposed to an airstream with constant sea level stagnation conditions. The lower frequency or "first mode" boundary exhibits a peak at about $M = 1.26$. The higher frequency or "second mode" boundary is present at Mach numbers less than 1.5 and is critical in the neighborhood of $M = \sqrt{2}$. A discontinuity in the slope of the stability boundaries appears where the boundaries corresponding to each of these different modes intersect. A similar discontinuity also appeared in the modal analysis of a clamped edge plate reported in Reference 6 and was suggested by the authors to be due to a change of flutter mode. A more extensive analysis by Fung (Ref. 1) failed to reveal this feature and it was suggested that the discontinuity could be due to the small number of modes employed in the analysis of Reference 6. However, the calculations presented in Reference 1 were undertaken for values of the reduced frequency k up to 0.45. The critical "second mode" flutter of Reference 6 involves values of k of the order of 0.7 and above. The

non-appearance of the critical "second mode" flutter boundary in the analysis of Reference 1 is therefore due to the small values of k employed in the calculations. The good agreement between the first mode boundaries calculated in References 1 and 6 indicates that the approximate method of analysis converges satisfactorily and that reasonable predictions may be obtained for the critical flutter boundaries of flat panels, with zero mid-plane stress, when employing a two-mode flutter analysis (i.e. the stiffness requirements predicted by the two mode analysis are expected to be only slightly affected by the inclusion of more terms in the analysis).

The effect of structural damping upon the flutter boundaries was next investigated. Calculations employing values of the structural damping coefficient g up to 0.05 were undertaken at Mach numbers 1.2. and 1.3. The results for $M = \sqrt{2}$ were estimated from Reference 6. The inclusion of structural damping has a very marked effect upon the flutter boundaries in the low supersonic region. The "second mode" boundary disappears completely for sufficiently large values of g and the thickness ratio requirements of the lower frequency flutter mode are reduced considerably from the values corresponding to zero structural damping (see Figure 19).

The effect of a specified initial curvature upon the panel flutter phenomenon in the low supersonic region was studied at $M = 1.3$. It has been shown by Yates and Zeijdel (Ref. 17) that at the higher Mach numbers ($M \geq 1.5$) a specified constant initial curvature will be destabilizing up to some critical value of the curvature. At this critical value the first and second natural frequencies of the plate (in vacuum)

coalesce. A two-mode analysis in the low supersonic region was undertaken at Mach number 1.3. The panel was assumed to have an initial deflection surface in the form of a half sine wave with an amplitude of one plate thickness. Calculations were also made at Mach number 1.56 with the same initial deflection. Structural damping was neglected in both cases. The results of these calculations are presented in Figures 20 and 21. There it is seen that such initial curvature is stabilizing at $M = 1.3$ and destabilizing at $M = 1.56$. It will also be noted that the critical flutter mode has been changed at $M = 1.3$.

The different effects of initial curvature at the two Mach numbers considered is not entirely unexpected because the ideal theory indicates that panel flutter at the higher Mach numbers ($M \geq 1.5$) is associated with a frequency coalescence phenomenon which is not present in the low supersonic region. The form of initial curvature assumed produces an increase in the first natural frequency of the panel (in vacuum) and a reduction in the difference between the first two natural frequencies. This latter effect appears to be the important one for flutter at the higher Mach numbers and is expected to be destabilizing. On the other hand, the most important effect upon flutter in the low supersonic region is probably the increase in the fundamental plate frequency which may be regarded as a stiffening influence. It should also be remarked that the presence of sufficient structural damping should prevent the change of critical flutter mode at Mach number 1.3.

The first mode thickness ratio requirements $(\frac{h}{2b})$ at M = 1.3, for panels representative of the experimental conditions, are found to be reduced by about 40 per cent from the results for perfectly flat panels. This reduction in the thickness ratio requirement is due to the development of mid-plane stresses in the panels. The development of such stresses in the test panels is greatly reduced by the presence of the flexure support at the trailing edge of these panels. The flexure support will therefore reduce the structural effect of any initial curvature upon the flutter boundaries. A rough estimate of the effectiveness of the flexure in this respect may be obtained by comparing the mid-plane stresses developed in a deformed panel when first assuming that the leading and trailing edges of the panel are fixed and secondly considering the case where the leading edge of the panel is fixed and the trailing edge is mounted upon a flexure support. For a given deformation of the plate the mid-plane stress developed by the second configuration may be expressed as $Rx(\sigma_x)_f$, where $(\sigma_x)_f$ denotes the mid-plane stress developed when the plate is assumed to have fixed edges and R denotes a relief factor $(R < 1)$. The term appearing in the flutter equations of motion (equation 2.10), that represents the effect of initial curvature, contains the mid-plane stress and is therefore also expected to be reduced by the factor R when account is taken of the flexure support. This reduction may be expressed by using $\sqrt{R}\ B_1$ as an "effective" amplitude of the specified initial deflection, i.e. the amplitude of a specified initial deflection B_1 of a panel with a flexure support would correspond to an effective amplitude of $\sqrt{R}\ B_1$ for a similar panel with fixed leading and trailing edges.

The value of R corresponding to the experimental conditions is of the order of 4×10^{-4}.

The experimental flutter boundaries for "flat" panels that are presented in Figure 15 were obtained for test panels where the measured amplitudes of static deflection of the panels were less than one plate thickness. The effective amplitudes of these panels, insofar as the structural effect of plate curvature upon the flutter boundaries is concerned, are therefore of the order of 0.02h (where h denotes the plate thickness). A few calculations were made at $M = 1.3$, using such effective amplitudes, and it was found that the inclusion of this effect produced less than 1 per cent change of the flutter boundaries from the results for perfectly flat panels. Changes of the same order of magnitude are expected at the other Mach numbers in the low supersonic range. It is therefore seen that negligible error is incurred when neglecting the appropriate curvature effects in the flutter calculations that are used in comparison with the experimental flutter boundaries for "flat" panels.

Section 2.3. - Analysis of the Energy Transfer at Flutter.

2.3.1. General Remarks

The following section describes an examination of some previous panel flutter investigations that employed the ideal theory. By examining the energy transfer between the airstream and the plate at flutter it is found that considerable light may be thrown upon the phenomenon as described by the idealized theory and that the reason for the breakdown of the quasi-steady aerodynamic theory for panel

flutter analysis in the low supersonic region becomes readily apparent. The energy analysis is effected by examining the flutter modes obtained in the previous investigations of Fung and Houbolt (Ref. 1 and 16 respectively).

2.3.2. Energy Analysis

The aerodynamic pressure expression for supersonic flows (2.1) may be written

$$p_a(\bar{x}, o^+, t) = \frac{\rho U^2}{\sqrt{M^2-1}} \left[\frac{\partial Z_a}{\partial \bar{x}} + \frac{(M^2-2)}{(M^2-1)} \frac{1}{U} \frac{\partial Z_a}{\partial t} + I \right], \tag{3.1}$$

where $Z_a(\bar{x}, t)$ denotes the deflection surface of the plate and I denotes the integral term appearing in (2.1). The rate at which work is done by the plate against the aerodynamic pressure is

$$\frac{d}{dt} E = -\int_o^{2b} p_a(\bar{x}, o^+, t) \frac{\partial Z_a}{\partial t} d\bar{x}, \tag{3.2}$$

where E denotes the sum of the kinetic and strain energy of the plate. For harmonic oscillations the deflection surface is expressed as

$$Z_a(\bar{x}, t) = Y(\bar{x}) \cos (\omega t + \psi(\bar{x})).$$

The contribution in (3.2) from the $\frac{\partial Z_a}{\partial \bar{x}}$ term arising in equation (3.1) is

$$\frac{-\rho U^2 \omega}{\sqrt{M^2-1}} \left[\int_o^{2b} (Y(\bar{x}) \sin (\omega t + \psi))^2 \frac{d\psi}{d\bar{x}} d\bar{x} - \right.$$

$$\left. \int_o^{2b} Y(\bar{x}) \frac{dY}{d\bar{x}} \sin(\omega t + \psi) \cos (\omega t + \psi) d\bar{x} \right]$$

The contribution to (3.2) from the $\frac{\partial Z_a}{\partial t}$ term in (3.1) is

$$-\frac{\rho U(M^2-2)\,\omega^2}{(M^2-1)^{3/2}} \int_0^{2b} \left[Y(\bar{x}) \sin\left(\omega t + \psi(\bar{x})\right)\right]^2 d\bar{x}.$$

Writing $\lambda = \omega t + \psi(\bar{x})$, equation (3.2) may be expressed as

$$\frac{d}{dt}E = -\frac{\rho U^2 \omega}{\sqrt{M^2-1}} \left[\int_0^{2b} \left[Y(\bar{x}) \sin\lambda \right]^2 \frac{d\psi}{d\bar{x}}\, d\bar{x} - \int_0^{2b} Y \frac{dY}{d\bar{x}} \sin\lambda\cos\lambda\, d\bar{x} \right.$$

$$\left. -\frac{\omega(M^2-2)}{U(M^2-1)} \int_0^{2b} (Y(\bar{x}) \sin\lambda)^2\, d\bar{x} + \tilde{I} \right],$$

where $\tilde{I}$ denotes the contribution from the integral term I that appears in the aerodynamic pressure expression. The results of Fung (Ref. 1) and Houbolt (Ref. 19) indicate that $\psi(\bar{x})$ is a monotonic function of $\bar{x}$ (See Figure 22). Using the mean value theorem and the monotonic nature of $\psi(\bar{x})$ the first term in the above expression may be written

$$\int_0^{2b} \left[Y(\bar{x}) \sin\lambda \right]^2 \frac{d\psi}{d\bar{x}}(\bar{x})\, d\bar{x} = \frac{d\psi}{d\bar{x}}(\bar{x}^*) \int_0^{2b} \left[Y(\bar{x}) \sin\lambda \right]^2 d\bar{x},$$

where $(0 \leq \bar{x}^* \leq 2b)$.

Employing this result and integrating $\frac{d}{dt}E$ over one period T of the flutter motion, we obtain

$$E(t+T)-E(t) = \frac{-\rho U^2 \omega}{\sqrt{M^2-1}} \left[\int_t^{t+T} \hat{I}\, dt + \right.$$

$$\left. \left\{ \frac{d\psi}{d\bar{x}}(\bar{x}^*) - \frac{(M^2-2)}{U(M^2-1)} \right\} \int_t^{t+T} dt \int_0^{2b} (Y(\bar{x}) \sin\lambda)^2 \, d\bar{x} \right]$$

At the flutter boundary the net exchange of energy between the panel and the flow must vanish. Hence

$$E(t+T) - E(t) = 0$$

The results of Reference 1 indicate that in the low supersonic region

$$\frac{d\psi}{d\bar{x}}(\bar{x}^*) \approx \frac{\Delta\psi}{2b},$$

where $\Delta\psi$ is the change of ψ over the panel chord. Letting R_T denote the energy contribution over one cycle of the motion from the $\frac{\partial Z_a}{\partial t}$ term in the aerodynamic pressure, R_x denote the $\frac{\partial Z_a}{\partial \bar{x}}$ contribution and R_I the integral term contribution, then employing data from Reference 1 the following table may be constructed to evaluate the relative importance of these three terms insofar as the flutter process is concerned.

M	R_T	R_x	R_I	$\frac{R_I}{R_x}$
1.1	-1.56	0.3	1.26	4.24
1.2	-0.657	0.07	0.587	8.49
1.3	-0.214	0.027	0.187	6.84
1.4	-0.0062	0.0052	0.001	0.19

Although the values given in the above table are approximate they clearly indicate the importance of the integral term I for the flutter process in the low supersonic region. It is seen that at Mach numbers 1.1, 1.2, and 1.3, this term provides the major stabilizing factor to balance the influence of the $\frac{\partial Z_a}{\partial t}$ term, which is destabilizing at Mach numbers less than $\sqrt{2}$. The term becomes relatively more important as the Mach number is increased above 1.2, but it is completely dominated by the integral term at Mach numbers less than 1.4 (see Figure 23). The small contribution of the $\frac{\partial Z_a}{\partial \bar{x}}$ term to the energy exchange lies in the fact that although the magnitude of this term may be large compared to the other terms, the phase shift in the flutter mode at the low supersonic Mach numbers is so small that relatively little energy contribution is provided. Herein lies the reason for the failure of the approximate quasi-steady aerodynamic theory which neglects the integral term and retains the other two contributions. At the low supersonic Mach numbers the $\frac{\partial Z_a}{\partial t}$ term, which is destabilizing for $M < \sqrt{2}$,

cannot be balanced by the $\frac{\partial Z_a}{\partial \bar{x}}$ term alone, which fact leads to the unhappy conclusion of Reference 4 that all panels are unstable in a supersonic flow with Mach number less than $\sqrt{2}$.

The success of the approximate aerodynamic theories at high Mach numbers ($M > 1.6$) is readily apparent when the flutter modes in this region are studied. Examination of the results of Reference 19, wherein the linear piston theory is employed for the aerodynamic pressure, reveals that the flutter mode at high Mach numbers exhibits a considerable amount of phase shift (see Figure 22) which in this instance is destabilizing. The flutter boundary is obtained when the out of phase contribution from the $\frac{\partial Z_a}{\partial \bar{x}}$ term balances the damping term $\frac{\partial Z_a}{\partial t}$. Unlike the phenomenon in the low supersonic region such a flutter mechanism is adequately described by the approximate aerodynamic theories.

It is also instructive to examine the significance of the various terms in the aerodynamic pressure expression (2.1) now that their relative importance in the flutter process has been assessed. The integral term, which plays such an important role in the low supersonic region, represents the influence, at a given point along the chord and at a given time, of the disturbances produced at earlier times upstream of this point. These disturbances propagate through the fluid and are convected with the supersonic stream over the panel. For such "almost in phase" mode shapes exhibited in the low supersonic region it thus appears that the phase shifts between aerodynamic pressure and plate displacement introduced by such a convection process are of extreme importance in the flutter problem at these Mach numbers.

The remaining terms in the aerodynamic pressure are what might be termed "local", i.e. their contribution to the pressure at a point is governed entirely by the conditions of the plate surface at that point only. The phase shifts that arise in this case are due to the character of the plate motion. The $\frac{\partial Z_a}{\partial x}$ term will have no contribution to the energy exchange if there is no phase shift in the plate mode. The contribution from the other term (the $\frac{\partial Z_a}{\partial t}$ term) is always out of phase. Whether this term is stabilizing or destabilizing depends entirely upon the supersonic flow Mach number.

PART III

THE COMPARISON OF THEORY AND EXPERIMENT

3.1. General Remarks

The experimental results are now compared with the predictions of the ideal theory. The comparison is made in the low supersonic flow region between Mach numbers 1.15 and 1.5 and is based upon the assumption that the theoretical flutter boundaries corresponding to the test panels will be intermediate between the flutter boundaries calculated for the limiting cases of clamped edge and simply supported panels. The experimental flutter boundaries employed in the comparison are those corresponding to the "flat" panel results.

The changes of flutter speed that were noted when the test panels exhibited static deflection (see Figure 15) are discussed. The theory is examined in order to determine whether there is any possible theoretical explanation of this phenomenon.

The results of the transonic panel flutter analysis are discussed in the light of the experimental data.

3.2. Comparison of the Flutter Boundaries

Direct comparison of the experimental flutter boundaries for "flat" panels with the theoretical predictions is not possible because no flutter calculations have been undertaken for panels with boundary conditions corresponding to those of the test panels. These boundary conditions being considered to be clamped at the leading edge and partially restrained (against rotation) at the trailing edge. The predicted

flutter boundaries for such panels are assumed to be intermediate between the boundaries calculated for simply supported and clamped edge panels and the experimental results are compared against these two limiting cases. For these calculations to be representative of the experimental conditions it is necessary that realistic values of the structural damping be included in the analysis. Experimental determination of the damping coefficient for three different test panels yielded values of 0.0095, 0.010 and 0.012. The calculations employed in the comparison were therefore undertaken for $g = 0.01$, which value is considered to be representative of the experimental conditions. It should be noted that this value of g will be conservative because the measured damping coefficients arise from both internal and acoustic sources of damping. The effects of mid-plane stress and initial plate durvature are not included in the flutter calculations used in the comparison with the "flat" panel data.

The "flat" panel flutter boundary from Figure 15 is shown in Figure 24 together with theoretical flutter boundaries calculated from two mode analyses of simply supported and clamped edge panels. It is immediately seen that although the experimental and predicted flutter boundaries exhibit the same general trend, namely increased stiffness requirements in the low supersonic region, the magnitude of the respective requirements may differ appreciably. The difference is particularly pronounced at Mach numbers less than about 1.4. The theoretical predictions are seen to be conservative in this region, the maximum predicted thickness requirements being of the order of two to three times the experimental value. Agreement between theory and

and experiment appears to improve as the Mach number increases. This trend towards better agreement at the higher Mach number is further supported by the results of some flat panel flutter tests carried out at a Mach number of 2.81 by Anderson. These experiments are reported upon in Reference 22. The pertinent data from these experiments are presented in Table II, where it is seen that the experimental thickness ratio requirements $(\frac{h}{2b})$ at the two-dimensional flutter boundary are between 3 per cent and 18 per cent above the theoretically predicted values.

The large differences between the theoretical and the experimental flutter boundaries that are observed in the low supersonic region do not appear explainable by the inclusion of realistic values of mid-plane stress and plate curvature in the flutter analysis. As mentioned previously in Part I of this paper it is considered that the mid-plane stresses developed in the test panels would be less than 20 psi. The inclusion of such mid-plane stresses in the flutter analysis would produce only small changes in the theoretical predictions from the zero mid-plane stress case and would not explain the large differences in question*. The same conclusion applies to the structural effect of initial curvature upon the flutter boundaries, which is also greatly reduced by the flexure support.

The crucial test of any flutter theory is the comparison of the predicted flutter boundaries with experiment and in this instance it has

---

*The order of magnitude of the effect produced by such stresses may be estimated from the results of Reference 6. It is found that the thickness ratio requirements at $M = 1.3$, for panels similar to the test panels, are reduced by less than 3 per cent with the introduction of a mid-plane stress of 20 psi.

been found that the predicted flutter boundaries are very conservative at supersonic Mach numbers less than about 1.4. However, it should be remarked that certain other features of the flutter phenomenon in this region are predicted quite closely by the ideal theory. In particular the predicted frequency ratios $(\frac{\omega}{\omega_o})$ at flutter are quite close to the experimental results. The difference between the predicted and experimental values being on the order of 10 - 15 per cent. Furthermore the agreement between the measured phase shift and the predicted phase shift in the flutter modes appears to be good. Measurements of the phase shift between the plate flutter motion at points located at 0.22 and 0.65 chord lengths aft of the plate leading edge at Mach numbers of 1.18, 1.31 and 1.34 yielded values of 2.5°, 1°, and 1° respectively. These results compare very closely with values estimated from Reference 1, which are considered to be representative of the theoretical predictions. These findings indicate that the ideal theory can predict the correct flutter mode in the low supersonic region (the non appearance of the critical "second mode" flutter is accounted for by the inclusion of realistic values of structural damping in the analysis) however the predicted stiffness requirements corresponding to this mode can show considerable disagreement with the experimentally determined values and the theory appears to be inadequate for the prediction of these requirements at the lower supersonic Mach numbers.

3.3. Effect of Panel Deflection upon Flutter

A further source of disagreement between theory and experiment arises when the effect of static deflection of the test panels upon

the flutter speed is investigated. It was noticed during the experiments that the flutter speed of a given panel could be altered by causing the test panel to deflect out into the airstream (amplitudes of deflection of the order of 1 1/2 - 3 plate thicknesses). The changes of the flutter speed that were observed were destabilizing in the sense that the region of instability was enlarged from the "flat" panel region of instability (see Figure 15). The static deflection of the panels could be produced by slightly accelerating the airstream over the length of the panel and thereby changing the static pressure distribution over the panel. It was also found that these effects would be accompanied by an increase in the fundamental plate frequency over the frequency that the plate would exhibit, at the same Mach number, when in the "flat" condition.

It is considered most unlikely that the changes in the flutter speed and in the fundamental frequency of the test panels could arise from potential aerodynamic effects. The non-uniformity of the main flow and the perturbations produced by the static deflection are both small and, on the basis of the linear theory, would not affect the unsteady phenomenon. Furthermore, the flutter analysis of Part 2 indicates that the effect of plate curvature and any mid-plane tension introduced by the pressure loading would be stabilizing in this Mach number region and would reduce the region of instability. Although the flexure support greatly reduces the effectiveness of plate curvature and limits the development of mid-plane stresses it is most unlikely that the flexure would change their general effect upon the flutter phenomenon.

It therefore appears that such changes in the flutter speed are not explainable upon the basis of the ideal theory. The increase in the panel frequencies, as opposed to the changes in flutter speed, may however be explainable upon the basis of plate curvature and mid-plane tension.

3.4. Transonic Panel Flutter

The experimental data indicates that the two-dimensional panel flutter phenomenon is limited to the supersonic flow region. No subsonic flutter was observed for any of the panels that were tested. These findings support the results of the transonic flutter analysis which indicated, to the degree of approximation employed in the analysis, that panel flutter was not possible at $M = 1$. The results of this analysis could not be verified directly because of the shock wave interference problem that arose in the experiments at Mach numbers around unity.

3.5. Summary

The results of the preceding discussions may be briefly summarized as follows:

(1) Theory and experiment both indicate that the low supersonic region ($1 < M < 1.5$) is critical for the flutter of two-dimensional flat panels. No subsonic panel flutter was found for any of the panels that were tested, whereas flutter was found at supersonic Mach numbers. This finding supports the results of the transonic analysis, however, the result of this analysis could not be verified directly because of

shockwave interference with the test panels at Mach numbers around unity.

(2) The panel thickness ratio required for the prevention of flutter as predicted by the ideal theory in the low supersonic region is found to be quite conservative compared to the experimental data at Mach numbers less than about 1.4. In particular the maximum thickness ratio requirement as predicted by the theory is of the order of two to three times the experimental value for "flat" panels in the Mach number range 1.15 - 1.35.

(3) The agreement between the experimental and theoretical flutter boundaries improves with increasing Mach number. This trend is further supported by the experimental data presented in Reference 22.

(4) Although considerable disagreement exists between the theoretically predicted stiffness requirements and the experimental data at the lower supersonic Mach numbers, the theory does predict the correct flutter mode at all supersonic Mach numbers.

(5) The changes of flutter speed for a given test panel that were observed in the experiments when the airstream was slightly accelerated over the chord of the test panel and that are believed to be due to the static deflection of the test panels produced by the variable static pressure do not appear explainable by the ideal theory.

Accepting the basis of the above comparisons it appears that the ideal theory is inadequate for flutter predictions in the low supersonic region. The predictions of the theory appear to be more realistic at higher Mach numbers. The results of the theory at $M = 1$

are supported by the experimental data (this does not necessarily imply that the theory is adequate at this Mach number).

It is of considerable interest to examine more closely the results of theory and experiment in order to see if some indication may be obtained of the reasons for the apparent inadequacy of the ideal theory at the low supersonic Mach numbers. In this regard it is of some help that the inadequacy of the theory appears to be particularly acute in a specific flow region. Any feature of the flutter phenomenon that is peculiar to this region would thus be highly suspect and could possibly contain the reasons for the breakdown of the theory. The disagreement between theory and experiment may arise from the following contributing sources:

(1) Certain of the physical assumptions concerning the plate and fluid properties upon which the ideal theory is based, are particularly poor (for the accurate description of the flutter phenomenon) in the low supersonic region.

(2) The linearization of the problem and the approximate means of analysis that were employed to obtain solutions within the framework of the ideal theory have introduced large errors in the low supersonic region.

(3) The conditions of the experiments, against whose results the theory was compared, are poor representations of conditions assumed in the calculation of the flutter boundaries. In particular the representation of two-dimensional conditions and the representation of zero mid-plane stress conditions.

Review of the experimental data and pertinent flutter analyses suggests that the major source of disagreement between theory and experiment arises from the physical assumptions concerning the plate and fluid properties that form a basis for the ideal theory. Many of the factors mentioned in (2) and (3) above have been discussed previously in this paper. There it was considered that good two-dimensional and zero mid-plane stress conditions were obtained in the experiments and that the approximate methods of analysis employed to estimate the theoretical flutter boundaries in the low supersonic region were satisfactory. Although the application of these methods had been a previous source of controversy more exact theoretical analysis had indicated that the application to the flutter of plates (finite bending stiffness) was satisfactory. Furthermore the experimental data gave no indication that the linearization conditions were not satisfied. It should be noted that the severe restriction upon the amplitude of the plate motion (amplitude $\ll$ plate thickness) arises from the linear plate theory and is removed by the presence of the flexure support and is replaced by the requirement that

$$\left| \frac{\partial^2 Z_a}{\partial \bar{x}^2} \right|^{-1} \ll h, \qquad \left| \frac{\partial Z_a}{\partial \bar{x}} \right| \ll 1.$$

These conditions were certainly satisfied throughout the experiments.

The improved agreement between theory and experiment at the higher supersonic Mach numbers indicates that the source of error is dependent upon the flow Mach number. The possibility that the error

arises from the hypotheses concerning the plate properties is considered most unlikely. The experimental data certainly gives no cause to believe that the adequacy of the plate theory employed in the analysis will be dependent upon the flow Mach number. It appears more reasonable that the error arises from the assumptions concerning the fluid properties. The most suspect of these assumptions is that of an inviscid fluid. This assumption greatly simplifies the analysis however, in the process, the description of a flow field in the immediate neighborhood of a solid boundary becomes very poor. This is because the ideal theory takes no account of the boundary layer, which is probably the most important consequence of the fluid viscosity, that will be present over any solid surface. Typical velocity profiles of the boundary layer over the test panel installation have been presented in Figure 4. This boundary layer will be present for all Mach numbers (except the trivial case $M = 0$) and the question arises as to how this layer, assuming that its neglect is the major source of error, should have such a profound effect upon the flutter phenomenon in the low supersonic region whilst having a relatively small effect upon the phenomenon at the higher Mach numbers. A possible answer to this question could come from the results of the analysis of the energy exchange at flutter which is presented in Section 2.3. There it was found that the "non-local" contributions to the aerodynamic pressures acting upon the various points of an oscillating panel play an extremely important role in the flutter phenomenon in the low supersonic region, whereas at the higher Mach numbers the aerodynamic pressures of consequence are of "local" origin (see Section 2.3. for a more detailed

discussion). These flutter mechanisms are of course based upon the ideal theory, however, if such "non-local" and "local" pressure contributions have the same relative importance in the flutter phenomenon in a real fluid then it is conceivable that the boundary layer could have a more pronounced influence upon the phenomenon in the low supersonic region than at the higher Mach numbers. This is because the effect of the "non-local" pressure contributions will depend upon their passage over the plate surface. The description of this process afforded by the ideal theory is that these disturbances will be propagated in the uniform supersonic stream passing over the plate surface. In practice, however, these disturbances will be propagating through the mixed subsonic-supersonic boundary layer and their effect could be considerably different from the ideal theory description. If the aerodynamic pressures of "local" origin were only slightly affected by the presence of the boundary layer these changes in the effect of the "non-local" pressures could account for the inadequacy of the ideal theory in the low supersonic region and the apparent success of the theory at the higher supersonic Mach numbers. The boundary layer effect could provide an explanation of the curious changes of flutter speed that are believed to be due to the static deflection of the test panels (see Figure 15). To seek evidence to support this suggestion some boundary layer profiles were measured over a surface of constant curvature (the radius of curvature was 9.5") to determine whether the curvature of the surface would affect the velocity profile of the layer. Assuming that the boundary layer played an important role in the flutter

phenomenon it is considered that any change of the effect of the layer would be associated with changes in the velocity profile. The results of these measurements are presented in Figure 4 and it will be noted that these latter velocity profiles are noticeably different from the profiles measured over the flat surface.

It should be stressed that the above arguments, although based upon careful review of the theoretical and experimental research, are hypothetical and are included in this paper to suggest a cause for the large differences between theory and experiment that were observed in the low supersonic flow region. To establish the importance of the boundary layer upon the panel flutter phenomenon at these Mach numbers would require the realistic inclusion of the boundary layer effects in the actual prediction of the flutter boundaries*. Furthermore, the argument does not imply that the other factors that were mentioned previously do not contribute to the differences between theory and experiment. These factors are certainly expected to have some contribution, however, the review of the experimental data and pertinent theoretical analysis indicates that such factors are unlikely to produce the large differences that were observed.

*It should be remarked that boundary layer effects have been included in an analysis considering the degree of instability of a traveling wave in an elastic sheet exposed to an airstream (see Ref. 23).

REFERENCES

1. Fung, Y. C.: On Two-Dimensional Panel Flutter. Journal of the Aeronautical Sciences, Vol. 25, No. 3, pp. 145-160 (1958).

2. Isaacs, R. P.: Transtability Flutter of Supersonic Aircraft Panels. Report P-101, The Rand Corp., Santa Monica, Calif., (1949).

3. Hayes, W.: A Buckled Plate in a Supersonic Stream. Report AL-1029, North American Aviation, Inc. (May 10, 1950).

4. Miles, J. W.: Dynamic Chordwise Stability at Supersonic Speeds. Report AL-1140, North American Aviation, Inc. (Oct. 18, 1950).

5. Eisley, J. G.: The Flutter of Simply Supported Rectangular Plates in a Supersonic Flow. Ph. D. Thesis, Guggenheim Aeronautical Laboratory, California Institute of Technology (1955). AFOSR TN 55-236.

6. Nelson, H. C., and Cunningham, H. J.: Theoretical Investigation of Flutter of Two-Dimensional Flat Panels with One Surface Exposed to Supersonic Potential Flow. NACA Report 1280 (1956), (Supersedes NACA TN 3465).

7. Luke, Y. L., Goland, M., and Constant, P. C.: Panel Flutter at Supersonic Speeds. Progress Report, Contract No. AF 33(616)-2897, Midwest Research Institute (1955).

8. Ashley, H., and Zartarian, G.: Piston Theory - A New Aerodynamic Tool for the Aeroelastician. Journal of the Aeronautical Sciences, Vol. 23, No. 12, pp. 1109-1118 (1956).

9. Hedgepeth, J. M.: Flutter of Rectangular Simply Supported Panels at High Supersonic Speeds. Preprint No. 713, Institute of Aeronautical Sciences (1957).

10. Shen, S. F.: Flutter of a Two-Dimensional Simply-Supported Uniform Panel in a Supersonic Stream. Contract No. N5ori-07833, Office of Naval Research, Dept. of Aero. Eng., Massachusetts Institute of Technology (1952).

11. Sylvester, M. A., and Baker, J. E.: Some Experimental Studies of Panel Flutter at Mach Number 1.3. NACA TN 3914 (1957), (Supersedes NACA RM L52116).

12. Dhawan, S.: The Design and Use of a Flexible Nozzle for the GALCIT Transonic Wind Tunnel. Ae. E. Degree Thesis, Guggenheim Aeronautical Laboratory, California Institute of Technology (1949).

13. Warburton, G. B.: The Vibration of Rectangular Plates. Proceedings of the Institution of Mechanical Engineers, Vol. 168, pp. 371-384 (1954).

14. Lin, C. C., Reissner, E., and Tsien, H. S.: On Two-Dimensional Nonsteady Motion of a Slender Body in a Compressible Fluid. Journal of Mathematics and Physics, Vol. 27, pp. 220-231 (1948).

15. Nelson, H. C., and Berman, J. H.: Calculations on the Forces and Moments for an Oscillating Wing-Aileron Combination in Two-Dimensional Potential Flow at Sonic Speed. NACA Report 1128 (1953), (Supersedes NACA TN 2590).

16. Van Wijngaarden, A., and Scheen, W. L.: Table of Fresnel Integrals. Report R49, Computation Dept., Mathematical Centre, Amsterdam (1949).

17. Wittrick, W. H.: Buckling of Oblique Plates with Clamped Edges under Uniform Compression. Aeronautical Quarterly, Vol. 4, pp. 151-163 (1953).

18. Luke, Y. L., and St. John, A.: Supersonic Panel Flutter. WADC Technical Report 57-252 (1957).

19. Houbolt, J. C.: A Study of Several Aerothermoelastic Problems of Aircraft Structures. Doctoral Thesis, Eidgenössische Technische Hochschule, Zurich (1958).

20. Yates, J. E., and Zeijdel, E. F.: Flutter of Curved Panels. AFOSR TR 59-163, Midwest Research Institute (1959).

21. Johns, D. J.: Some Panel Flutter Studies using Piston Theory. Journal of the Aeronautical Sciences, Vol. 25, No. 11, pp. 679-684 (1958).

22. Anderson, W. J.: Experimental Studies of the Flutter of Flat Panels at Mach Number 2.81. Progress Report No. 9, Office of Scientific Research, Contract No. AF 49(638)-220, Appendix A, (1960).

23. Miles, J. W.: On Panel Flutter in the Presence of a Boundary Layer. Journal of the Aero/Space Sciences, Vol. 26, No. 2, pp. 81-93 (1959).

24. Lock, M. H.: The Flutter of Two-Dimensional Flat Panels. Progress Report No. 3, Office of Scientific Research, Contract No. AF 49(638)-220 (1958).

APPENDIX A

PHYSICAL SIGNIFICANCE OF THE TRANSONIC AERODYNAMIC THEORY

It is of some interest to seek the physical significance of the unsteady transonic aerodynamic theory that was employed in Part I, particularly in light of the failure of the linearized aerodynamic theory in the steady flow case ($k = o$) at these Mach numbers. An insight into the significance of the theory may be obtained by developing the theory from the solution for a source in a supersonic stream. The complete solution is obtained by integrating over a distribution of such sources. It is found that the transonic solution may be obtained (within a small multiplicative factor) by modifying the limits of the integration and the nature of this modification reveals the physical significance of the theory.

Consider a uniform supersonic stream of velocity U and choose a rectangular cartesian co-ordinate system (X, Y, Z) with the X axis in the direction of the flow. Now consider an elementary line source pulse (in the plane $Z = o$ and perpendicular to the direction of the flow) which is located at ξ on the X axis. The source pulses at time T and the resulting potential observed at the station (x, o, o) is

$$\phi(x, o, t) = \frac{A(\xi, o, \tau)}{\sqrt{a^2\tau^2 \left[(x-\xi)^2 - U\tau\right]^2}}, \qquad (A.1)$$

where $\tau = t - T$ and a denotes the speed of sound of the fluid. No disturbance will have arrived at the station (x, o) before the time

$$\tau_1 = \frac{(x-\xi)}{a(M+1)} .$$

The disturbed fluid will have been swept downstream of the point (x, o) by the time

$$\tau_2 = \frac{(x-\xi)}{a(M-1)} .$$

The observer at (x, o) will therefore see a signal during the time interval τ_1 to τ_2. The duration of the signal due to the source pulse is

$$T_s = (\tau_2 - \tau_1) = \frac{2(x-\xi)}{a(M^2-1)} .$$

If $A(\xi, o, T)$ is finite the disturbance is of infinite strength on the two wave fronts bounding the disturbed fluid passing over the plane $Z = o$. The downstream or fast wave front moves at a velocity $U + a$ relative to the observer. The slow or upstream wave front moves at a velocity $U - a$ relative to the observer.

Consider now a distribution of line source pulses in the plane $Z = o$. The sources being positioned on the positive X axis. The disturbance potential at (x, o, t) for $M \geq 1$ is

$$\phi(x,o,t) = \int_0^x d\xi \int_{\tau_1}^{\tau_2} \frac{A(\xi, t-\tau)}{\sqrt{(\tau-\tau_1)(\tau_2-\tau)}} d\tau \; \frac{1}{a\sqrt{M^2-1}} . \qquad \text{(A. 2)}$$

Assuming that the sources are harmonic in time we write

$$A(\xi, t) = -\frac{W_a(\xi)\, a}{\pi} e^{i\omega t} .$$

The potential $\phi(x, o, t)$ is therefore

$$\phi(x,0,t) = \frac{-e^{i\omega t}}{\pi\sqrt{M^2-1}} \int_0^x W_a(\xi)\, d\xi \int_{\tau_1}^{\tau_2} \frac{e^{-i\omega\tau}}{\sqrt{(\tau-\tau_1)(\tau_2-\tau)}}\, d\tau .$$

We now assume that the effects of the slowly moving wave fronts (i.e. the wave fronts that travel at velocity $U - a$ relative to the observer) may be neglected and that the effect of a source pulse is observed over a time interval τ_1 to $\tau^* = \frac{(x-\xi)}{Ma}$, instead of the time interval τ_1 to τ_2. Therefore, we write

$$\phi(x,0,t) \approx \frac{-e^{i\omega t}}{\pi\sqrt{M^2-1}} \int_0^x W_a(\xi)\, d\xi \int_{\tau_1}^{\tau^*} \frac{e^{-i\omega\tau}}{\sqrt{(\tau-\tau_1)(\tau_2-\tau)}}\, d\tau .$$

The term $(\tau_2-\tau)^{-1/2}$ is essentially constant over the range of integration so that

$$\int_{\tau_1}^{\tau^*} \frac{e^{-i\omega\tau}}{\sqrt{(\tau-\tau_1)(\tau_2-\tau)}}\, d\tau \approx \int_{\tau_1}^{\tau^*} \frac{e^{-i\omega\tau}}{\sqrt{(\tau-\tau_1)(\tau_2-\tau_1)}}\, d\tau$$

and we write

$$\phi(x,0,t) \approx \frac{-b\, e^{i\omega t}}{\pi\sqrt{2kM}} \int_0^x \frac{W_a(\xi)\, e^{-\frac{ikM(x-\xi)}{M+1}}}{\sqrt{(x-\xi)}}\, d\xi \int_0^{\frac{k(x-\xi)}{M+1}} \frac{e^{-i\sigma}}{\sqrt{\sigma}}\, d\sigma .$$

For sufficiently large k and $\xi \neq x$ the integral

$$\int_0^{\frac{k(x-\xi)}{M+1}} \frac{e^{-i\sigma}}{\sqrt{\sigma}}\, d\sigma \approx e^{-i\frac{\pi}{4}} \sqrt{\frac{\pi}{2}} .$$

Therefore if k is sufficiently large and $M \approx 1$ the potential that results when the slow moving wave fronts are neglected may be written as

$$\phi(x,0,t) \approx \frac{-be^{i\omega t}}{\sqrt{2\pi k i M}} \int_0^x \frac{W_a(\xi)\, e^{-\frac{ik}{2}(x-\xi)}}{\sqrt{(x-\xi)}\sqrt{2}}\, d\xi. \qquad \text{(A. 3)}$$

This expression differs from the earlier transonic result (equation 1.4) only by a small multiplicative factor. The major features of the transonic theory have been obtained by this process of modifying the effects of an elementary source pulse.

The following interpretation of the unsteady transonic aerodynamic theory is offered upon the basis of the preceding analysis: In the transonic flow range the upstream wave fronts (associated with the velocity U - a) travel extremely slowly over the panel chord with the result that a large number of such wave fronts will be present at each point of the panel at any given time. For the case of an <u>oscillating</u> plate these disturbances have both positive and negative sign. If the frequency of oscillation is sufficiently large a destructive interference may result which would prevent the development of large perturbations. If the interference was extremely effective we could assume that the effects of disturbances that persist upon the panel could be neglected. We have shown above that the main features of the transonic theory may be obtained by such an assumption. The physical significance of the unsteady transonic theory therefore lies in the neglect of the disturbances that persist upon the panel. This neglect is possible

because of the interference phenomenon that may arise for sufficiently unsteady flows. The interference phenomenon prevents the development of large disturbances and makes possible the use of a linear theory to describe flows that are sufficiently unsteady.

APPENDIX B

GENERALIZED AERODYNAMIC FORCE COEFFICIENTS

1. Simply Supported Panels in a Transonic Airstream

The nth generalized force $Q_n^{(s)}$ was written in Section 2.1 as

$$Q_n^{(s)} = \frac{-\rho U^2 e^{i\omega t}}{\sqrt{2\pi k i M^2}} \sum_{m=1}^{N} T_{mn}^{(s)} A_m$$

and the coefficients $T_{mn}^{(s)}$ were expressed in terms of the coefficients C_i^{mn}. These latter coefficients are defined as follows:

$$C_1^{mn} = B_1^{mn}\left[\frac{+1}{(m+n)} \mp \frac{1}{(m-n)}\right]; \quad C_2^{mn} = B_2^{mn}\left[\frac{+1}{(m+n)} \mp \frac{1}{(m-n)}\right] \begin{matrix}(m+n)\ \text{even}\\ (m+n)\ \text{odd}\end{matrix}$$

$$C_3^{mn} = \left[\frac{B_2^m}{(m-n)} - \frac{B_1^m}{(m+n)} + \frac{m\pi^2}{2}\right]; \quad C_4^{mn} = \left[\frac{B_1^m}{(m-n)} - \frac{B_2^m}{(m+n)} - \frac{m\pi^2}{2}\right];$$

$$C_5^n = \left[\frac{1}{2\pi i}\left\{\frac{k^2}{n} - \frac{n\pi^2}{4}\right\} - \frac{B_1^n}{2}\right]; \quad C_6^n = \left[\frac{B_2^n}{2} - \frac{1}{2\pi i}\left\{\frac{k^2}{n} - \frac{n\pi^2}{4}\right\}\right];$$

$$C_7^n = \sqrt{\theta}\left\{C_5^n\left(\frac{2\pi}{\theta}\right)^{1/2} - \frac{i B_1^n}{4\theta^{3/2}}\left(\frac{\pi}{2}\right)^{1/2}\right\};$$

$$C_8^n = \sqrt{\delta}\left\{C_6^n\left(\frac{2\pi}{\delta}\right)^{1/2} - \frac{i B_2^n}{4\delta^{3/2}}\left(\frac{\pi}{2}\right)^{1/2}\right\};$$

$$C_9^n = \left\{\frac{B_1^n e^{-2i\theta}}{\theta} + \frac{B_2^n e^{2i\delta}}{\delta}\right\};$$

$$B_1^m = \left\{\left(\frac{m\pi}{2}\right)^2 + km\pi + k^2\right\};$$

$$B_2^n = \left\{km\pi - \left(\frac{m\pi}{2}\right)^2 - k^2\right\}.$$

2. Clamped Edge Panels in a Transonic Airstream

The nth generalized force $Q_n^{(c)}$ was written in Section 2.1 as

$$Q_n^{(c)} \quad \frac{-\rho U^2 e^{i\omega t}}{\sqrt{2\pi k i M^2}} \sum_{m=1}^{N} T_{mn}^{(c)} A_m$$

The coefficients $T_{mn}^{(c)}$ are defined as follows:

$$T_{\substack{mn \\ m \neq n}}^{(c)} = \left\{ S_0^{mn} + S_1^{mn} \int_0^k \tilde{J}(t)\,dt + S_2^{mn} \int_0^{n\pi+k} J(t)\,dt + S_3^{mn} \int_0^{n\pi-k} \tilde{J}(t)\,dt + S_4^{mn} \int_0^{m\pi+k} J(t)\,dt + S_5^{mn} \int_0^{m\pi-k} \tilde{J}\,dt \right\}$$

$$T_{mn}^{(c)} = \left\{ S_6^{n} + S_7^{n} \int_0^k \tilde{J}(t)\,dt + S_8^{n} \int_0^{n\pi+k} J(t)\,dt + S_9^{n} \int_0^{n\pi-k} \tilde{J}\,dt \right\}$$

$$\tilde{J}(t) = J_{-1/2}(t) - i J_{1/2}(t); \qquad J_{-1/2}(t) = \left(\frac{2}{\pi t}\right)^{1/2} \cos t;$$

$$J(t) = J_{-1/2}(t) + i J_{1/2}(t); \qquad J_{1/2}(t) = \left(\frac{2}{\pi t}\right)^{1/2} \sin t.$$

The following relationships hold:

$$S_2^{mn} = (-1)^{m+n} S_4^{nm}; \qquad S_3^{mn} = (-1)^{m+n} S_5^{nm};$$

$$S_0^{mn} = (-1)^{m+n} S_0^{nm}; \qquad S_1^{mn} = (-1)^{m+n} S_1^{nm}.$$

The coefficients S_i^{mn} are functions of k alone for given m and n. The explicit forms of these coefficients are extremely lengthy and will not be given here. These expressions can be found in Reference 24.

3. Simply Supported Panels in a Supersonic Airstream

The nth generalized force $Q_n^{(s)}$ was written in Section 2.2 as

$$Q_n^{(s)} = \frac{-\rho U^2 e^{i\omega t}}{\sqrt{M^2-1}} \sum_{m=1}^{N} C_{mn}^{(s)} A_m .$$

The coefficients $C_{mn}^{(s)}$ are defined as follows:

$$C_{nn}^{(s)} = \frac{ik(M^2-2)}{(M^2-1)} + \frac{k^2}{(M^2-1)^2}\left\{ \sum_{j=1}^{4} a_j H_j^{nn} \right\}.$$

$$C_{mn}^{(s)} = \frac{k^2}{(M^2-1)^2}\left\{ \sum_{j=1}^{4} a_j E_j^{mn} \right\}. \qquad m \neq n \quad (m+n) \text{ even.}$$

$$C_{mn}^{(s)} = \frac{2mn}{(n^2-m^2)} + \frac{k^2}{(M^2-1)^2}\left\{ \sum_{j=1}^{4} a_j \widetilde{F}_j^{mn} \right\}. \qquad m \neq n \quad (m+n) \text{ odd.}$$

$$H_j^{nn} = \left[\frac{-2W_j}{\left(W_j^2 - \left(\frac{n\pi}{2}\right)^2\right)} + \frac{\left(e^{2iW_j}(-1)^n - 1\right)}{2i}\left\{ \frac{n\pi}{\left(W_j^2 - \left(\frac{n\pi}{2}\right)^2\right)} \right\}^2 \right].$$

$$\widetilde{F}_j^{mn} = \left[\frac{mn\pi^2 e^{2iW_j}(-1)^n}{2i\left(W_j^2 - \left(\frac{m\pi}{2}\right)^2\right)\left(W_j^2 - \left(\frac{n\pi}{2}\right)^2\right)} + \frac{(n^2+m^2)}{(n^2-m^2)} - \frac{8W_j^2}{(n^2-m^2)\pi^2} \right].$$

$$E_j^{mn} = \left[\frac{mn\pi^2\left\{-1 + e^{2iW_j}(-1)^n\right\}}{2i\left(W_j^2 - \left(\frac{m\pi}{2}\right)^2\right)\left(W_j^2 - \left(\frac{n\pi}{2}\right)^2\right)} \right].$$

$$a_1 = a_2 = \frac{-(M^2+2)}{8i} ; \qquad a_3 = -a_4 = \frac{(2 \max J_1) M}{4i}.$$

$$W_{1,2} = \pm \frac{\bar{\omega}}{2M}\left\{ \frac{\pi}{d_1} \mp M \right\} ; \qquad W_{3,4} = \pm \frac{\bar{\omega}}{2M}\left\{ \frac{\pi}{d_2} \mp M \right\}.$$

TABLE I

DETAILS OF THE TEST PANELS

Test Panel No.	Panel Dimensions		Natural Frequencies of Lateral Vibration (cycles/sec)					
	Thickness (Inches)	Thickness Ratio $(\frac{h}{2b})$	Experimental		Clamped-Simply Supported		Clamped-Clamped	
			Mode 2,0	Mode 3,0	Mode 2,0	Mode 3,0	Mode 2,0	Mode 3,0
3	0.010	0.00297	95	308	91	295	132	364
22	0.0125	0.0033	112	328	90	291	130	360
25	0.0125	0.00353	118	363	103	333	149	412
23	0.0125	0.0037	133	398	114	368	165	455
26	0.0125	0.004	152	471	133	431	193	533
24	0.0155	0.00438	144	440	128	414	185	511
27	0.0155	0.0046	163	505	141	458	205	565

TABLE II

RESULTS OF

TWO-DIMENSIONAL PANEL FLUTTER EXPERIMENTS

PERFORMED AT MACH NUMBER 2.81 (see Ref. 22)

Thickness Ratio $(\frac{h}{2b})$		$\frac{(\frac{h}{2b})_{experiment}}{(\frac{h}{2b})_{theory}}$
Theory	Experiment	
0.00147	0.00163	1.11
0.0014	0.00165	1.18
0.00144	0.00165	1.15
0.0020	0.00205	1.03

Note: Two types of panel flutter were observed in the experiments described in Reference 22. The first type was characterized by a three-dimensional flutter mode and the second type by a two-dimensional flutter mode. The experimental results quoted above pertain to the two-dimensional flutter.

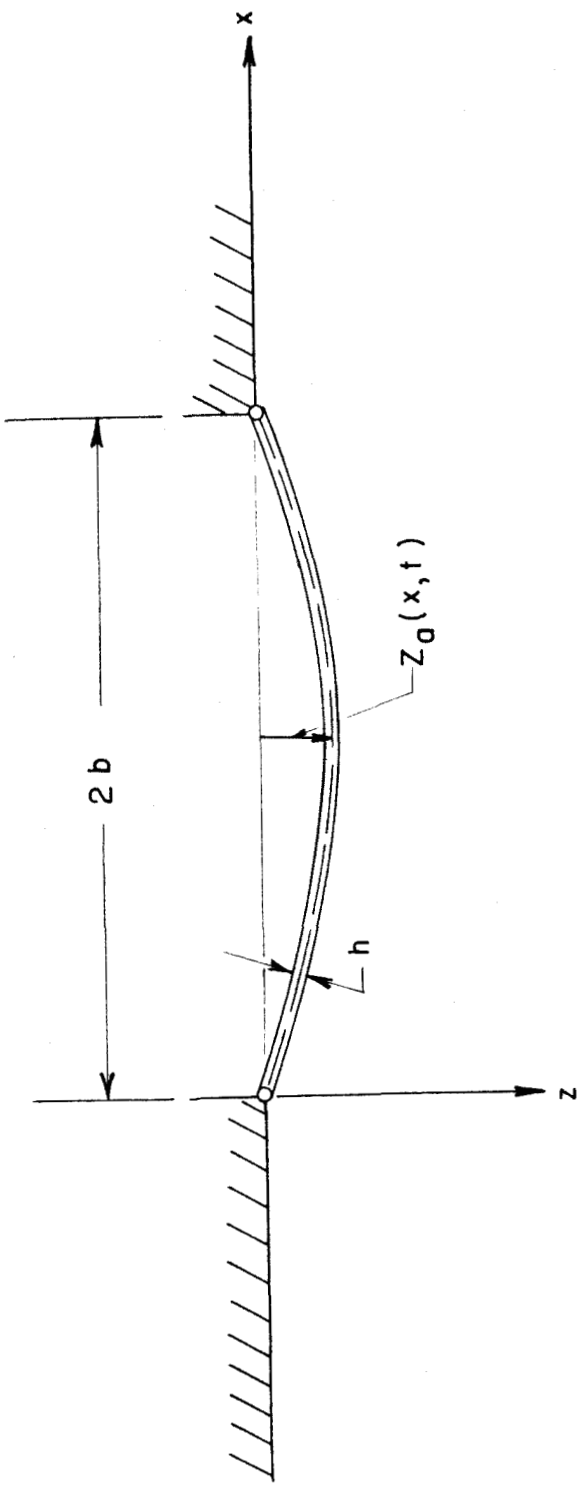

$U, p_o, M \gtrless 1$.

FIG. 1 – PANEL CONFIGURATION

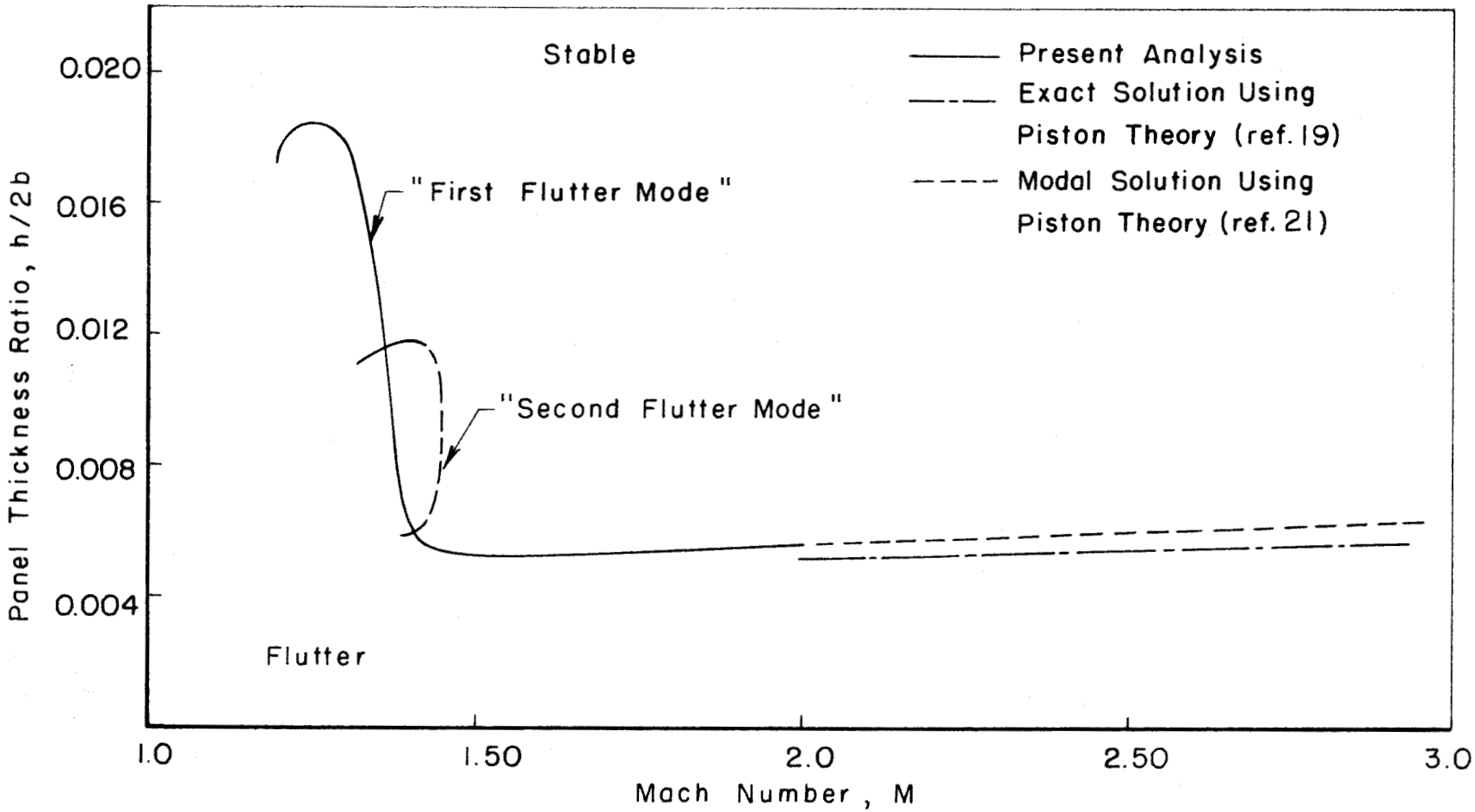

FIG. 2 – THEORETICAL PANEL THICKNESS REQUIREMENTS TO PREVENT THE FLUTTER OF SIMPLY SUPPORTED ALUMINUM PANELS IN SEA LEVEL AIR. TWO DIMENSIONAL FLOW

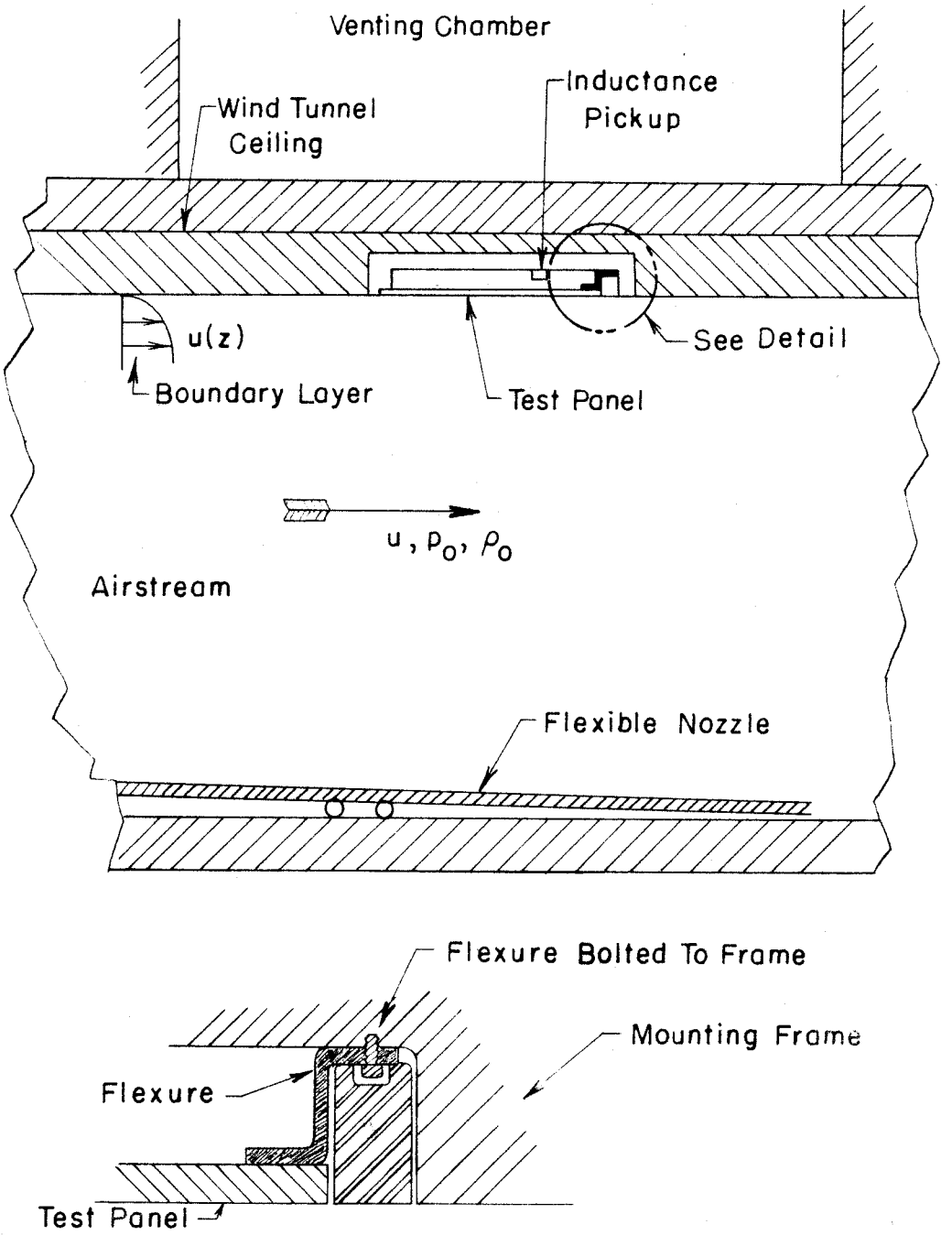

Detail Of Flexure Support

FIG. 3 – SCHEMATIC DIAGRAM OF THE TEST PANEL INSTALLATION IN THE CEILING OF THE TRANSONIC WIND TUNNEL

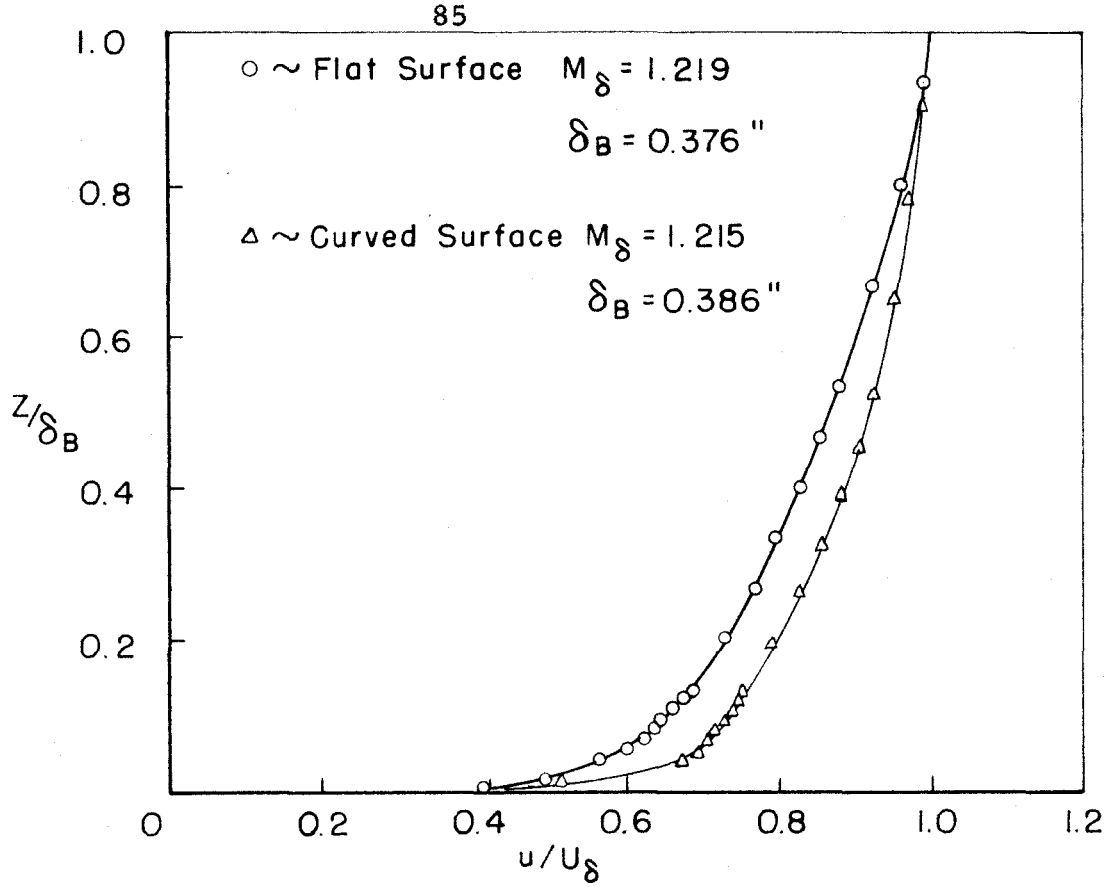

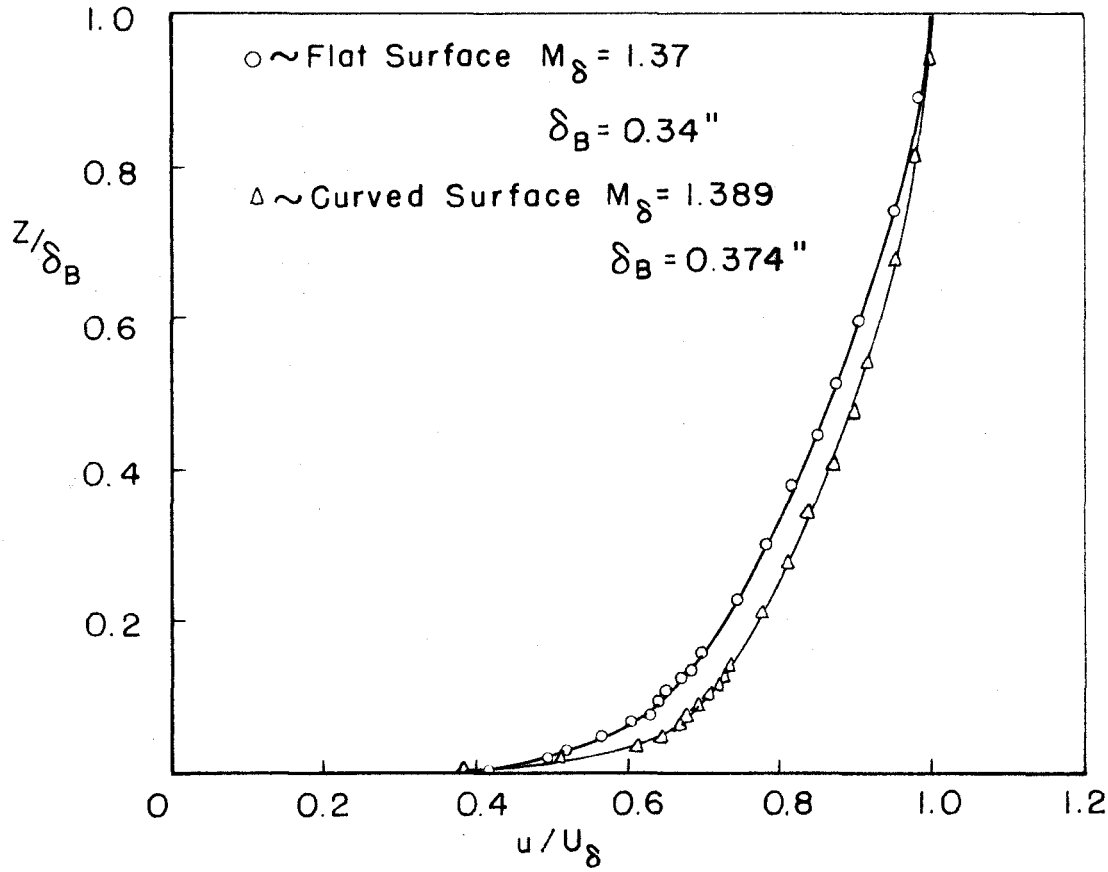

FIG. 4 - TYPICAL VELOCITY PROFILES OF THE BOUNDARY LAYER OVER THE TEST PANEL INSTALLATION IN THE WIND TUNNEL CEILING

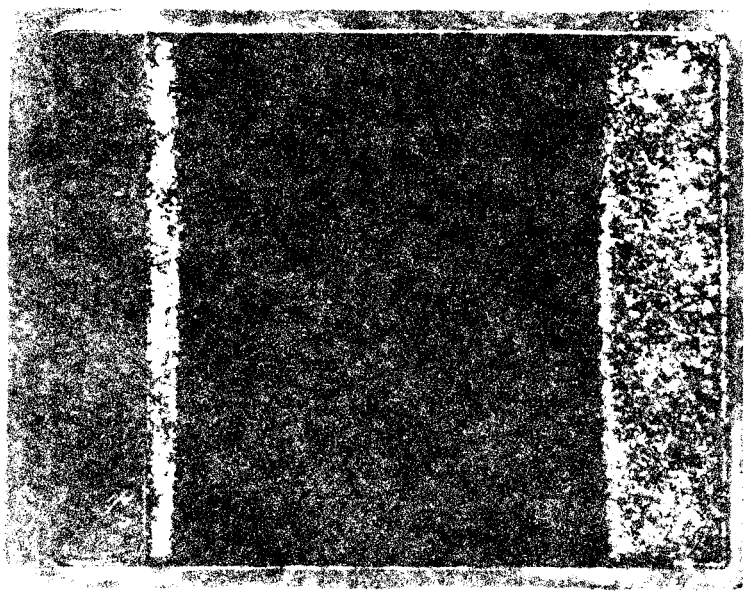

FIG. 5 (a) NODAL LINES FOR PANEL MODE (2,0)

Note: The notation (a, b) denotes the number of nodal lines perpendicular and parallel to the free edges of the plate respectively. The concentrations of salt crystals occur along the nodal lines for the various modes and are clearly visible in the following sequence of pictures.

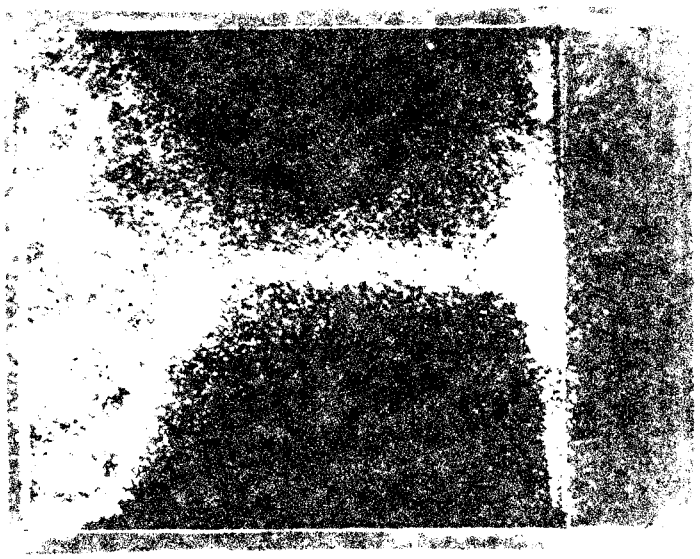

FIG. 5 (b) PANEL MODE (2, 1)

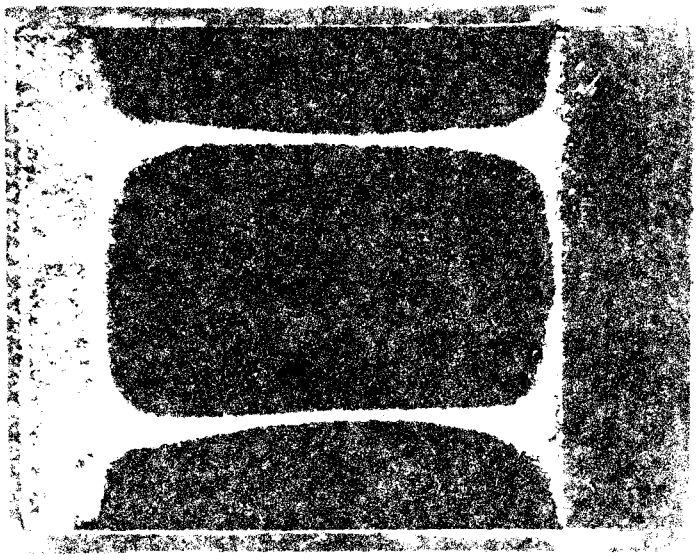

FIG. 5 (c) PANEL MODE (2, 2)

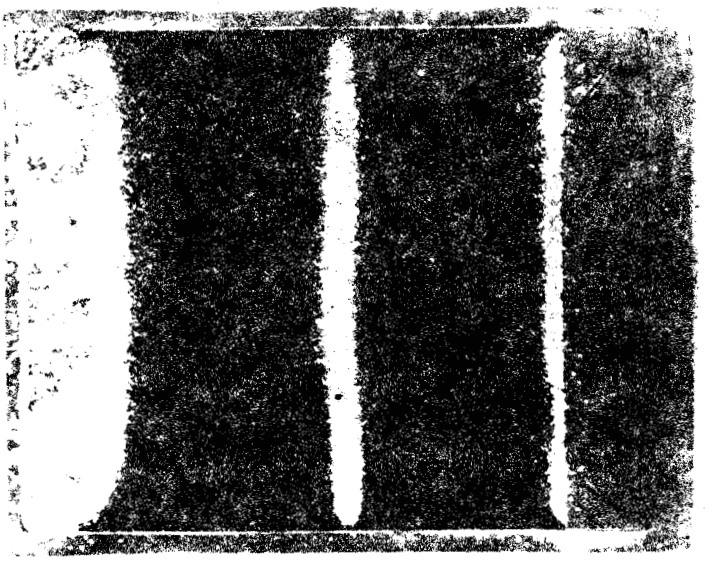

FIG. 5 (d) PANEL MODE (3,0)

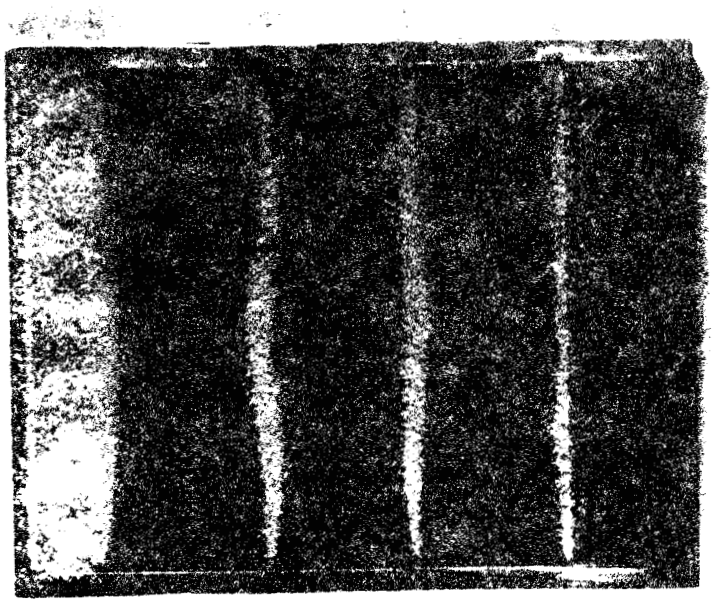

FIG. 5 (e) PANEL MODE (4,0)

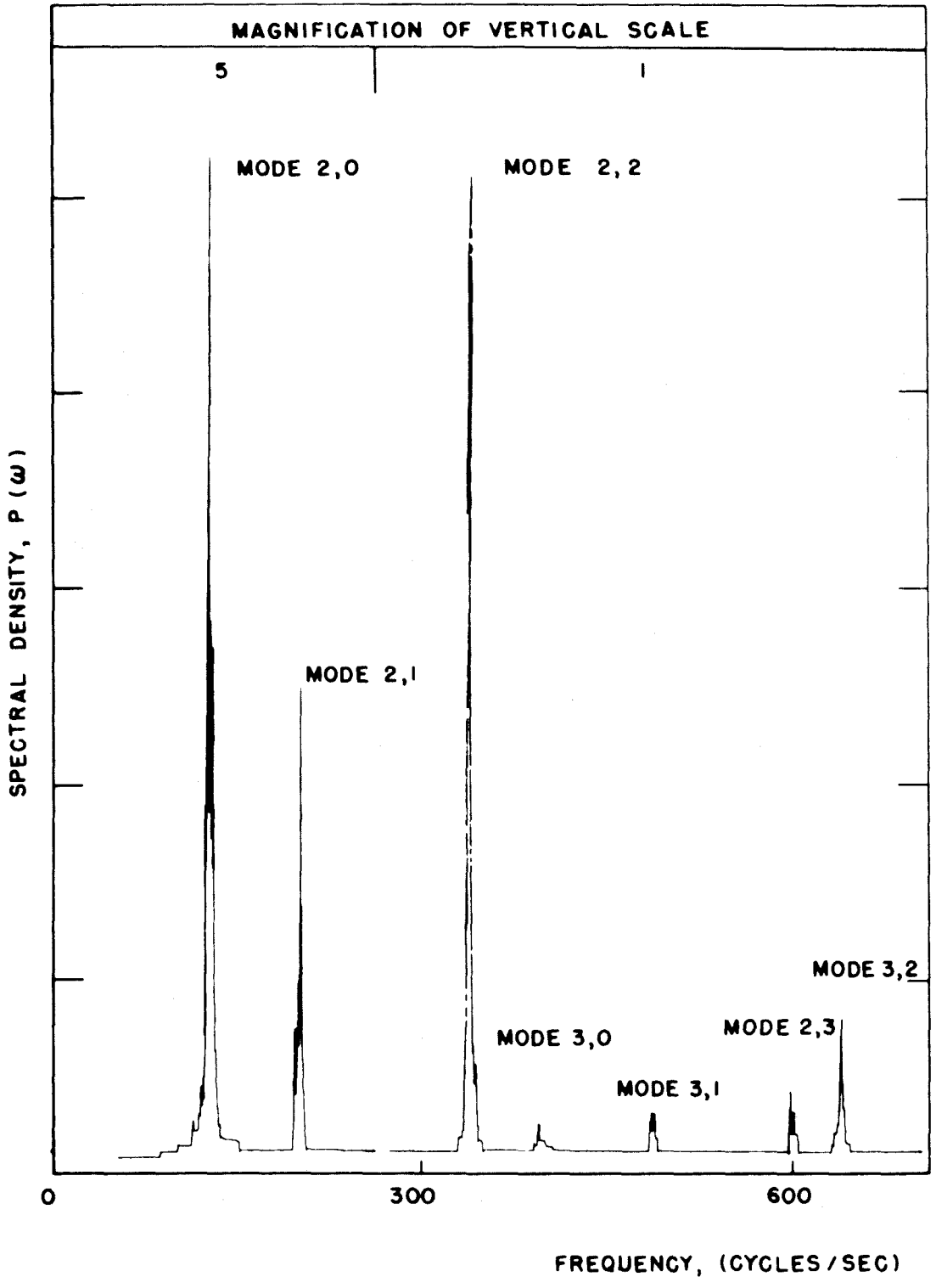

Fig. 6. A typical power spectrum of the test panel response to jet noise. Spectral peaks are exhibited at the natural frequencies of the panel. The spectrum was obtained using a 2 c/s bandwidth filter.

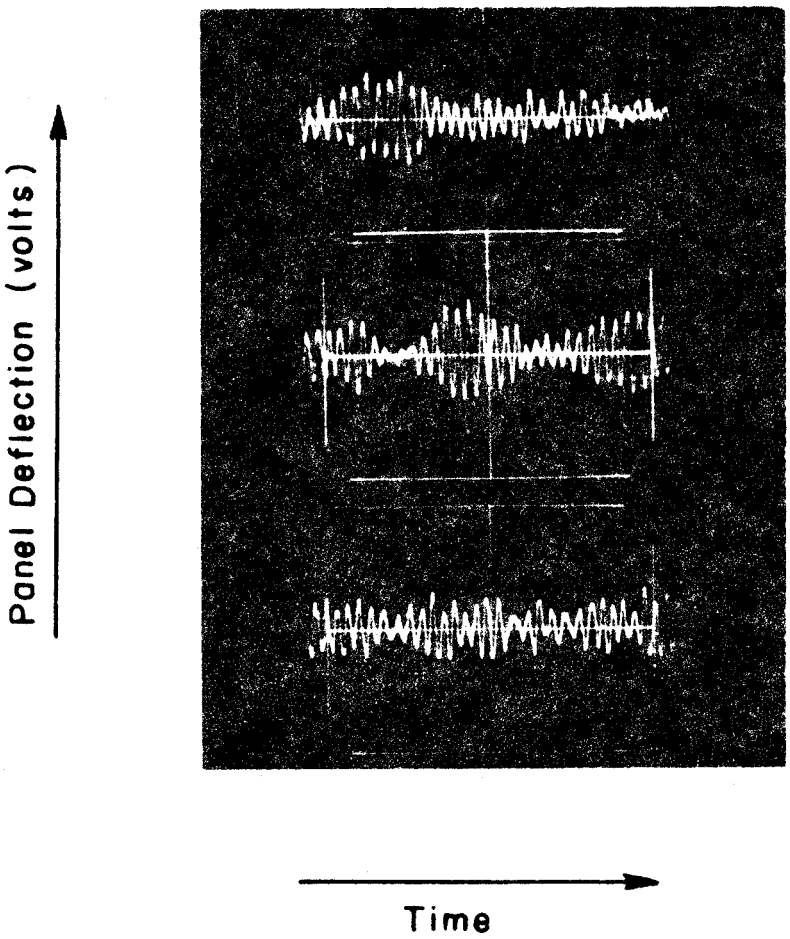

Fig. 7a. Panel response prior to flutter. The oscilloscope trace shows the pre-flutter response of a test panel exposed to a supersonic airstream. The major contribution to the response arises from the frequency band around the fundamental frequency of the panel. Estimated sweep speed was of the order of 0.022 seconds per major division of the scale.

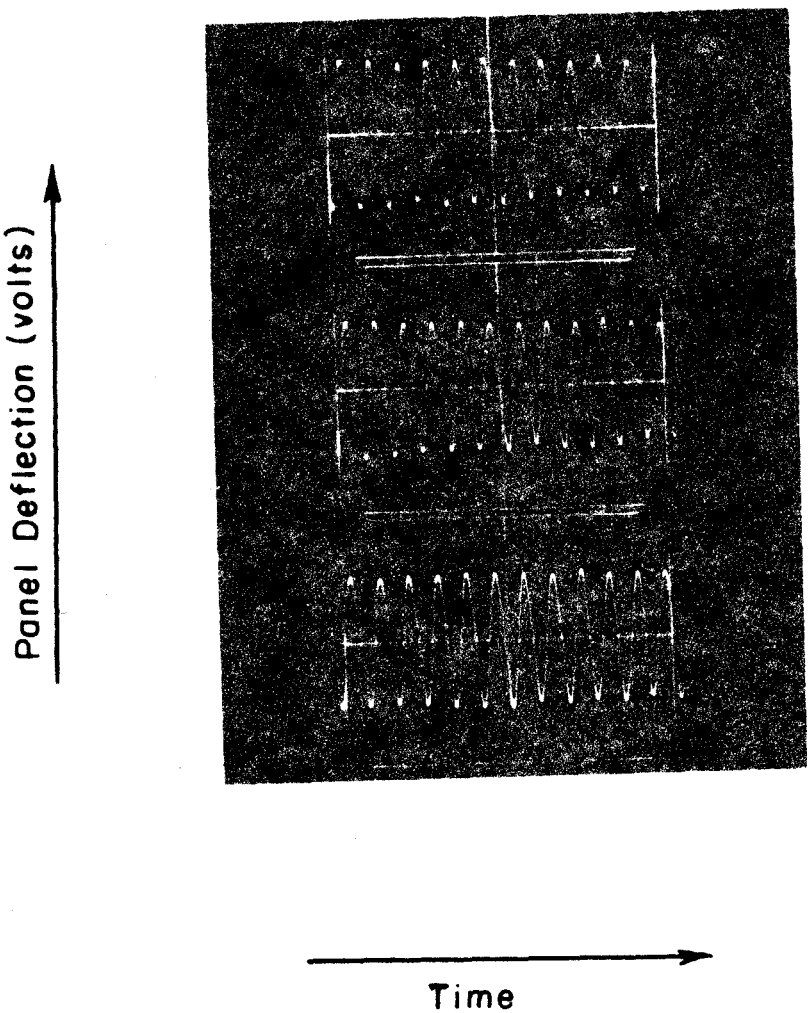

Fig. 7b. Panel response during flutter. The oscilloscope trace shows the response of a test panel at flutter. Estimated sweep speed was 0.0093 seconds per major division of the scale.

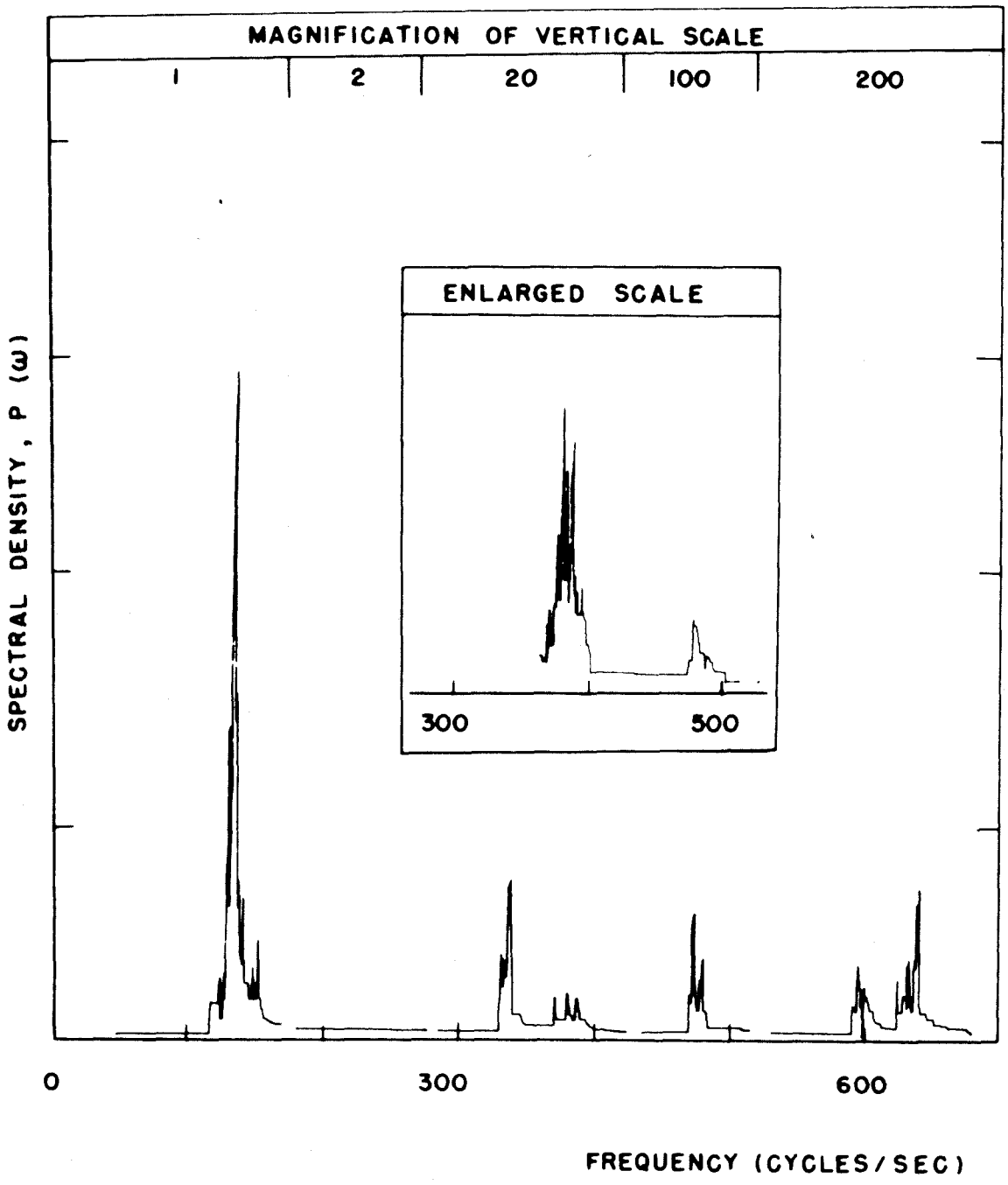

Fig. 8. A typical power spectrum of the test panel response to wind tunnel noise. The spectrum was obtained using a 2 c/s bandwidth filter.

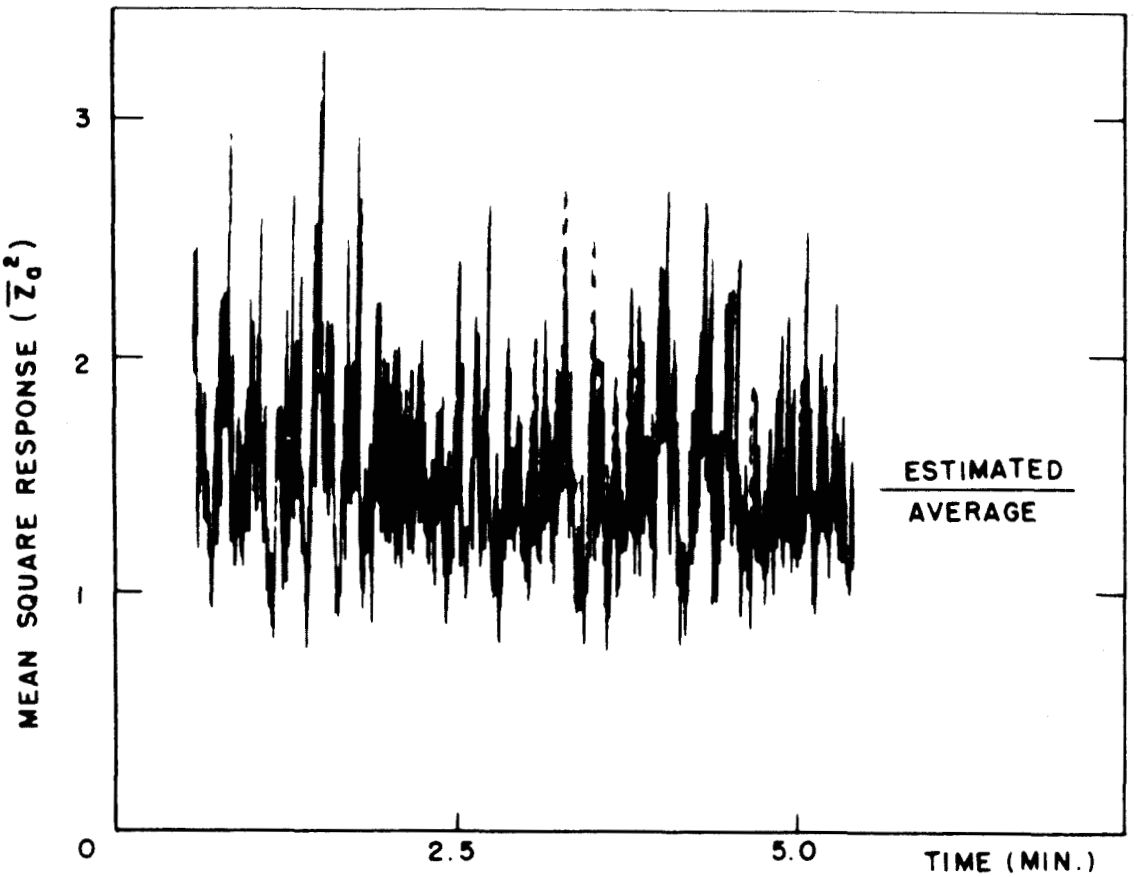

Fig. 9a. Variation of the mean square plate response with time in the non-flutter region.

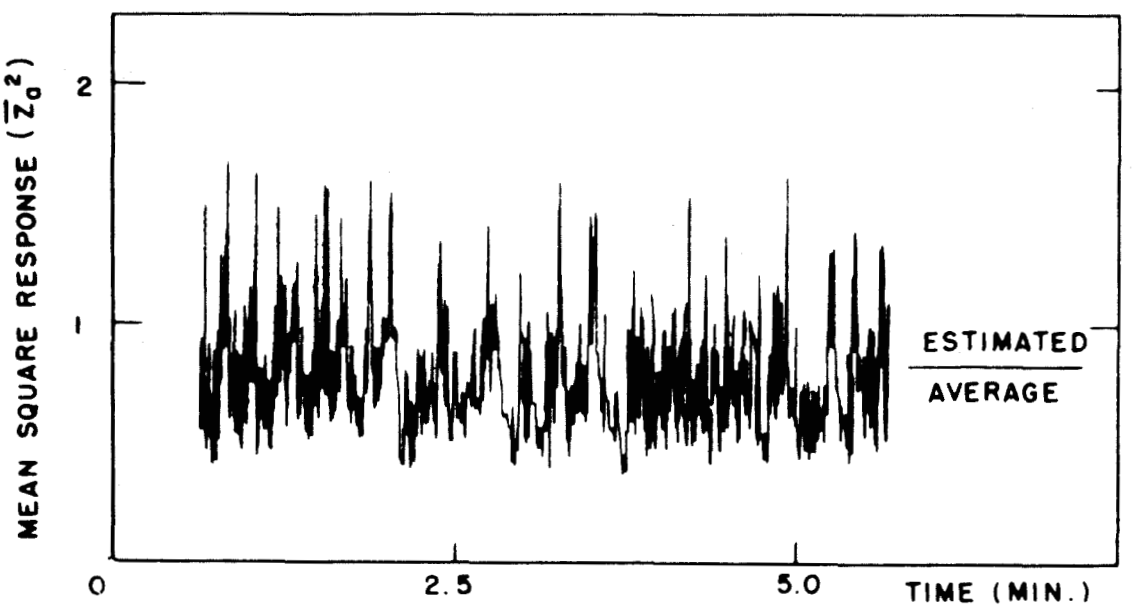

Fig. 9b. Variation of the filtered mean square response with time in the non-flutter region. The total signal has been passed through a 50 c/s bandwidth filter at the fundamental plate frequency.

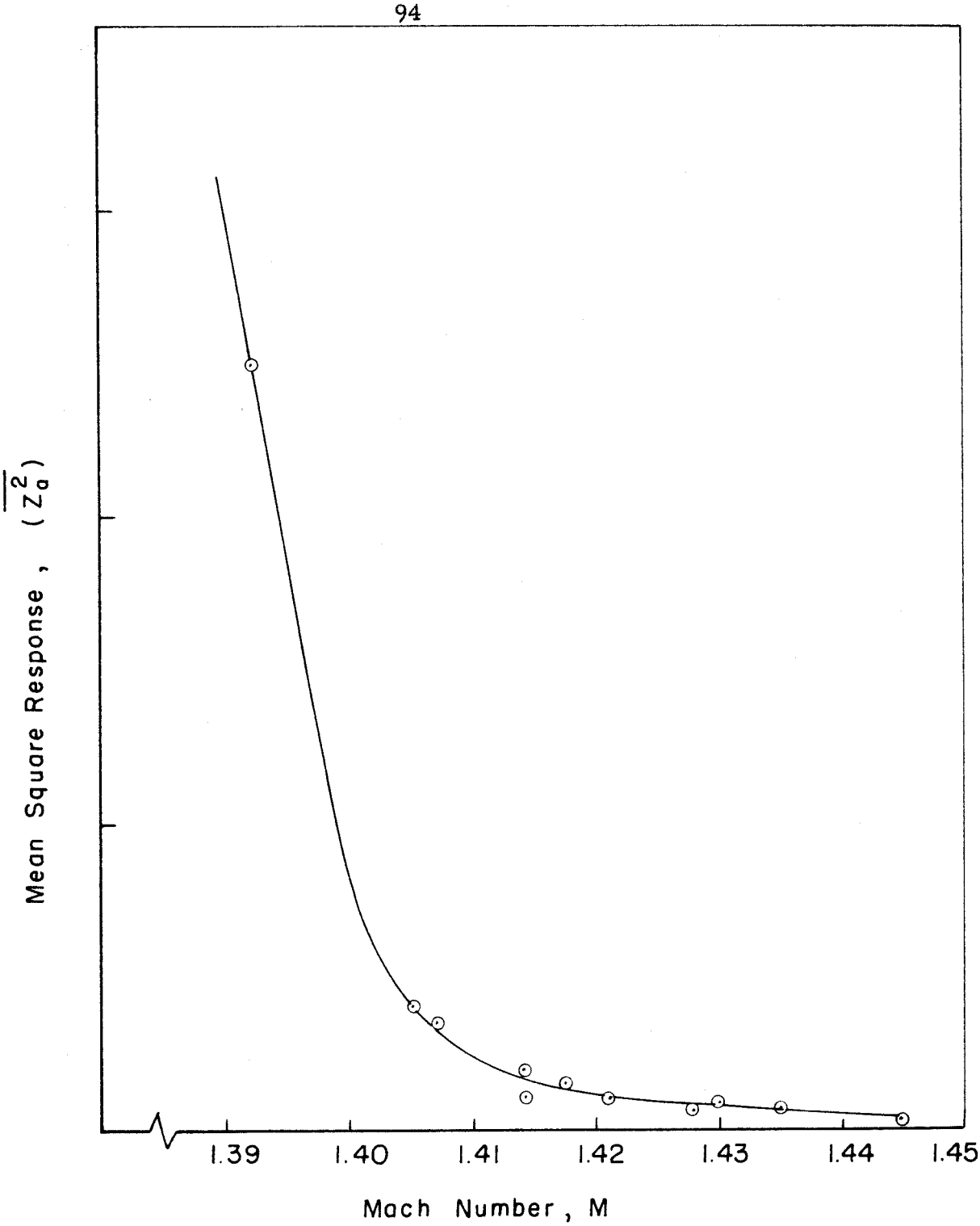

FIG. 10 - TYPICAL VARIATION OF THE MEAN SQUARE RESPONSE OF A TEST PANEL AT THE FLUTTER BOUNDARY

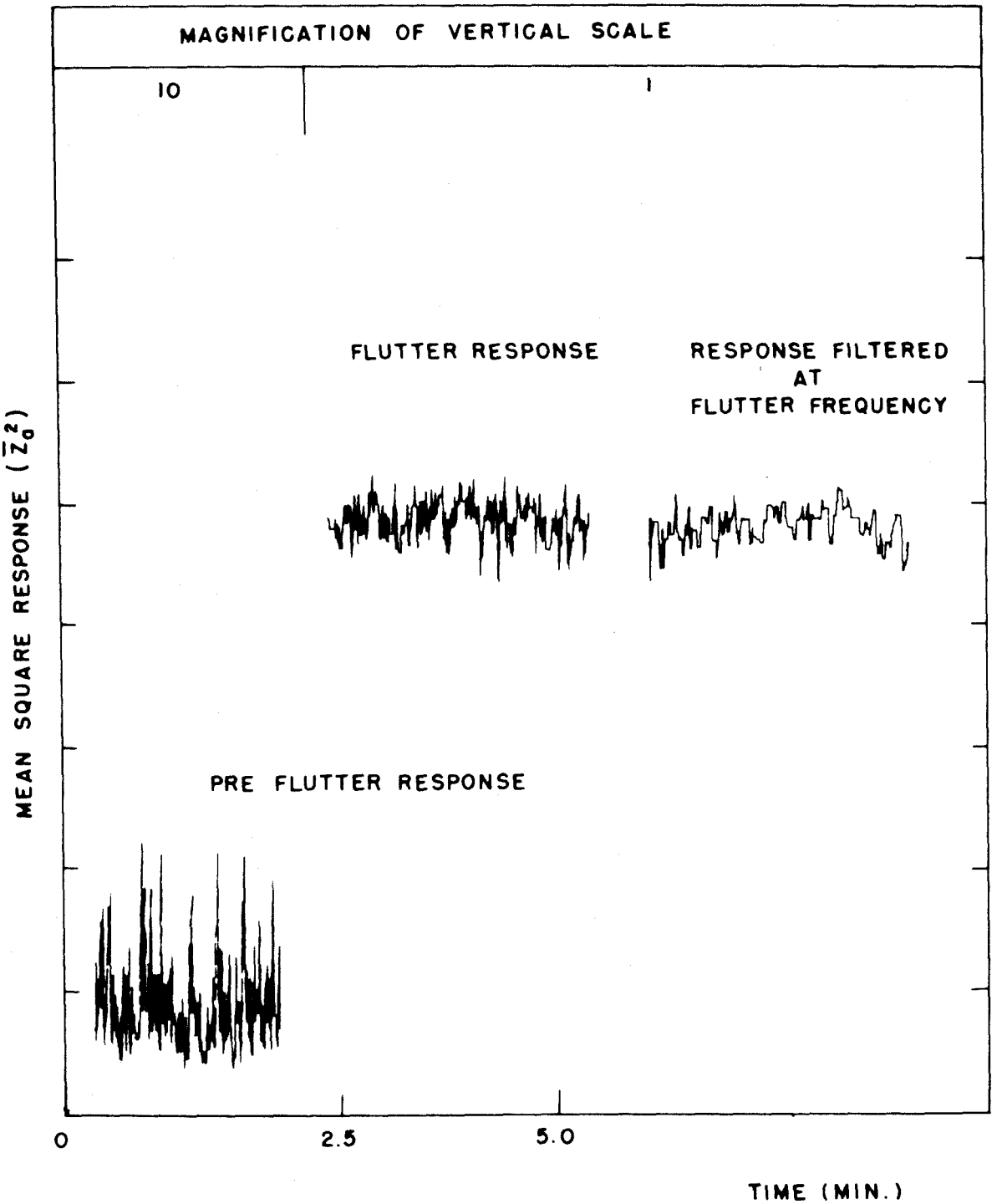

Fig. 11. Comparison of the mean square plate response in the flutter and non-flutter region. The flutter response was filtered at the flutter frequency using a 2 c/s bandwidth filter.

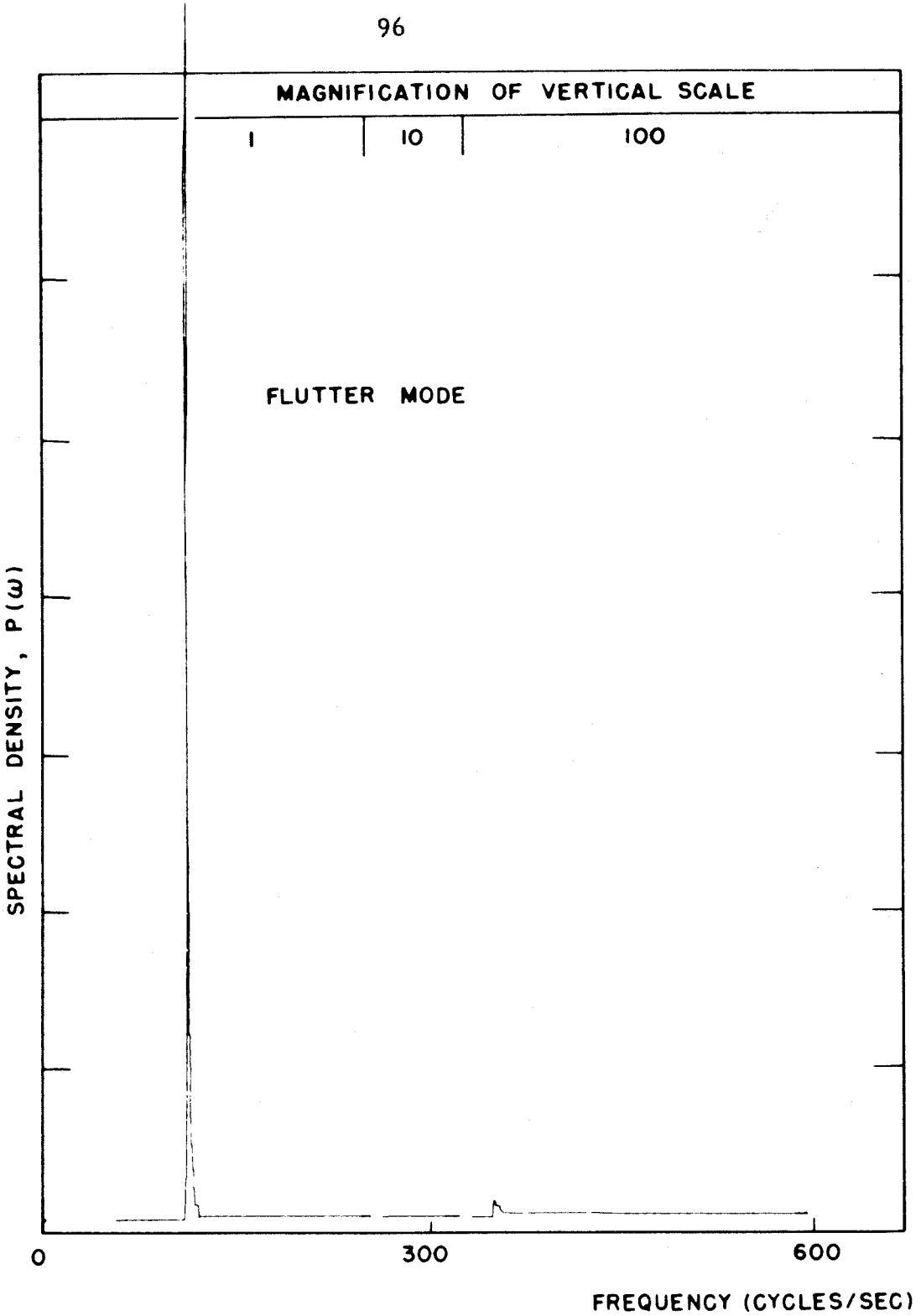

Fig. 12. A typical power spectrum of the test panel at the flutter Mach number. The spectrum was obtained using a 2 c/s bandwith filter.

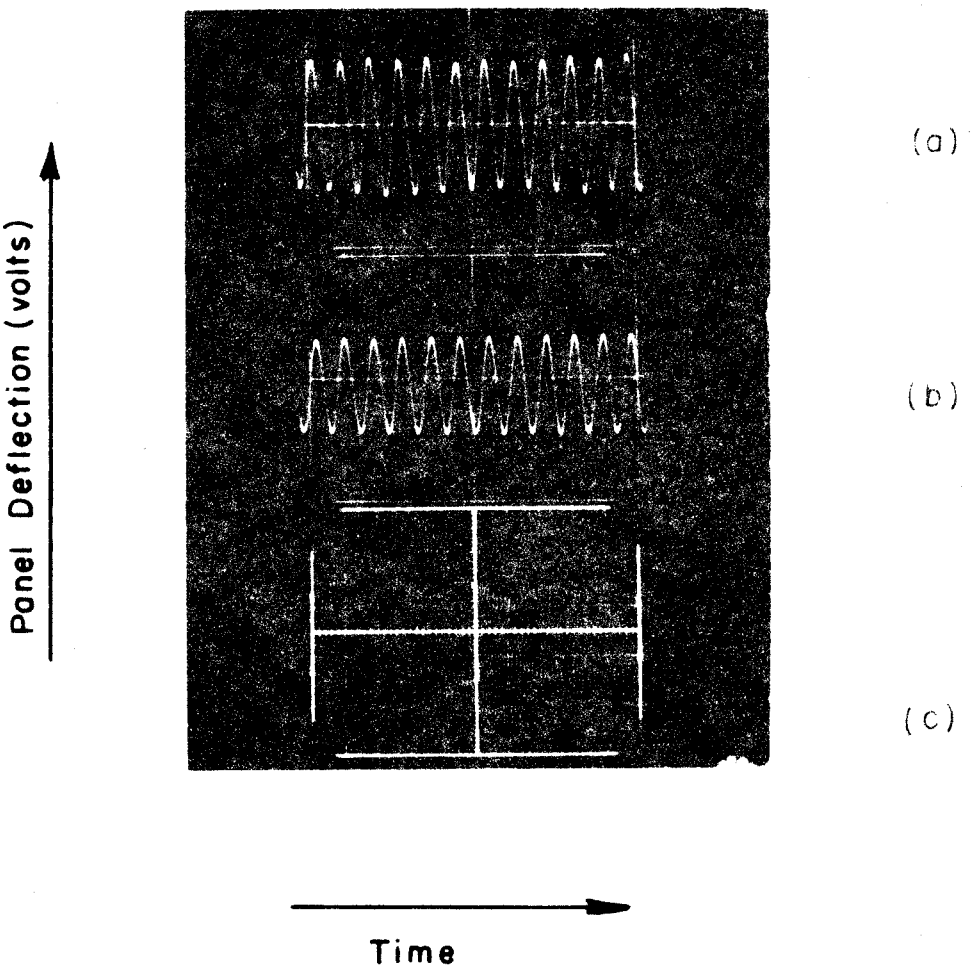

Fig. 13. Panel response during flutter.

(a) Panel response, total signal

(b) Panel response filtered at the flutter frequency

(c) Panel response filtered at the frequency of the second two-dimensional mode

Note: A 2 cycle/sec bandwidth filter was employed to obtain traces (b) and (c). Vertical scales are different for all three traces.

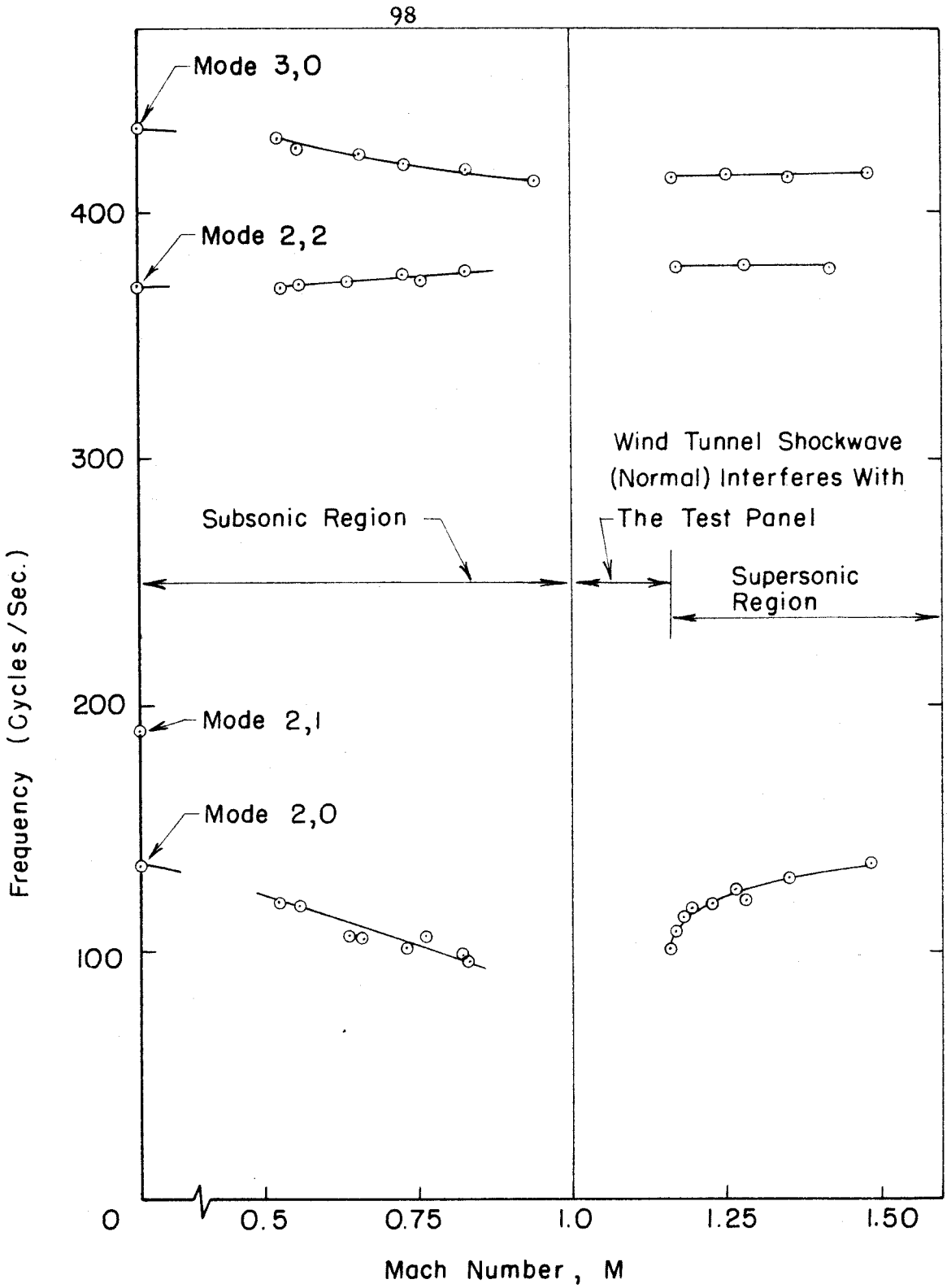

FIG. 14 - THE VARIATION WITH MACH NUMBER OF THE FREQUENCIES OF LATERAL VIBRATION OF A TEST PANEL

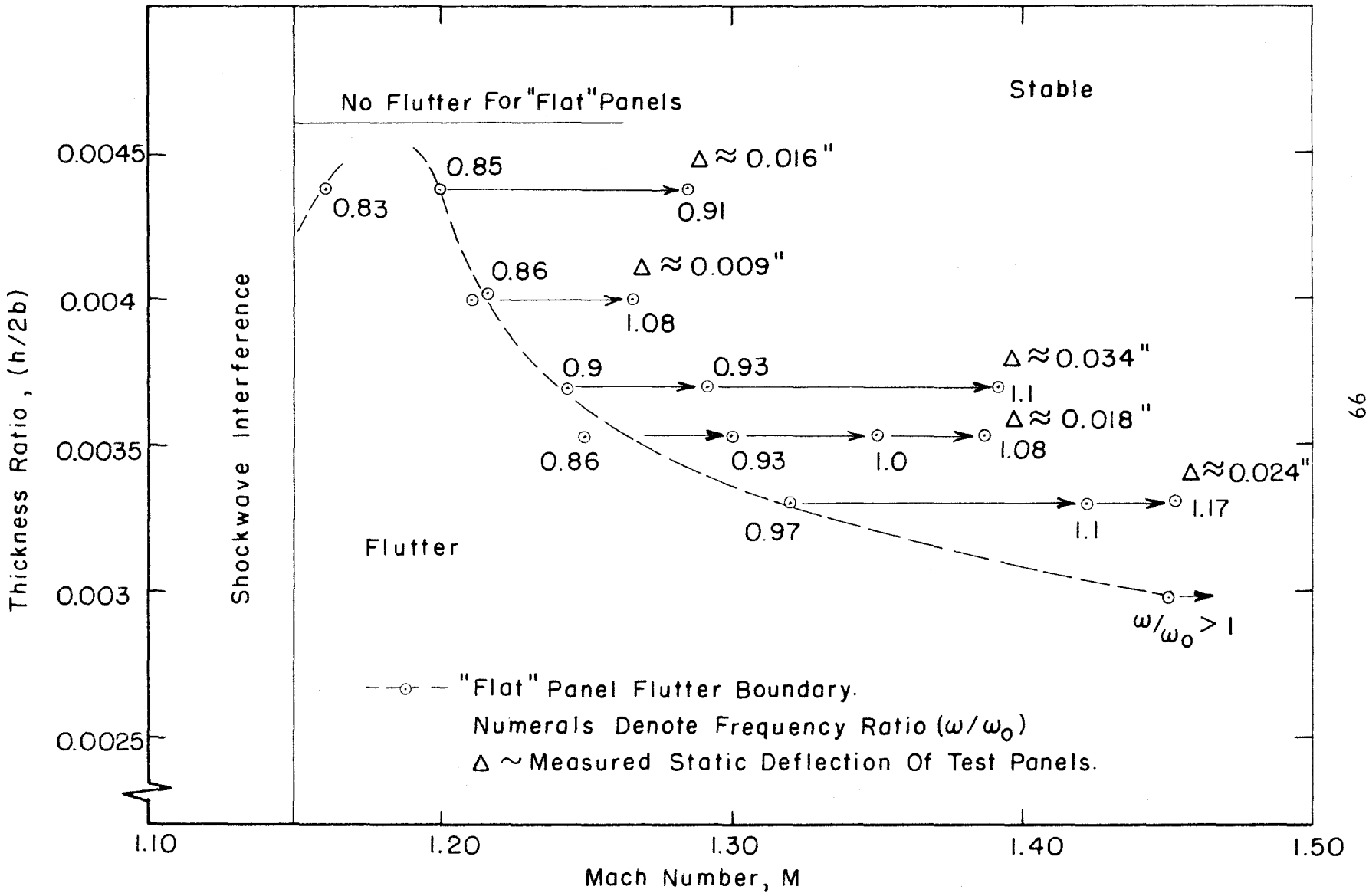

FIG. 15 - EXPERIMENTAL FLUTTER BOUNDARIES FOR BRASS PANELS EXPOSED TO AN AIRSTREAM WITH SEA LEVEL STAGNATION CONDITIONS

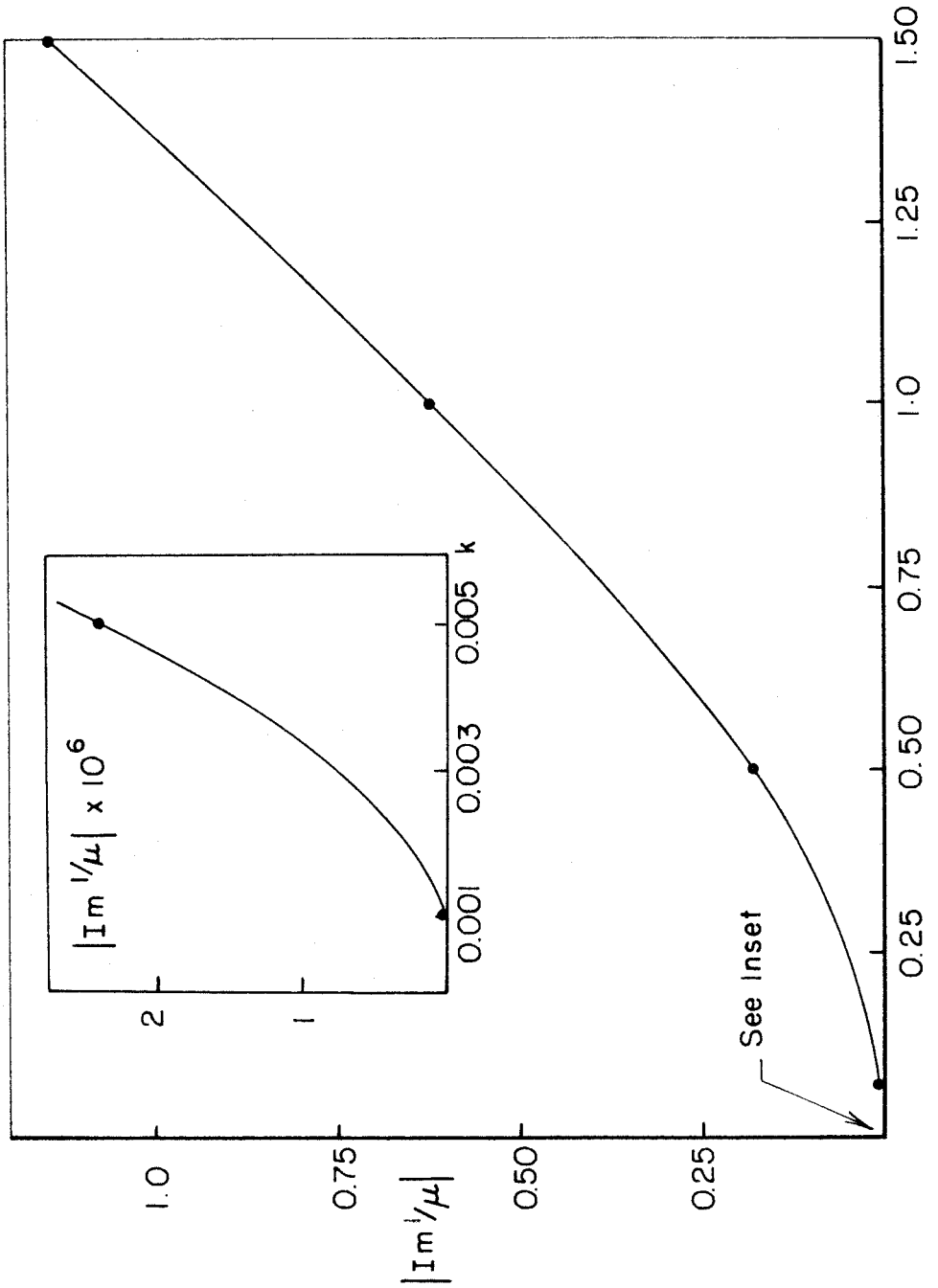

FIG. 16a-TRANSONIC FLUTTER SOLUTIONS FOR A SIMPLY SUPPORTED PLATE IN A SONIC AIRSTREAM

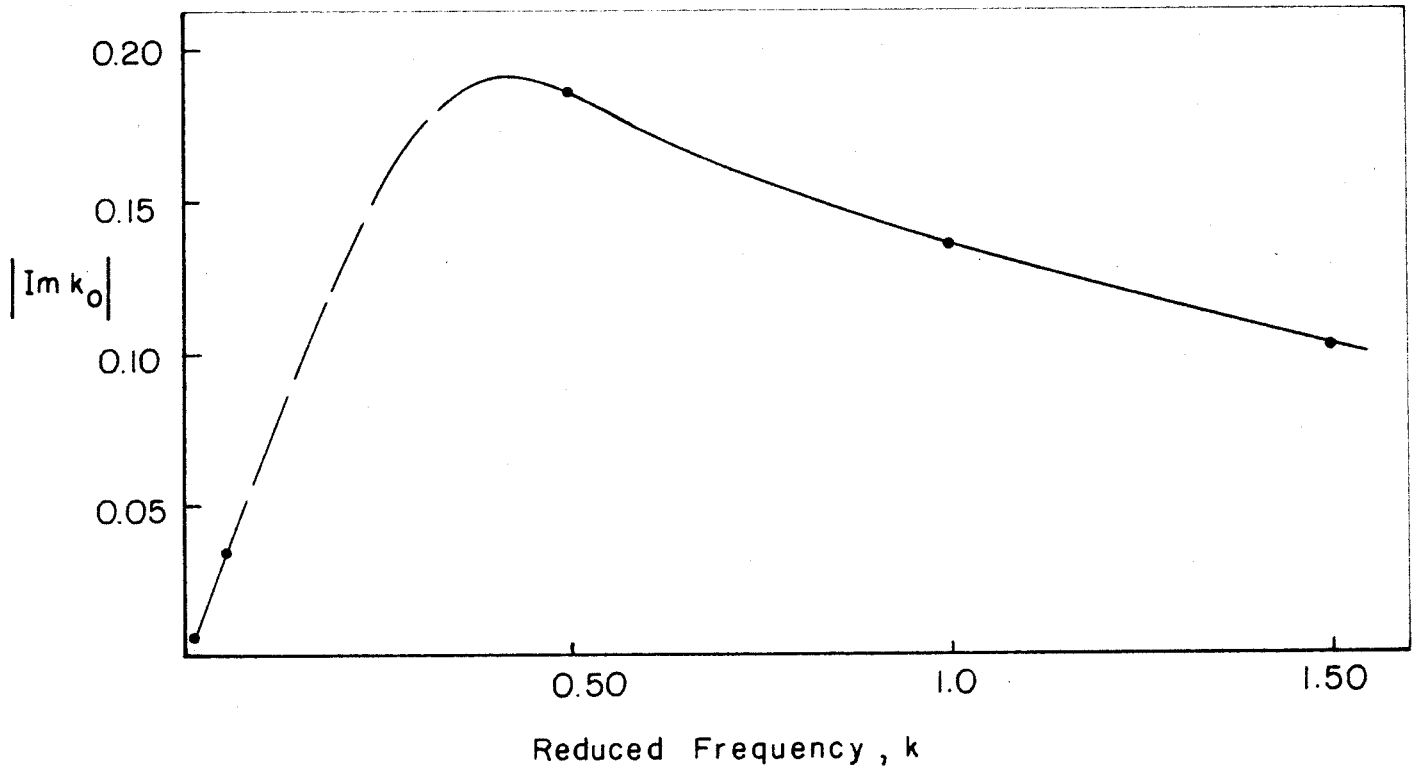

FIG. 16b-TRANSONIC FLUTTER SOLUTIONS FOR A SIMPLY SUPPORTED PLATE IN A SONIC AIRSTREAM

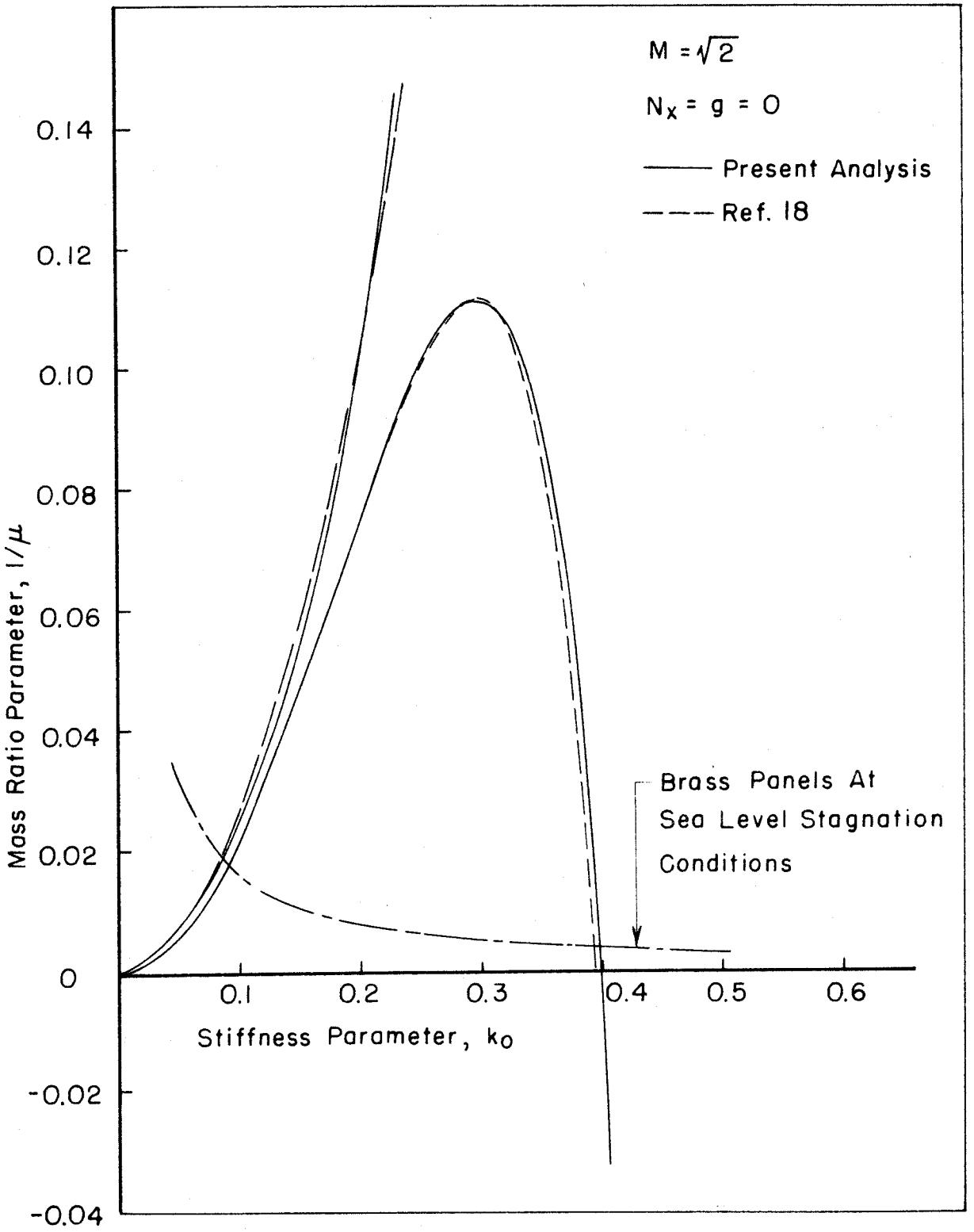

FIG. 17 - FLUTTER BOUNDARIES FOR SIMPLY SUPPORTED PANELS AT $M = \sqrt{2}$ FROM A TWO MODE ANALYSIS

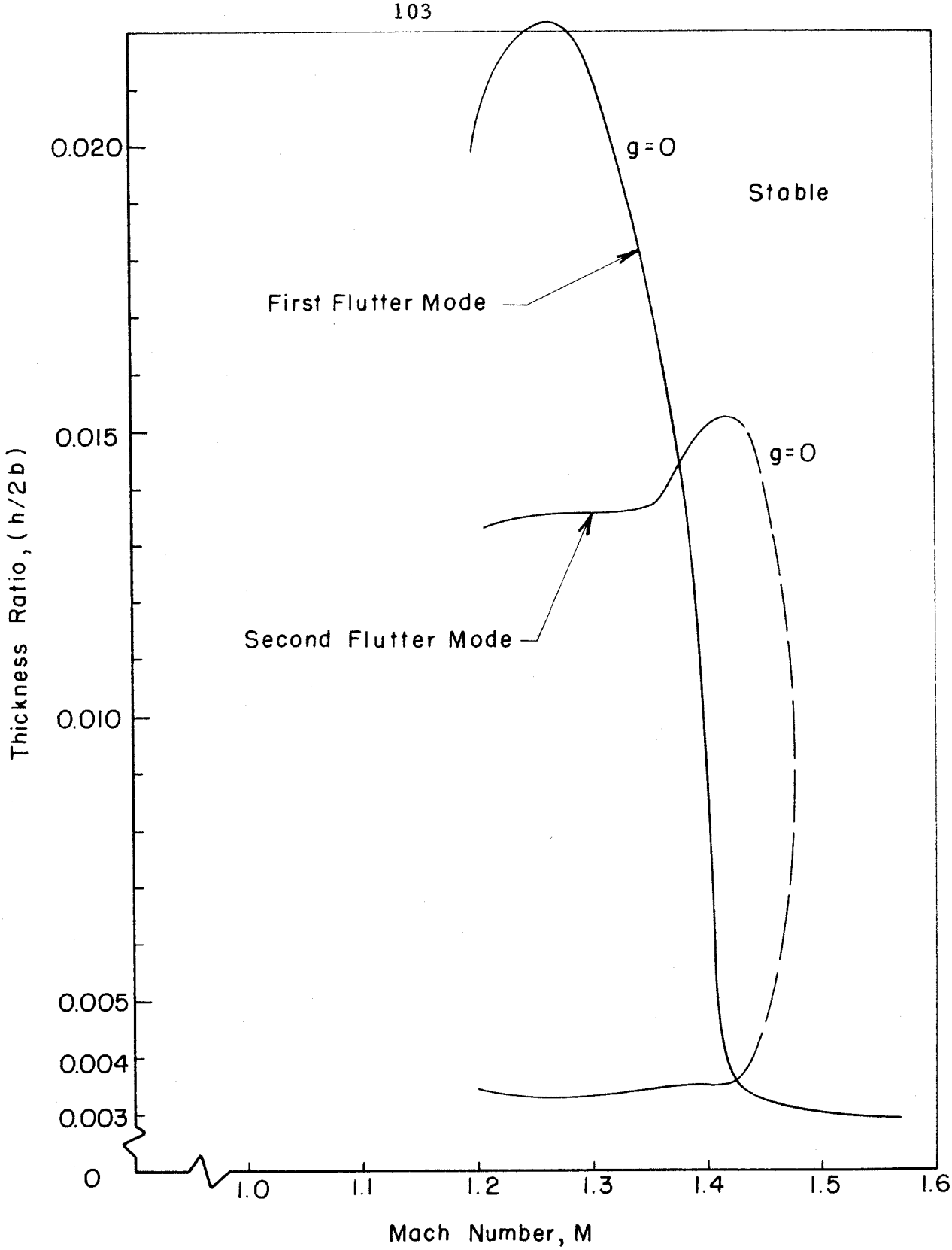

FIG.18-FLUTTER BOUNDARIES FOR BRASS PANELS AT CONSTANT SEA LEVEL STAGNATION CONDITIONS FROM A TWO MODE ANALYSIS. SIMPLY SUPPORTED EDGE CONDITIONS.

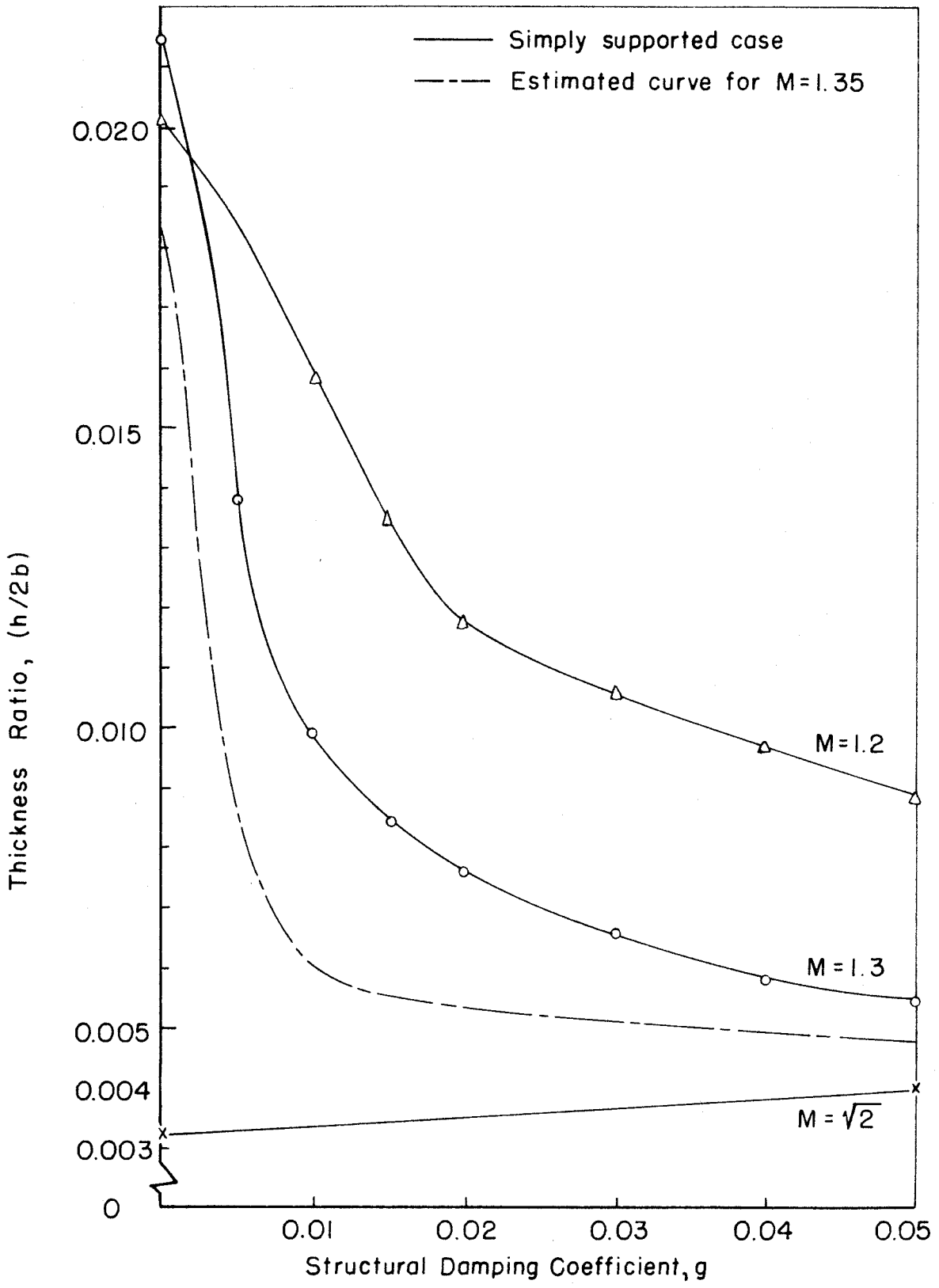

FIG. 19 - VARIATION OF "FIRST MODE" THICKNESS REQUIREMENTS WITH THE STRUCTURAL DAMPING COEFFICIENT g. BRASS PANELS AT CONSTANT SEA LEVEL STAGNATION CONDITIONS

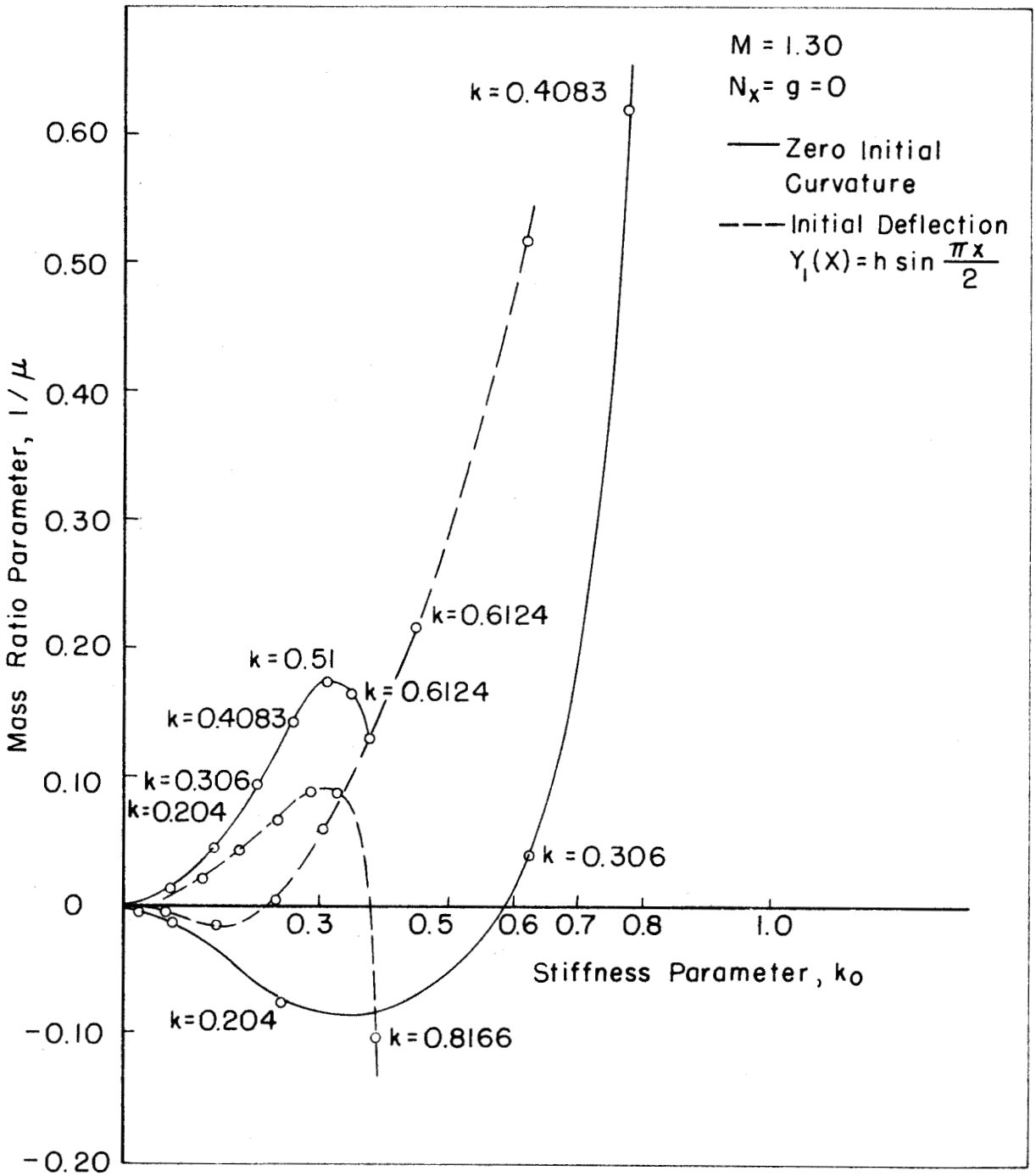

FIG. 20-EFFECT OF INITIAL CURVATURE UPON FLUTTER BOUNDARIES AT M = 1.3 ACCORDING TO A TWO MODE ANALYSIS

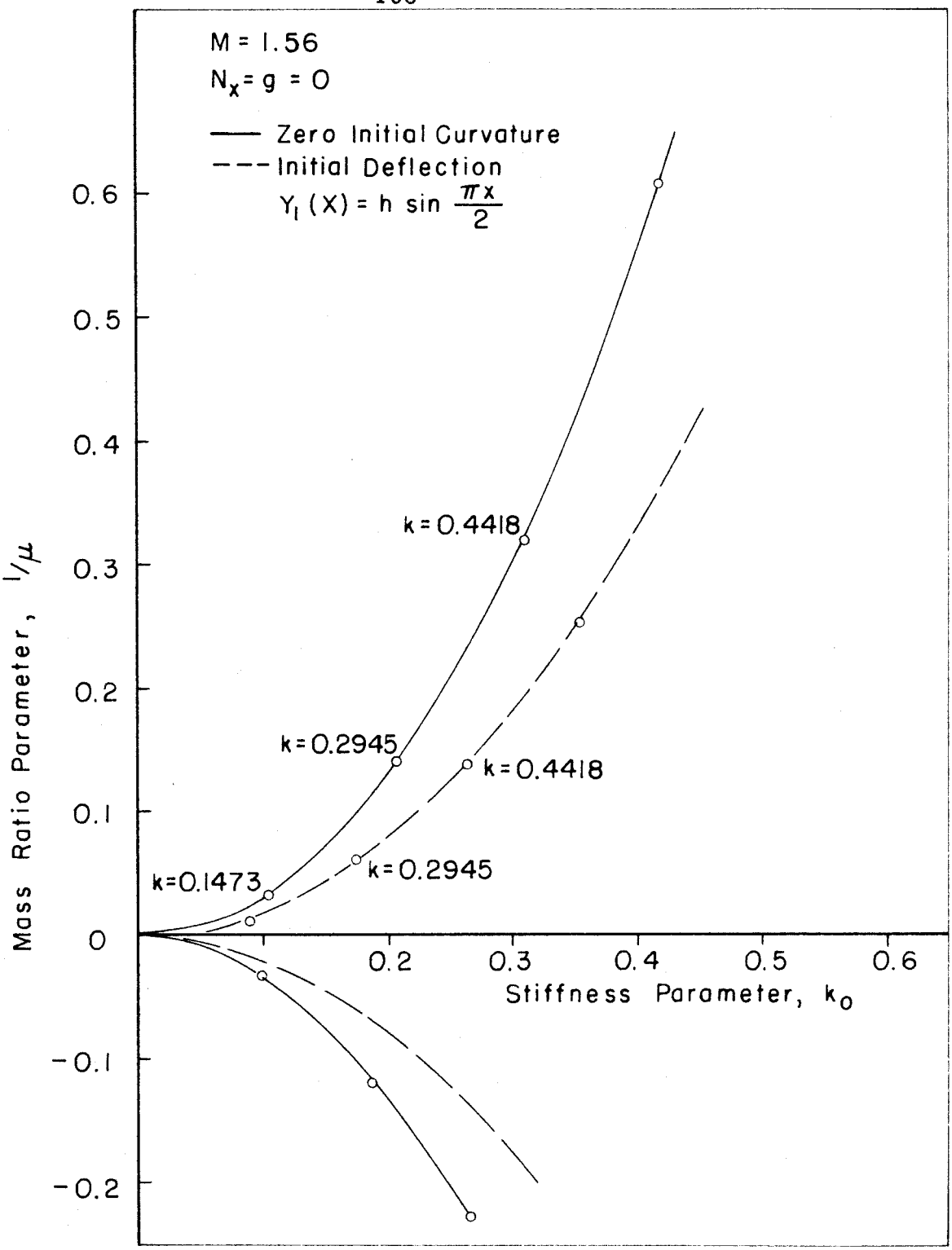

FIG. 21-EFFECT OF INITIAL CURVATURE UPON FLUTTER BOUNDARIES AT M = 1.56 ACCORDING TO A TWO MODE ANALYSIS

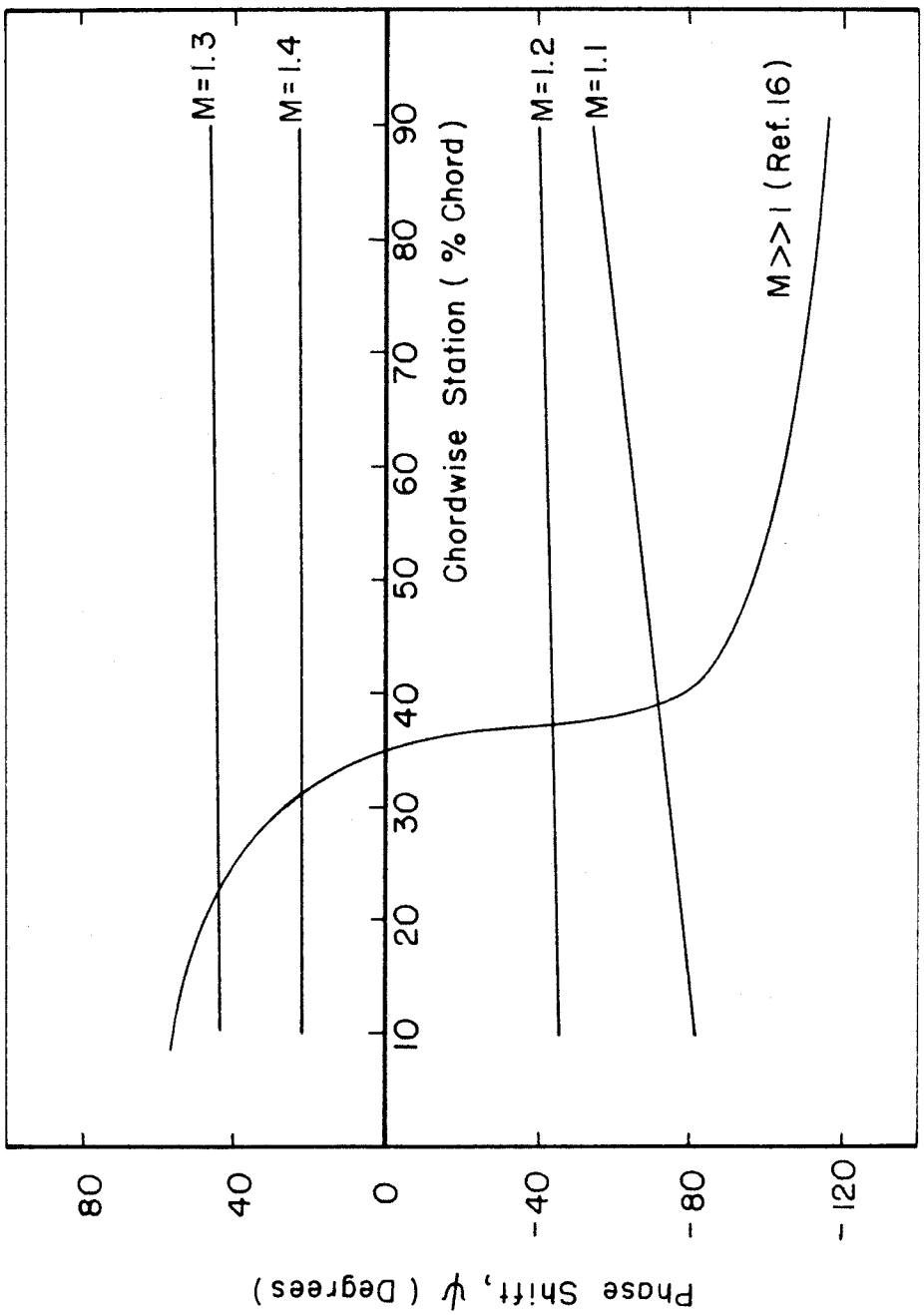

FIG.22-PHASE SHIFT PRESENT IN THE FLUTTER MODES AT VARIOUS MACH NUMBERS. THE RESULTS FOR MACH NUMBER 1.1, 1.2, 1.3, 1.4 ARE ESTIMATED FROM REF. 1.

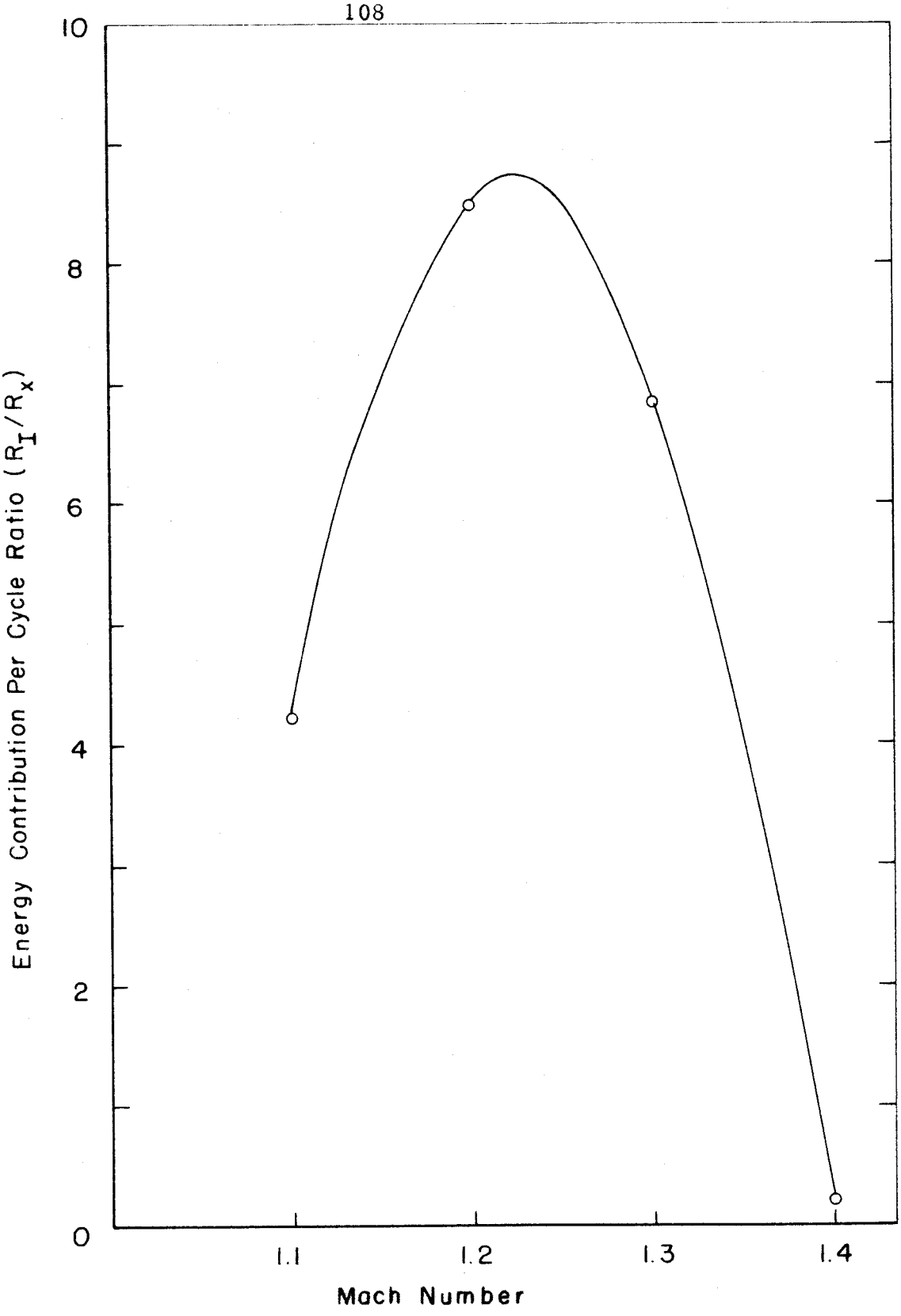

Fig. 23. Ratio of the energy contribution per cycle at flutter originating from the static aerodynamic term and the integral term in the aerodynamic pressure expression. The results are estimated from the flutter analysis of reference 1.

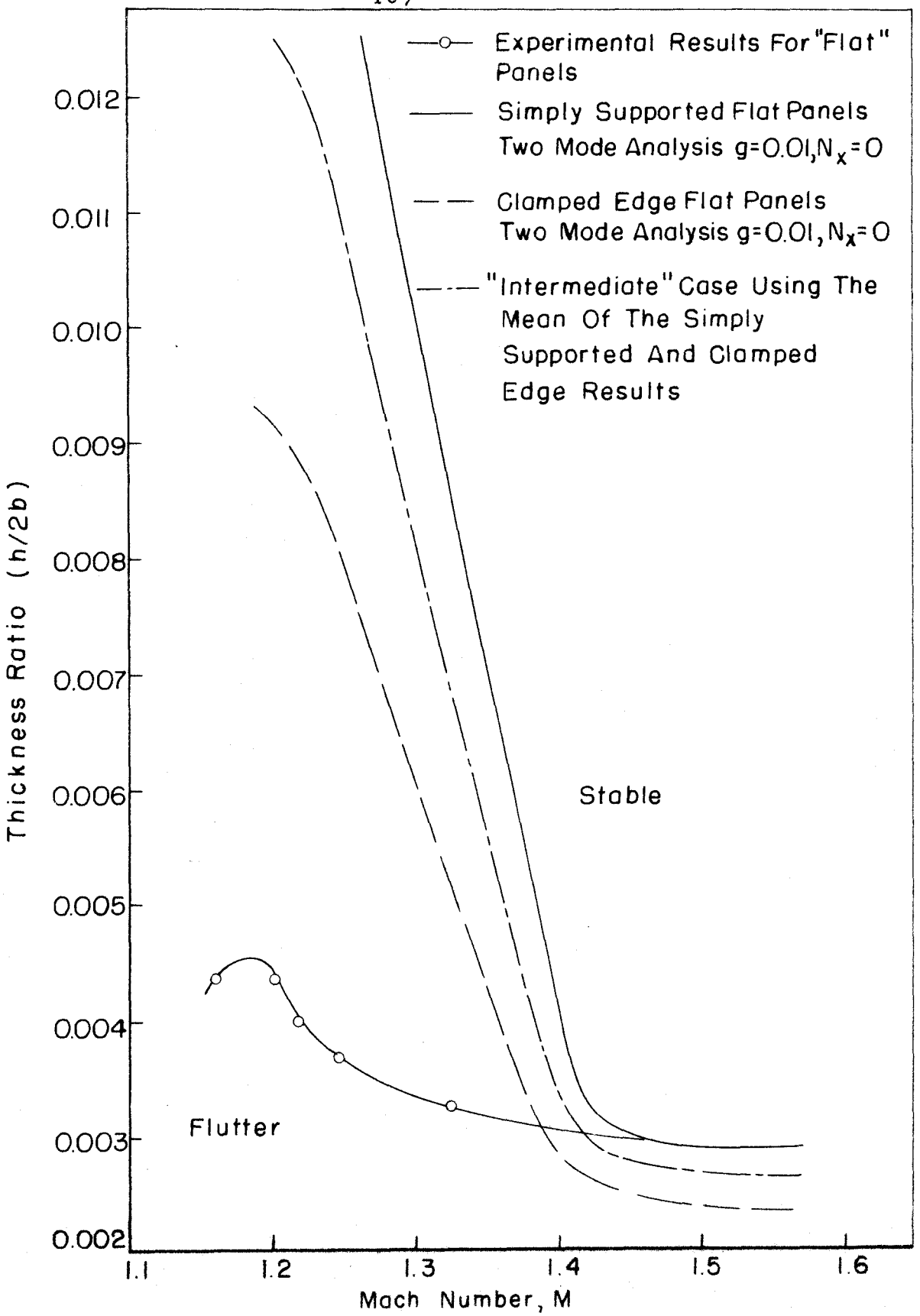

FIG. 24 - COMPARISON OF THE THEORETICAL FLUTTER BOUNDARIES WITH THE EXPERIMENTAL RESULTS